SOLAR ER 1473-15

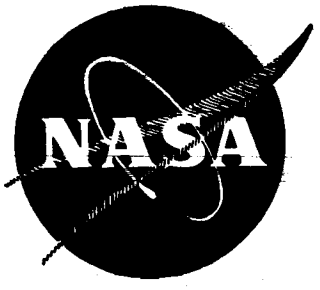


# LIQUID HYDROGEN FLEXIBLE DUCTING TECHNOLOGY

by

H. T. MISCHEL



Prepared for

NATIONAL AERONAUTICS AND SPACE ADMINISTRATION

CONTRACT NAS 8-11303



SOLAR, A DIVISION OF INTERNATIONAL HARVESTER COMPANY

SAN DIEGO, CALIFORNIA 92112

NOTICE

This report was prepared as an account of Government sponsored work. Neither the United States, nor the National Aeronautics and Space Administration (NASA), nor any person acting on behalf of NASA:

A.) Makes any warranty or representation, expressed or implied, with respect to the accuracy, completeness, or usefulness of the information contained in this report, or that the use of any information, apparatus, method, or process disclosed in this report may not infringe privately owned rights; or

B.) Assumes any liabilities with respect to the use of, or for damages resulting from the use of any information, apparatus, method or process disclosed in this report.

As used above, "person acting on behalf of NASA" includes any employee or contractor of NASA, or employee of such contractor, to the extent that such employee or contractor of NASA, or employee of such contractor prepares, disseminates, or provides access to, any information pursuant to his employment or contract with NASA, or his employment with such contractor.

SOLAR ER 1473-15

FINAL REPORT

# LIQUID HYDROGEN FLEXIBLE DUCTING TECHNOLOGY

by

H. T. MISCHEL

Prepared for
NATIONAL AERONAUTICS AND SPACE ADMINISTRATION
30 JUNE 1966

CONTRACT NAS 8-11303

TECHNICAL MANAGEMENT
NASA MARSHALL SPACE FLIGHT CENTER
HUNTSVILLE, ALABAMA

MR. P. G. HAAS

SOLAR, A DIVISION OF INTERNATIONAL HARVESTER COMPANY
2200 PACIFIC HIGHWAY
SAN DIEGO, CALIFORNIA 92112

## FOREWORD

This report was prepared by Solar, a Division of International Harvester Company, San Diego, California, on NASA MSFC Contract NAS 8-11303. The work was performed under the direction of the Propulsion and Vehicle Engineering Division of the George C. Marshall Space Flight Center, Huntsville, Alabama. Mr. P. G. Haas was the contracting officer's technical representative.

The work presented herein began in June 1964 and was concluded in January 1966. Solar was the prime contractor and the effort was under the direction of the Aerospace Engineering Activity with Mr. H. T. Mischel as Program Manager. Major contributors to the program were Messrs. C. S. Martin, O. Abegg, and D. H. Betts of the design group; Mr. D. T. Shen, Stress Analysis; and Messrs. M. A. Gould and R. L. Neher, Testing. Mr. A. E. Maruniak contributed in providing project liaison services. Mr. D. T. Shen is particularly acknowledged for his contribution in the improvement of the bellows instability prediction method.

## ABSTRACT

12280

This report presents a description of the work performed in attempting to improve the state-of-the-art in the technology of liquid hydrogen flexible ducting for space flight vehicle applications.

The various components which make up a typical $LH_2$ flexible ducting system were segregated and individually studied for areas of possible improvement. Areas where information was lacking were designated for further analytical and empirical studies.

A boltless flange concept was developed and subjected to limited testing. Tubing was studied from a material substitution standpoint; and a flexible elbow concept was developed but not tested. Flexible joints were studied at length and a low-profile gimbal joint was fabricated and tested. Various materials and material combinations were tested to obtain data for designing spherical ball joints which could operate in a vacuum. An improved analytical method for predicting critical squirm pressure of bellows was verified in an extensive testing program. A non-rigid vacuum insulation was conceptualized but not tested.

Author

CONTENTS

ILLUSTRATIONS

ILLUSTRATIONS (Cont)

# 1

## INTRODUCTION

This is the final report of the work performed by Solar, a Division of International Harvester Company on the study to improve the state-of-the-art of the technology of flexible ducting for liquid hydrogen space flight vehicle applications.

The work was performed under National Aeronautics and Space Administration, George C. Marshall Space Flight Center, Huntsville, Alabama, Contract No. NAS 8-11303. The period during which this work was performed was June 1964 to January 1966.

The purpose of this program was to investigate flexible ducting designs and the properties of materials applicable to liquid hydrogen flight service. In addition, the program was to develop new and unique designs and determine their feasibility in this demanding realm of performance requirements.

All the study work was performed in pursuit of the following desirable system and components features:

- Improved reliability
- Increased fatigue resistance
- Increased bellows stability
- Increased fabricability
- Reduced weight
- Reduced deflection forces
- Reduced heat transfer

In designing a system for specific vehicle applications, the desired reliability consists of first, the establishment of a design which will demonstrate, analytically, adequate margins of safety to do the job; and second, the selection of basic design techniques which stipulate the use of predictable and consistently reliable materials and manufacturing processes. For the initial part of the study, the second reliability criteria was the measure against which component improvements were compared. For the actual development of hardware the entire concept of reliability was applied.

Seeking improved fatigue resistance required the consideration of the performance parameters which generate the cyclic stresses and the components which are the particular failure points in these regimes.

To seek increased bellows stability narrowed the discussion to studies of the flexible joints.

To seek reduced weight required the determination of those components which make up the largest percentage of the total system weight and those components which have complex systems of load distribution.

Reduced deflection forces were assumed for this study to require the consideration of only flexible joints; however, a concept for a flexible elbow is advanced.

For reduced heat transfer, this study was restricted to nonvacuum jacketed systems. For clarification it is necessary to state that this did not include nonvacuum systems but simply metallic, rigid vacuum jacket structures. It is postulated that the presence of a vacuum is essential to the achievement of the insulation quality required for liquid hydrogen flight service.

Increased fabricability was an underlying requirement for all the concepts which were generated during this study. Experience gained by Solar during the development of systems, such as the liquid hydrogen feed ducting for the Saturn S-II stage, formed this necessary discipline.

An evaluation of the various components which make up liquid hydrogen transfer lines was made early in the study. This evaluation was to determine those components which most affected the areas of improvement and, therefore, those which when improved would result in the greatest benefit. The following components are found in a typical liquid hydrogen flexible ducting system:

- Flanges
- Tubing
- Flexible joints
- Insulation (including associated equipment such as found in rigid vacuum jackets)

The study effort was devoted to each of these component types; however, the degree of study concentration was proportional to the total system improvement which would result from the improvements of each.

The study of flanges was aimed at weight reduction since the flanges make up a considerable portion of the weight of relatively short systems.

During this program a concept for a boltless flange, which appeared to offer the greatest benefits in the areas of weight reduction, was developed. A model was constructed and limited testing was performed.

For the sake of the study, the tubing was considered to be an area where considerable effort would result in the least gain. Admittedly, the weight of tubing forms a large percentage to the total weight of long systems. However, the simplicity of the structure precludes much gain from design improvements. Suggestions are offered for the use of new materials to afford weight reductions and increased fatigue resistance.

Flexible joints offer the most fertile area for improvement since the flexible joint, besides being one of the larger mass members of the system, essentially determines the deflection forces and the fatigue limits of the entire system under dynamic environments. The joints are also the source of greatest difficulty from the standpoint of fabrication. A considerable amount of effort during the study was devoted to investigating the gimbal joint as an assembly, and to improving the individual components which make up the gimbal joint.

Insulation was treated from a design standpoint, and a concept for a nonrigid vacuum jacket is advanced.

As previously mentioned, the major portion of the work was concentrated on the gimbal joint. Early in the program, design parameters for gimbal joint components of liquid hydrogen flexible systems were studied. Following this, a gimbal joint optimization study was performed resulting in three concepts for optimum gimbal joints. Of these, one gimbal joint was fabricated and tested.

Work was also performed in the area of bellows instability. This work resulted in the improvement of the analytical techniques which has greatly increased the accuracy of instability prediction methods. An extensive testing program was conducted to verify the improved method.

One of the suggested concepts, a ball joint, was analyzed to determine the design areas where information is insufficient for optimization purposes. The primary area was found to be the fatigue life and friction forces of surfaces in sliding contact in a vacuum. Therefore, to provide this necessary data, a test program was performed.

In summary, this program has permitted the attention of the investigator to focus on the individual subassemblies which make up a production system and the details of those subassemblies where improvements can be achieved. A new gimbal joint design has been demonstrated to achieve higher structural efficiency with much lighter weight. An improved analytical technique has been developed for predicting the critical instability pressure of bellows. A basis for permitting the designer a more definitive choice of materials and surface loadings for use in bellows-sealed ball joint designs has been developed. The program has by no means tapped all the avenues where improvements can be made and, in those areas investigated, has not reached the final degree of optimization that is possible. This report therefore presents the work, designs, test data, and comparisons to existing hardware that was developed during the program and also presents the conclusions reached by the investigators. Finally, this report presents the recommendations for future study which is felt to be the next logical step from this completed work.

# 2

## FLANGES

A concept for a boltless flange was developed as an outgrowth of NASA Industrial Applications Flash Sheet (identified as LEWIS-51), which depicted an approach to the attachment of end caps to tubes for creating inexpensive, high-pressure cryogenic bottles for laboratory use.

The concept involved the use of a low-melting temperature metal as a seal, and a structural attachment for joining flanges without the use of bolts. The joining concept is shown schematically in Figure 1. The advantages to the concept are:

- Boltless attachment, thereby eliminating the problems of flange orientation, bolt installation clearances, and bolt torque relaxation
- Reduced envelope and weight
- Accommodation of axial and angular misalignments
- Seals can be made regardless of flange face finishes
- Less costly

A design of the boltless flanges was made using the design requirements of Saturn S-II stage, 3-inch hydrogen tank pressurization system flanges for comparison. A set of these flanges have a total weight of 5.3 pounds without bolts and seals. The boltless flange set has a weight of 1.5 pounds or a reduction of 71 percent. The dimensions of these two flange sets are compared in Figure 2.

A set of flanges was fabricated and welded to tubing for experiments to optimize design details and the selection of low melting metal. The actual experimental flanges are shown in Figure 3.

Initial experiments used a solder which had been subjected to cryogenic testing by General Dynamics/Convair under Contract AF33(616)-7984. The solder used was a lead solder, commercially sold as Claude-Michael No. 20. This material did not appear to be successful in creating a seal since, without flux, it tended to ball up and contract in the cavity. The joint was again remade with Cerrobend, a low-melting,

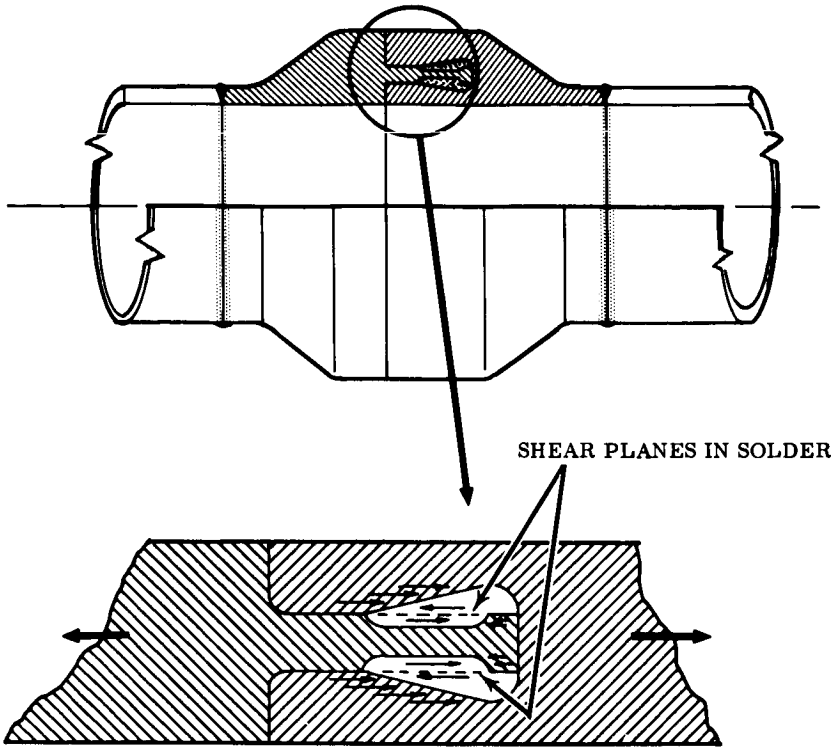


FIGURE 1. BOLTLESS FLANGE CONCEPT

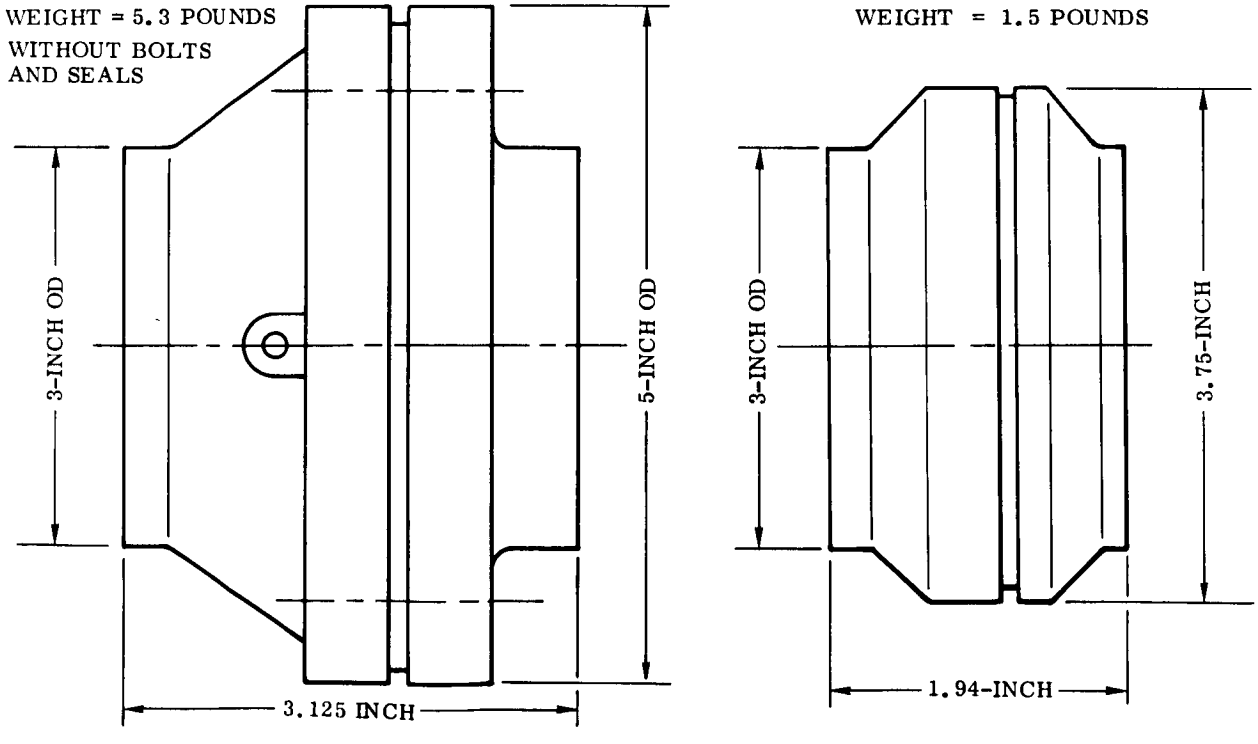


SATURN S-II $LH_2$ TANK PRESSURIZATION SYSTEM - 200 psi

3-INCH BOLTLESS FLANGE - 200 psi

FIGURE 2. DIMENSIONAL COMPARISON OF EXISTING AND BOLTLESS FLANGES

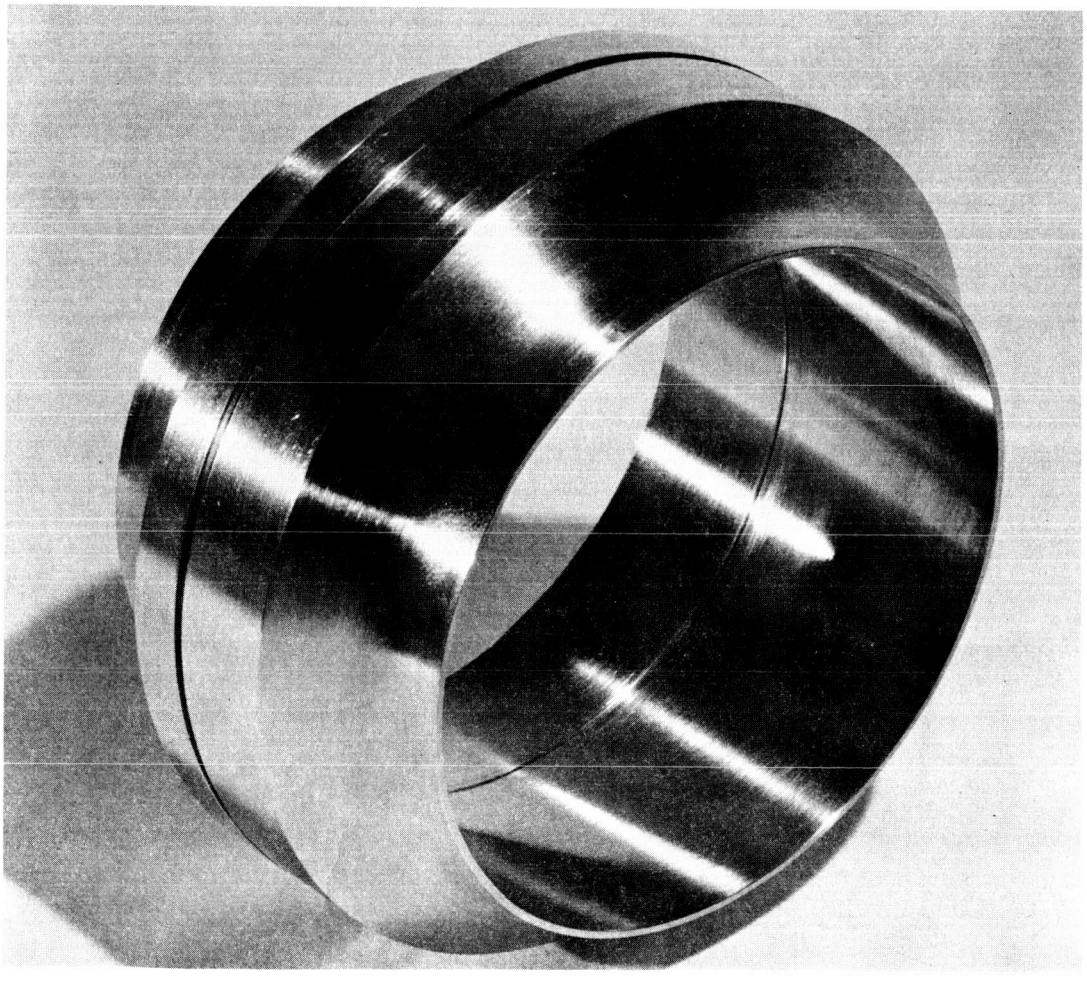

FIGURE 3. EXPERIMENTAL BOLTLESS FLANGE

lead-tin-antimony-bismuth alloy with a melting temperature below boiling water. This Cerrobend alloy is currently being used by NASA-LeRC in their pressure bottle applications. This joint did seal at low pressures, but leaked at approximately 50 psi. Pressurization to 150 psi verified the strength of the joint, however.

Investigation of the joint indicated the need for changes in the groove design to prevent entrapment of air and to determine the complete filling of the cavity with the liquid metal.

While it was generally agreed that the concept was sound, subsequent work was discontinued due to the inability of the solder-type materials to accept temperature cycling. Further development would necessitate extensive experimentation with various other media, such as nonmetallics, which this program could not support.

# 3

## TUBING

As a result of their simplicity as structures, the tubing components of ducts offered the fewest avenues of improvement over those currently used. The most flexible area of tubing, with respect to changes, is the basic materials of construction. An obvious improvement would be to utilize higher strength-to-density materials to achieve weight savings. However, experience has indicated that the substitution might not be as simple as it sounds. For example, the dynamic characteristics of various materials, i.e., the amounts of internal damping or energy absorption which can be realized is not well understood and requires a separate analytical and empirical study. The practical problems of joining and fabrication of adjacent flexible components of the same materials must be considered, but are not unsolvable.

Coincident with this program was another in which a materials survey was made. The purpose of that program was to solve the problems of fabricating bellows of lighter materials such as aluminum and titanium alloys.

Two materials are presently in use for high-pressure and low-pressure systems. Corrosion resistant stainless steels, primarily Type 321, is the material used in low-pressure systems where practical handling and rigidity considerations preclude wall thicknesses based wholly on hoop strength and low bending load considerations. Inconel 718, a nickel-base, age hardenable, material is the choice for high-pressure applications where hoop stresses are the deciding criteria.

In future ducting systems for $LH_2$ service, it can be envisioned that low-pressure applications can be handled by aluminum tubing which, for the same wall thickness determined by the same considerations as Type 321 stainless steel applications, would result in ratio of densities weight reduction. High-pressure service may be handled by titanium alloy (Ti-5Al-2.5Sn) which exhibits adequate properties at -423 F.

During the program, a concept for a flexible elbow was advanced. In actuality, the concept involved the entire ducting system in that a series of flexible tubing elbows replace flexible joints. The flexible elbows are basically ovalized, multilayer tubing

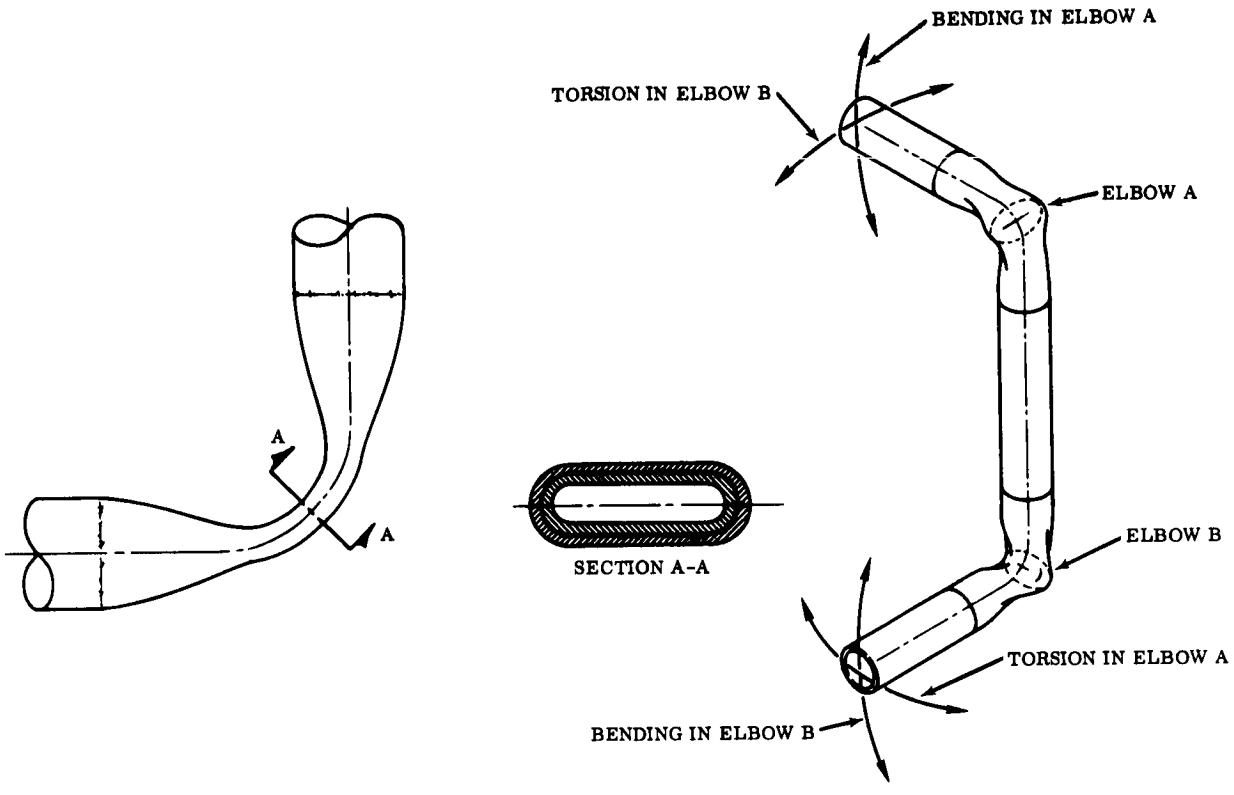


FIGURE 4. FLEXIBLE ELBOW CONCEPT

elbows as shown in Figure 4. Multilayering and ovalizing reduces deflection forces about axis A-A. Multilayering also retains the pressure carrying capability of the system. Resistance to torsional deflections is also reduced in this structure.

The multilayering achieves the low deflection forces in a manner similar to multilayered, or multiply bellows. This is accomplished by substituting thinner bending members with zero shear interfaces for thick members with relatively high section moduli. Ovalizing reduces the overall section modulus and lower resistance to further flattening is obtained by the multilayered radii at the neutral axis A-A.

As shown in Figure 4, an "S" shaped duct with two elbows capable of bending and twisting could replace a three gimbal system. The flat plate at the inside and outside elbow surfaces appear to present problems in resisting bowing due to internal pressure. Lateral stiffening members could solve this problem.

Time and funding did not permit further efforts in pursuit of this concept and its presentation in this work is based upon idealizations. The possibilities of benefits to ducting systems warrants its mention, however, and the recommendation for further investigation.

# 4

## FLEXIBLE JOINTS

Flexible joints offer the most fertile area for improvement with the greatest possible degree of success. The type of flexible joint most commonly used in space vehicle ducting is the bellows-sealed, gimbal-type joint. The details which make up a gimbal joint (Fig. 5) are a bellows seal, two end flanges with integral lugs, a gimbal ring, and four rotational pins. The primary use of the gimbal joint is to provide a point of flexibility in the ducting system. Flexibility is necessary for accepting relative motion between the end flanges caused by deflections in the vehicle structure or the duct system itself. These motions can be induced by the dynamic environment or by thermal changes. The standard gimbal joint is heavy with respect to the tubular portions of the line since, in order to provide flexibility, the transmission of loads across the bellows is complex. This complexity is the result of point loadings of the gimbal flanges and the gimbal ring. An additional function of the gimbal joint is to provide, by friction in the pins, a degree of damping for energy absorption during dynamic conditions.

Optimizing this flexible member can be accomplished by two approaches:

- Studying the deficiencies of the existing gimbal joint design methods with the goal of improving this basic design.
- Generating new concepts of flexible joints to replace the gimbal type universal joint.

This study did both since the benefits to be gained by both methods warranted the effort.

The existing gimbal-type universal joint has been the subject of considerable refinement over the years and its advantages as a flexible joint are attested to by its use in practically all ducting systems found on space vehicles. The optimization study

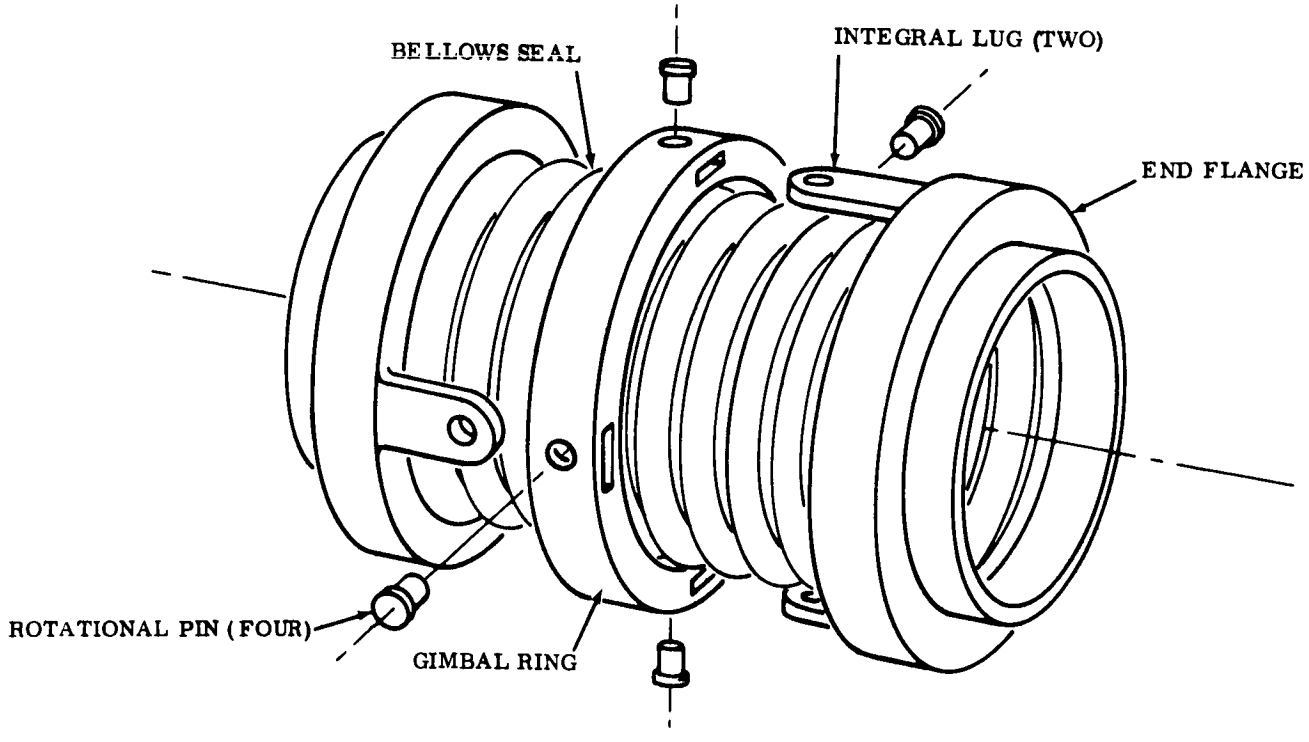


FIGURE 5. TYPICAL GIMBAL JOINT

of this joint was performed in a logical manner with the guiding principle being to investigate:

- The parametric considerations which govern the design of each of the details which make up the assembly.
- The interrelationship of each detail and subassembly with regard to how each affects the design of the others.

## 4.1 DESIGN CONSIDERATIONS FOR GIMBAL JOINTS

The design considerations for gimbal rings are:

- The inside diameter of the ring is controlled by the outside diameter of the bellows and the required amount of angulation.
- The outside diameter of the ring is determined by strength and rigidity requirements and envelope limitations stemming from the proximity of other structure or equipment in the vehicle installation.
- The width of the ring has to provide sufficient material to accommodate the holes for the pins with adequate edge distance. The structural requirements for resisting bending and torsion stresses must be adequately provided for in gimbal ring width.

The design considerations for gimbal flanges are:

- The inside diameter of the flange is controlled by the inside diameter of the duct and the bellows.
- The outside diameter of the flange is controlled by the position of the lugs which have to mate with the gimbal ring. Thus, the outside diameter of the gimbal ring governs the outside diameter of the flange.
- The width of the flange lugs is controlled by structural considerations and must provide sufficient material to accommodate the gimbal pins.
- The length of the flange lugs is governed by envelope, structural, and angulation requirements. The greater the angulation the longer the lugs.
- The thickness of the flange lugs is governed by the structural and envelope requirements.

The design parameters for gimbal bellows are:

- The inside diameter is controlled by the inside diameter of the duct.
- The outside diameter of the bellows is controlled by spring rate, angular deflection, structural, and envelope requirements.
- The length of the bellows is controlled by spring rate, angular deflection, structural, and envelope requirements.

The design parameters for gimbal pins are:

- The diameter of the pin is governed by structural and envelope requirements. The pin must provide a large enough bearing area and be structurally adequate to resist shear loads transmitted through the bellows and gimbal ring.
- The length of the pin is governed by gimbal ring and clevis lug thickness.

The gimbal ring weight varies as the square of the ring diameter. When the gimbal ring diameter is increased the following equation applies:

$$W = w(D^2 - d^2)$$

where: $W$ = new weight

$w$ = existing weight

$D$ = new gimbal ring diameter

$d$ = existing gimbal ring diameter

The load the gimbal ring has to withstand is affected by the mean diameter of the bellows which determines the effective pressure area. Therefore, the weight of the gimbal ring is also affected by the bellows diameter.

When the bellows mean diameter is increased, the pressure induced load increases to:

$$F = f(D_m^2 - d_m^2)$$

where: $F$ = new load
$f$ = existing load
$D_m$ = new mean diameter
$d_m$ = existing mean diameter

This increased load affects the torsional stress ($\sigma_r$) in the gimbal ring:

$$\sigma_r = \frac{0.207\ Pr}{\alpha b h^2} \quad \text{(approx)}$$

where: $P$ = load per pin = $f/2$
$r$ = mean radius
$\alpha$ = shape coefficient
$b$ = width of gimbal ring
$h$ = thickness of gimbal ring

An increase in the bellows mean diameter therefore would increase P in the torsion formula by $(D_m^2 - d_m^2)$, resulting in an increase in the ring torsional stress. To maintain the same torsional stress, the denominator would have to be multipled by $(D_m^2 - d_m^2)$. Since "b" or "h" can be affected by $(D_m^2 - d_m^2)$, we choose the thickness "h" from the above expression for $\sigma_r$. This involves the least increase in weight and envelope size. Thus, the new "h" would be equal to:

$$\sqrt{h^2 (D_m^2 - d_m^2)}$$

The effect of increasing the mean diameter of the bellows on the bending stress ($\sigma_b$) in the ring must also be considered.

$$\sigma_b = \frac{Pr}{2\ (I/C)}$$

where: $P$ = load per pin = $f/2$
$R$ = mean radius
$I/C$ = section modulus = $\frac{hb^2}{6}$

The increased pressure load due to the increased bellows mean diameter would result in P being multiplied by $(D_m^2 - d_m^2)$ with a corresponding increase in ring bending stress. To maintain the same ring bending stress, the denominator must also be multipled by the same value. In this condition, we have the reverse of the torsional stress situation and must consider the width "b" as the parameter affected. Thus the new "b" would equal $\sqrt{b^2 (D_m^2 - d_m^2)}$.

Thus, in comparing the torsion and the bending condition, a different shape of gimbal ring would evolve to meet each condition. The width would be proportionally more than the thickness for bending, and the reverse would be true for torsion. The best compromise for torsion, bending, and weight consideration is somewhere between the optimum shapes for each.

## 4.2 DOUBLE-SHEAR AND SINGLE-SHEAR GIMBAL JOINTS

The double-shear gimbal appears favorable from the point of view of distribution of shear load on the pins and ease of assembly. To offset these advantages, the single-shear gimbal offers a smaller envelope, less weight, and less complex machining, with resultant lower cost. A disadvantage of the single-shear approach is pin support. It is difficult to make a rigid attachment when the pin is being supported at one end. The weld is much more critical and subject to proportionally higher loads than the pin weld in a double-shear assembly. There are problems in installing the pin and welding it in position. The diameter of the pin must be larger to withstand the higher shear load.

## 4.3 THE EFFECT OF ANGULATION

In comparing the 8-inch diameter gimbals for the liquid hydrogen and liquid oxygen feedlines for the Saturn S-II stage, it is interesting to note how a change in one design requirement drastically affects the weight. The operating considerations for both of these gimbals are very similar. The one condition that is considerably different is the amount of angulation required. The liquid hydrogen gimbal was required to angulate through a total angle of 12 degrees and the liquid oxygen gimbal was required to angulate through a total angle of 18 degrees. Because of this difference in angulation (requiring greater clearances), the weight of the gimbal had to be increased from 11.77 to 15.17 pounds (approximately 30 percent weight increase). The weight penalty for ±3 degrees is 3.40 pounds.

## 4.4 PROBLEMS ASSOCIATED WITH ANGULATION OF GIMBALS AT 45 DEGREES TO THE PINS

When a gimbal assembly is angulated in a plane at 45 degrees to a plane through the pin center lines, a torsional stress is imposed on the bellows. Because of pin clearance and small deflection of gimbal components, this torsion is not apparent in most gimbals which do not exceed 9 degrees angulation in a 45-degree plane. Consequently, this torsion has not constituted a problem in designing gimbals which do not have excessive angulation. However, when angulation is required in excess of 9 degrees in the 45-degree plane, the torsional stress rapidly increases and could have catastrophic consequences if not provided for in the gimbal design. The lugs would also be subjected to high torsional stresses which would be transmitted to the duct.

If an elbow or short straight section were adjacent to the gimbal, severe stresses may be imposed with resultant buckling. Particular attention should be given to the location of gimbals in the line and in gimbal orientation to avoid excessive angulation in a plane at 45 degrees to the pins.

## 4.5 GIMBAL JOINT OPTIMIZATION STUDY

With this understanding of how the design parameters affect the individual gimbal joint details, a study was made of an existing gimbal joint with the goal being to optimize the design. This work was a three phase effort consisting of:

- Optimizing the joint by concentrating on the gimbal ring and ring-lug attachment since the ring is the heaviest single member in the joint
- Investigating the possible weight reduction by simply changing materials
- Developing new flexible joint concepts to replace the existing gimbal joint

### 4.5.1 Phase I - Gimbal Ring and Attachment Optimization

The gimbal joint to which this optimization is being compared contains a double-shear, ring-pin-lug attachment. The double-shear attachment is desirable for easing the pin and pin attachment problems. Double-shear also loads the ring as shown below:

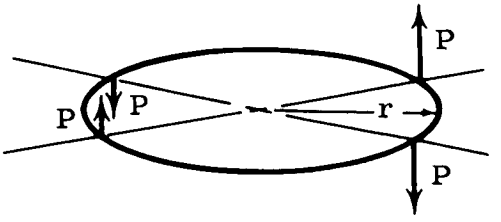


where: P = 1/2 pressure plug load

These loads produce bending and torsional moments in a ring which varies from zero to a maximum and which are out of phase by 45 degrees. These moments are shown by the expressions:

$$\text{Maximum bending moment} = \frac{Pr}{2} \text{ (in plane of pins)}$$

$$\text{Maximum torsional moment} = \frac{Pr(0.414)}{2} \text{ (at a 45-degree angle to plane of pins)}$$

If the ring can be loaded eccentrically such as shown below, additional moments occur.

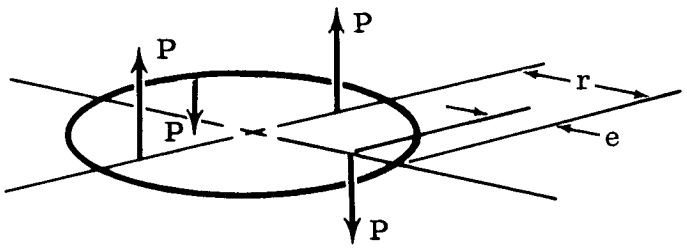


These moments are expressed as:

$$\text{Maximum bending moment}_e = \frac{-Pr}{2} \epsilon \text{ (at pins)}$$

$$(\text{torsional moment})_e = \frac{+Pr}{2} \epsilon \text{ (at pins)}$$

$$= \frac{-Pr}{2} \epsilon \sqrt{2} \text{ (at a 45-degree angle to the pins)}$$

Positive moments relate to those shown in the original case where:

$$\epsilon = \frac{e}{r} \text{ and } \epsilon < 0 \text{ if e is outside ring}$$

$$\epsilon > 0 \text{ if e is inside ring}$$

Summing these moments along the circumference of the ring yields moment distributions such as those shown in Figure 6. Loading the ring with an external eccentricity would induce higher ring stresses; therefore, it is advantageous to provide an eccentric load which is applied inside the ring. The attainment of the beneficial

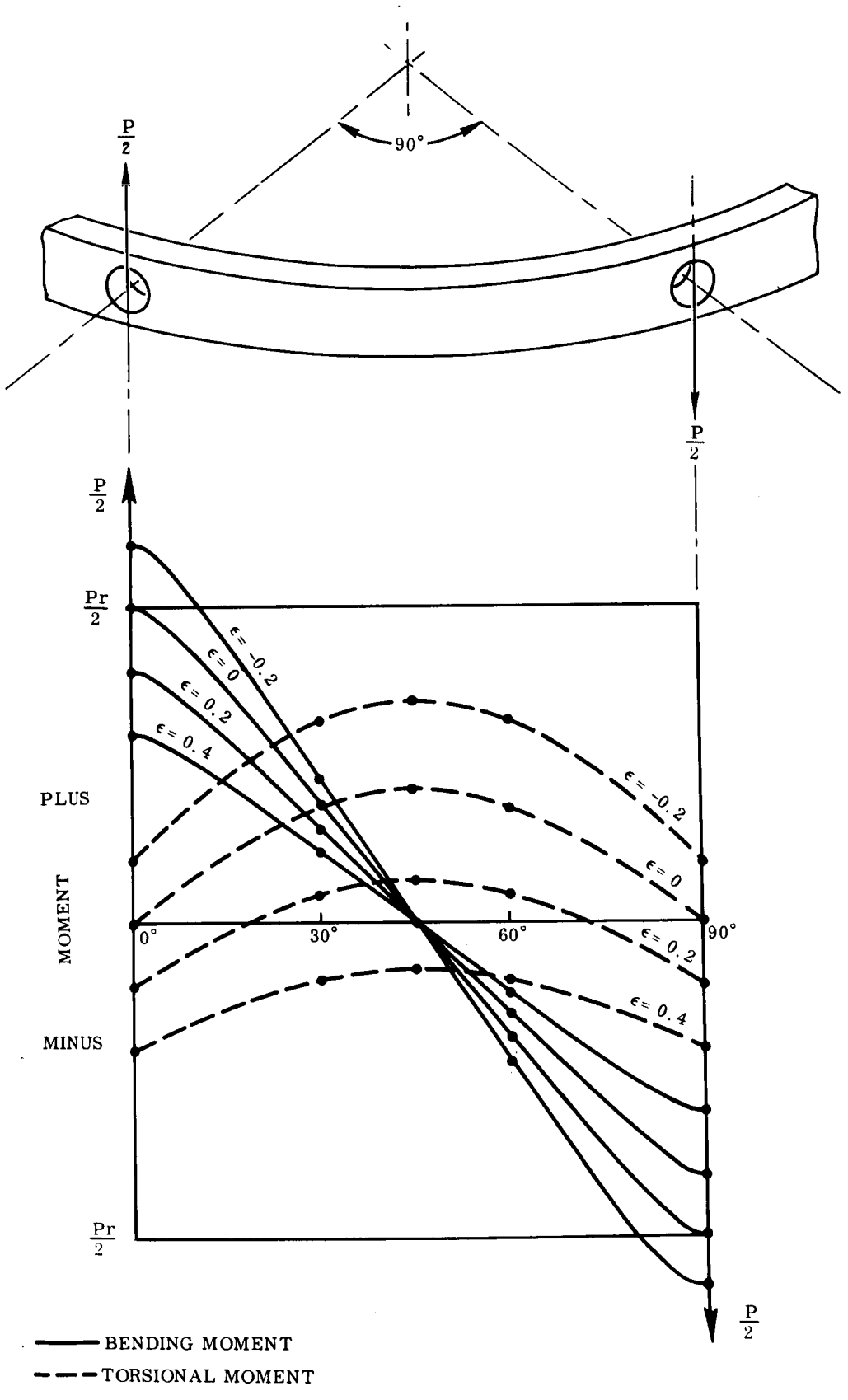


FIGURE 6. MOMENT DISTRIBUTION IN A GIMBAL RING

effects of this eccentric loading requires lug designs which do not resist the development of these moments. In other words, the lug attachment should be maximized for tensile loads and remain flexible to lateral loading and rotation. Therefore, the gimbal lug should, in theory, be nothing more than a plate or block heavy enough to attach the pin, or to reduce the bearing stresses induced by the pin during cycling and pressure loading. This plate or block would in turn be attached to the lug flange by a thin strap.

This simplified approach does not take into account the lateral load components which occur during angulation and vibration. Modifying the concept to accept this yields the idea of a lateral restraining device which is attached to the duct at more than 45 degrees to the plane of the pins and to the lug plate as shown in the following sketch.

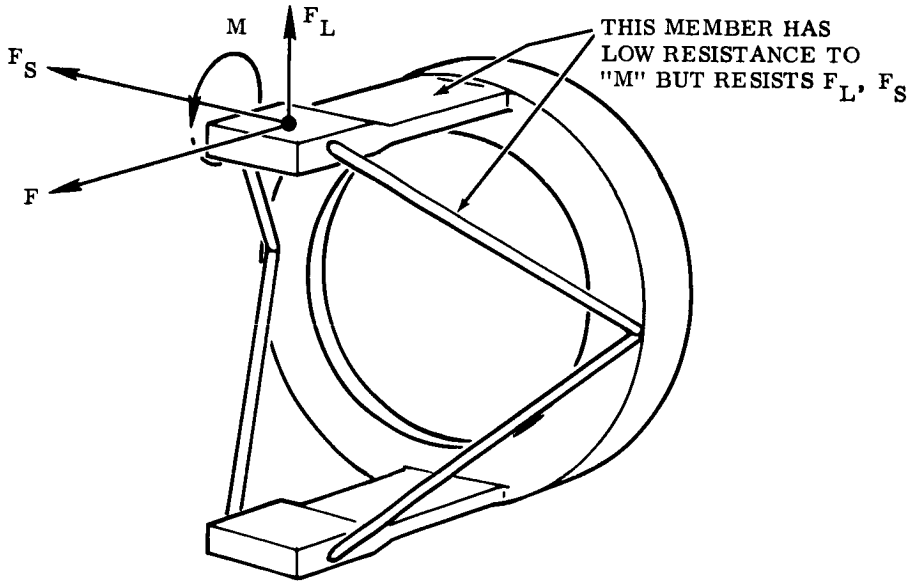


The optimum cross sectional shape of the ring would be a hollow box beam member from practical as well as strength considerations.

Since the ring need not be attached to the lug, a freer choice of materials is available. The use of titanium is recommended because of its high strength-to-density ratio. Sufficient sections can be maintained to overcome the low modulus of titanium with regard to the stainless steel or nickel-base alloys commonly used today.

4.5.2 Phase II - Retaining the Basic Gimbal Concept and Changing Materials

With the assumption that the bellows can be fabricated from a titanium alloy (Ti-5Al-2.5Sn), and investigating the stresses developed in the existing Inconel 718 design, no change in convolution geometry was necessary. Therefore, the weight reduction is simply a function of the ratio of densities.

Assuming no other changes in the shapes of the other gimbal components, their weight reduction is a function of the ratio of material densities which is:

$$\frac{\text{Titanium}}{\text{Inconel 718}} = 0.58$$

This assumption is felt to be valid since the yield strength of the titanium alloy under consideration is reported to be as high as Inconel 718 at cryogenic temperatures.

4.5.3 Phase III - New Flexible Joint Concepts

Low-Profile Gimbal Joint

Reducing the gimbal ring diameter results in a direct weight reduction. Normally, the gimbal ring of externally structured gimbal joints must have an inside diameter large enough to clear the bellows during angulation. The low-profile gimbal joint has the bellows divided into two segments (dumbbell-shape), the space between consisting of line-size tubing. This space is utilized for reducing the gimbal ring diameter.

The original concept considered a spherical surface in the space between the bellows segments. The spherical surface had its center at the center of rotation of the joint and was intended to suppress bellows instability by restricting lateral translation of the bellows centerline. A motion study revealed that the intermediate tube, if restrained to rotation only about the gimbal center, would cause excessive offset deflections in the bellows segments.

This flexible joint was chosen for further study and reduction to hardware. Since bellows fatigue life was not in question (the fatigue capability of the bellows is capable of being varied by design with little or no change in structure), only ultimate strength tests were performed on this unit. The joint dimensions are shown in Figure 7 and the actual joint is shown in Figure 8. The material of the joint is Type 321 stainless steel, including the bellows; the gimbal ring is titanium alloy, Ti-6Al-4V; and the pins are Haynes Alloy 25 (L605). The design was compared to ar

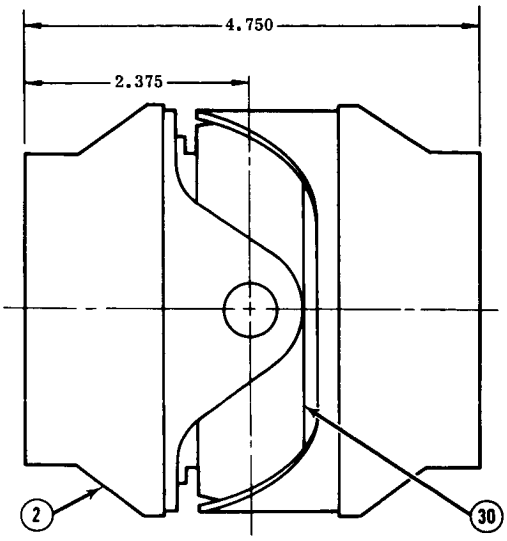


(-40) GIMBAL ASSEMBLY 3.00-INCH DIAMETER
(-30) BELLOWS AND RING ASSEMBLY (ONE REQUIRED)
(- 2) FLANGE (TWO REQUIRED)

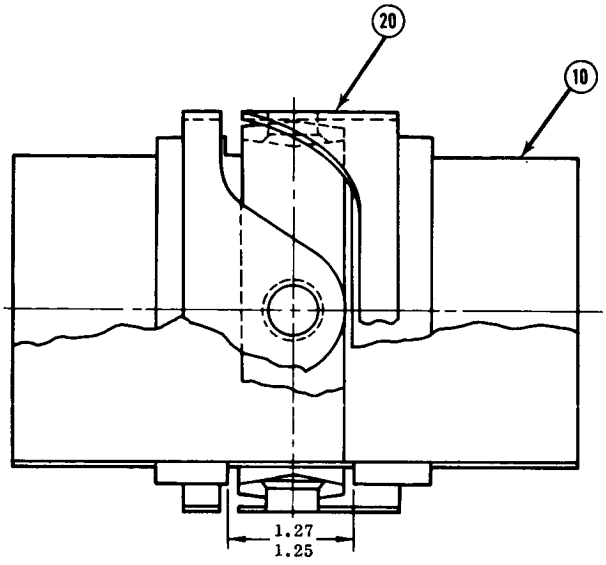


(-30) BELLOWS AND RING ASSEMBLY (ONE REQUIRED)
(-10) BELLOWS ASSEMBLY (TWO REQUIRED)
(-20) RING AND FORK ASSEMBLY (ONE REQUIRED)

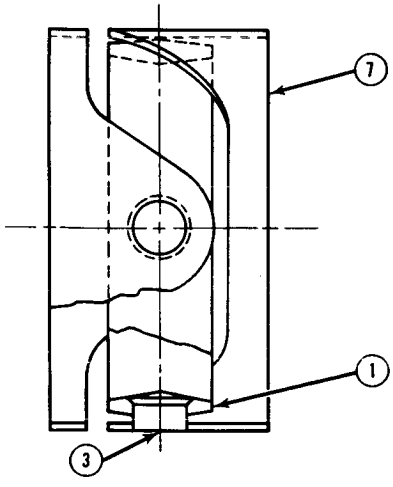


(-20) RING AND FORK ASSEMBLY (ONE REQUIRED)
(- 1) RING (ONE REQUIRED)
(- 3) PIN (FOUR REQUIRED)
(- 7) FORK (TWO REQUIRED)

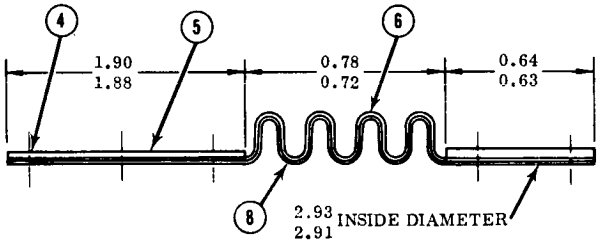


(-10) BELLOWS ASSEMBLY (TWO REQUIRED)
2 PLY OF 0.008-INCH CRES 321
4 CONVOLUTIONS
OD = ID +0.58 -0.48
(- 4) BELLOWS, DOUBLER END, MATERIAL:
0.020-INCH THICK CRES 321 (ONE REQUIRED)
(- 5) DOUBLER, CENTER, MATERIAL:
0.040-INCH THICK CRES 321 (ONE REQUIRED)
(- 6) BELLOW CONE (ONE REQUIRED)
(- 8) BELLOW CONE (ONE REQUIRED)

FIGURE 7. SCHEMATIC OF LOW-PROFILE GIMBAL JOINT (Sheet 1 of 2)

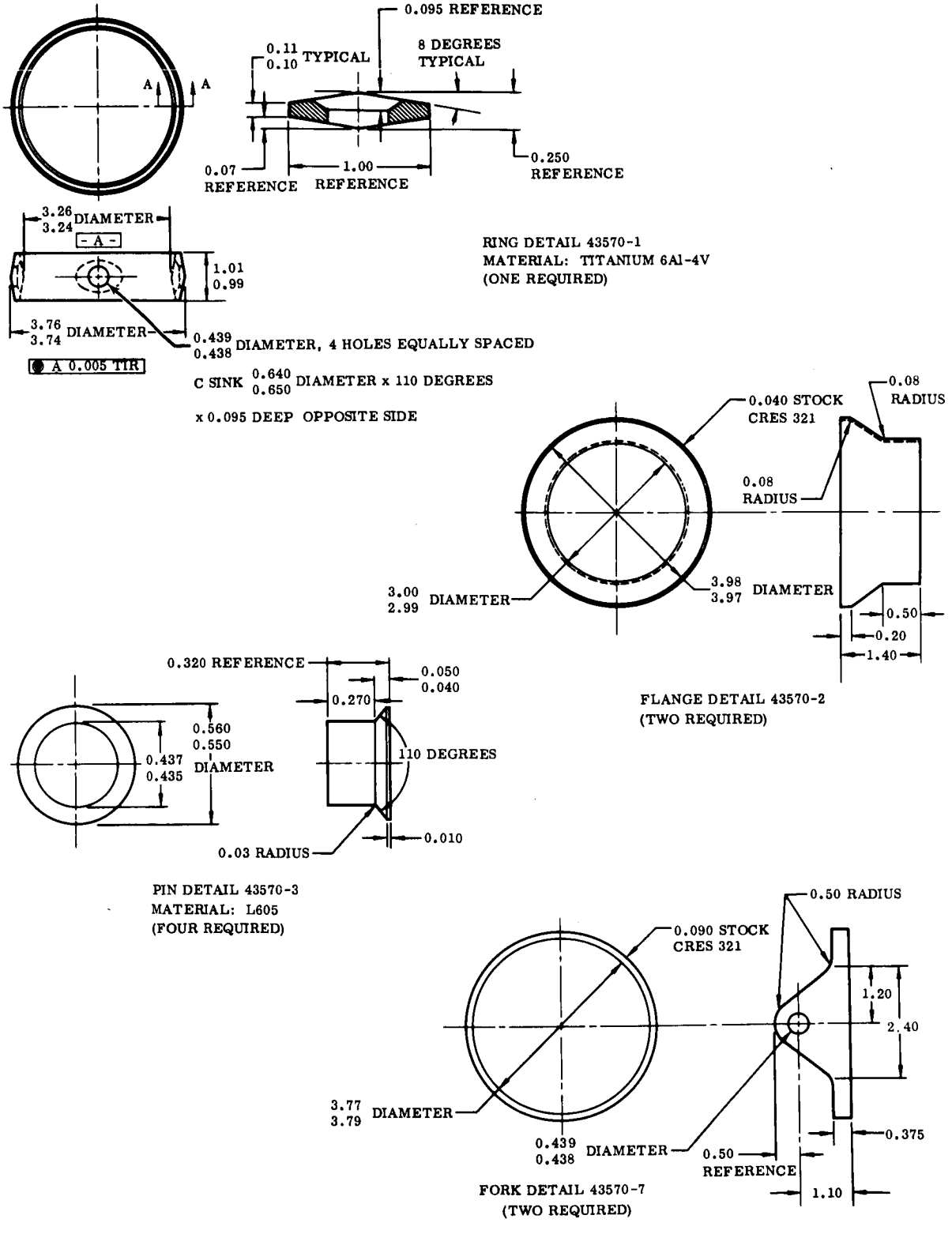


FIGURE 7. SCHEMATIC OF LOW-PROFILE GIMBAL JOINT (Sheet 2 of 2)

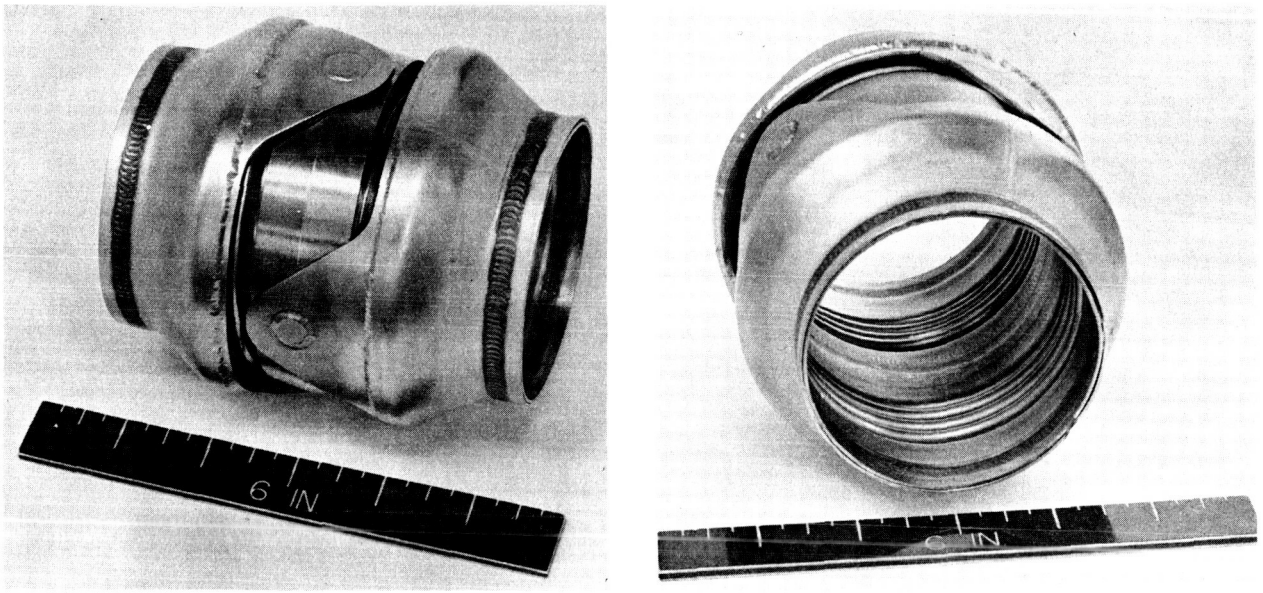


FIGURE 8. LOW-PROFILE GIMBAL JOINT

existing gimbal joint now being used on the Saturn S-1C stage fuel pressurization system. The existing gimbal joint was fabricated entirely from Inconel 718 and weighed approximately 4.5 pounds while the low profile joint weighed 1.7 pounds.

Admittedly, the low-profile design achieved part of its weight reduction by a reduction in margins of safety. These reductions, however, were not to levels below design ground-rules. Specifically, the gimbal ring margin of safety in torsion was reduced until the torsional stress was equal to ultimate at design burst pressure, whereas the Saturn S-IC gimbal joint ring did not yield at burst pressure. By this method, small increases in ring weight greatly increase ring section modulus and therefore the margin of safety. Also, the low-profile gimbal was not subjected to dynamic tests as an integral part of a ducting system. This dynamic environment however, is not expected to affect the assumptions since the decreased mass of the new design would contribute to lower system responses.

The basic weight reduction has been achieved by:

- The small gimbal ring
- Utilizing titanium for the gimbal ring material
- The reduced eccentricity in the lug-to-tube load path as a result of the smaller ring
- The use of a thin cone as a lug flange for carrying the load from the lug to the tube as opposed to a machined flange which is essentially a thick, flat plate

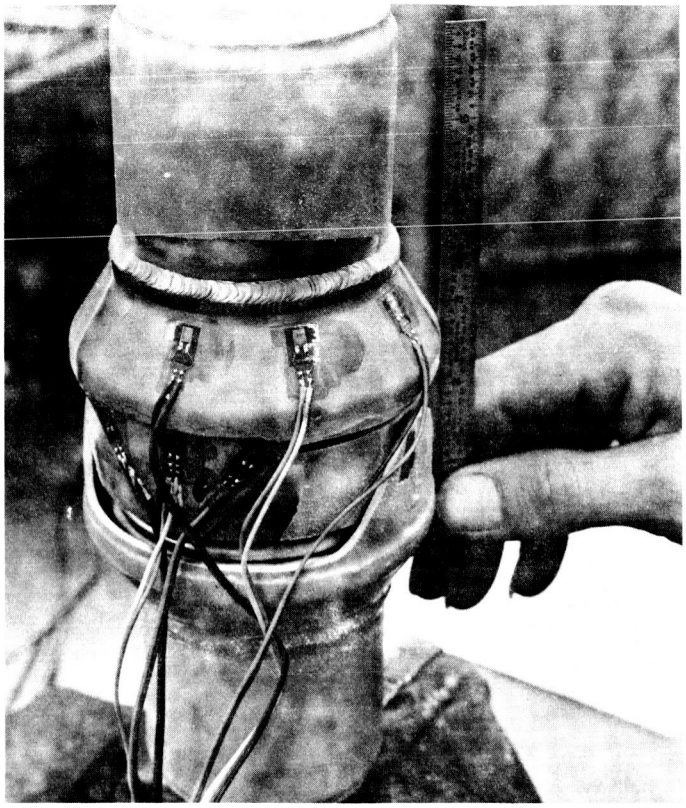

FIGURE 9.

INSTRUMENTATION FOR ULTIMATE STRENGTH TESTING OF THE LOW-PROFILE GIMBAL JOINT

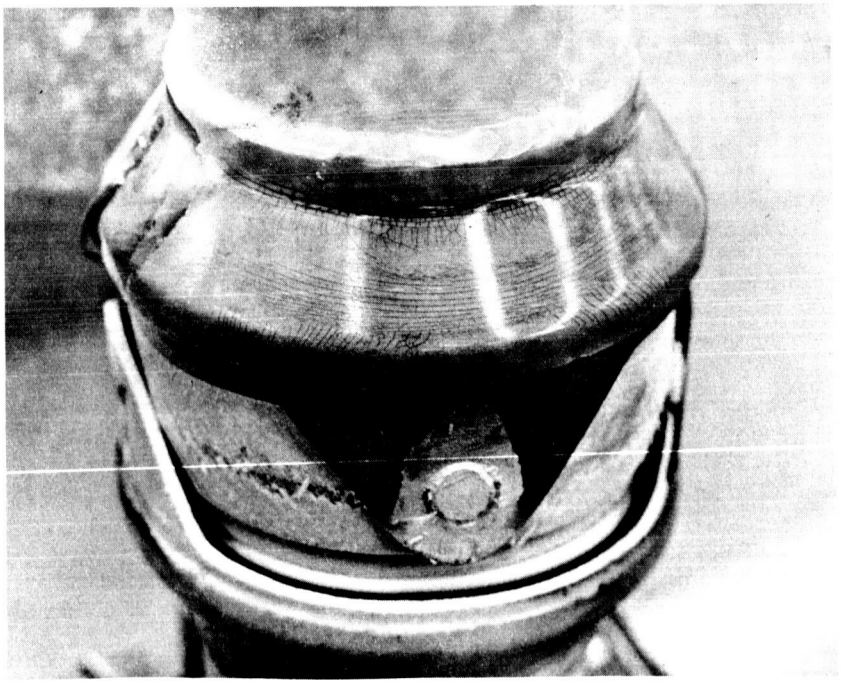

FIGURE 10. STRESS MEASUREMENT WITH STRESS-COAT LACQUER

The ultimate strength test consisted of pressurizing the flexible joint internally to failure. Six strain gages were fixed to the joint; three located on the lug adjacent to the lug-to-cone attachment weld, and three located on the cone itself (Fig. 9). The location of the strain gages was intended to determine the ability of the light lug and cone combination to distribute the concentrated pin load into the duct wall over a large part of the duct circumference. The unit was also coated with stress-coat lacquer to observe the strain which was occurring in all the gimbal members (Fig. 10). Failure occurred at 780 psig by failure of the pin-to-lug welds resulting in separation of the gimbal structure (Fig. 11). The failure is attributed to the torsional/bending failure of the titanium gimbal ring. The distortion of the lug and ultimate tearout of the pin from the lug was caused by the rotation of the ring at the pin.

Bellows squirm occurred between 550 and 600 psig. An instability analysis, using the method developed during the program, predicted that squirm would occur at 572 psig. At 650 psig, the convolution adjacent to the gimbal ring contacted the ring edge and continued thereafter to fold itself around the ring.

In summation, the gimbal structure (except for the ring) exhibited strengths in excess of that required for the burst requirement. The failure of the ring indicates an area where improvement can be achieved by a minor change if uprating of the gimbal is desired. For example, if the ring rigidity can be increased, thereby avoiding lug distortion, the cone appears to be capable of carrying additional loads. Increased rigidity of the ring can be gained by small increases in ring width. If additional strength is desired, another ring can be installed on the outside of the lug with no changes to the lug and cone designs; however, some modifications to the pin attachment would be required.

Four-Lug Gimbal Joint

The concept shown in Figure 12 is primarily intended for large diameter flexible joints where achieving rigidity in lug flanges, subjected to the standard two-point loading, offers weight penalties which can be excessive. The joint consists of two concentric gimbal rings, each carrying half the end load. Each end-flange contains four lugs, one set pinned to the outer rings and the other set in a plane 90-degrees from the plane of the first set and pinned to the inner ring. Each flange is identical except rotated 90-degrees from the other. In essence, two gimbal joints are created which are coincident with each other. Each lug carries one-fourth the end plug load;

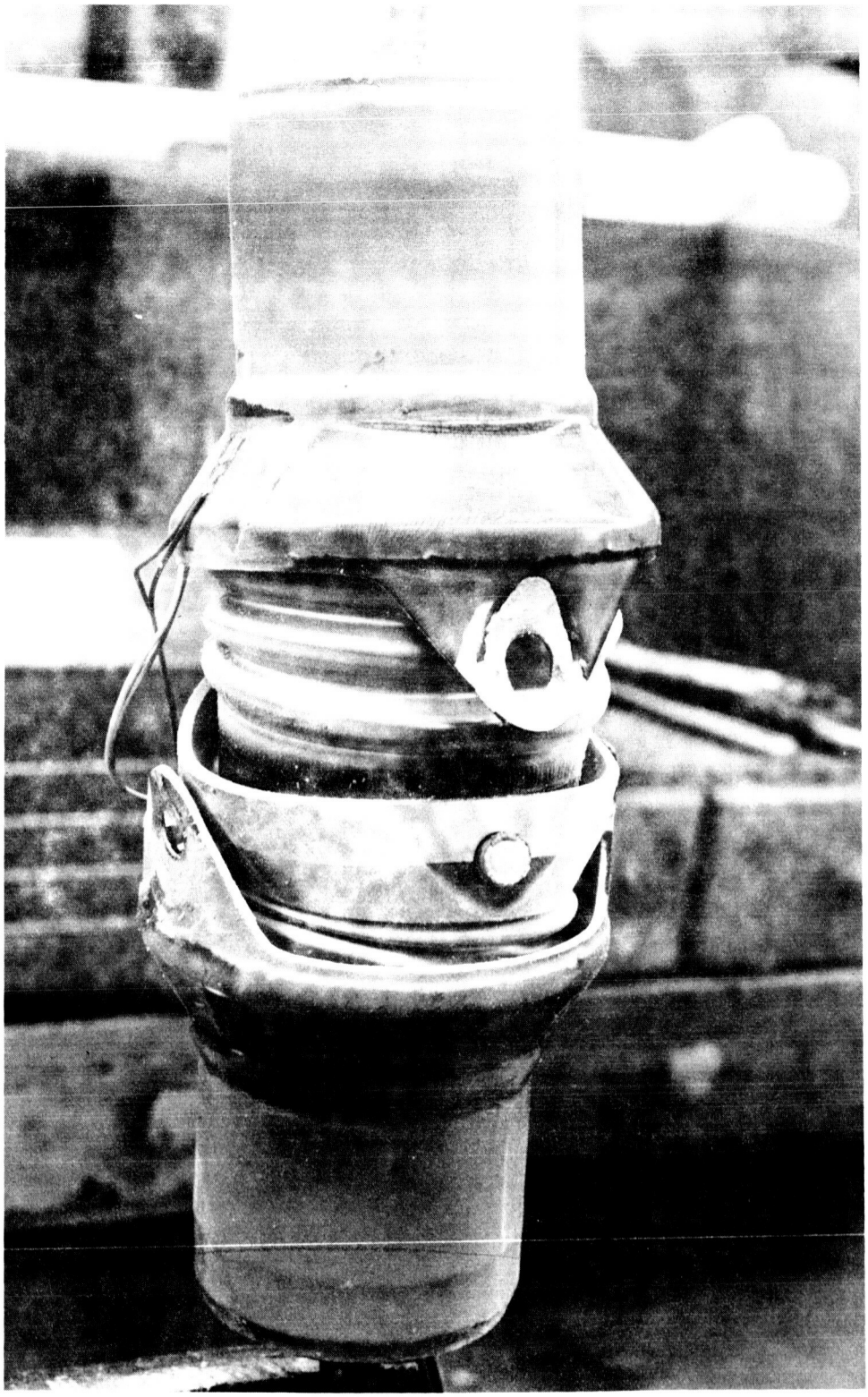

FIGURE 11. FAILURE OF THE LOW-PROFILE GIMBAL JOINT

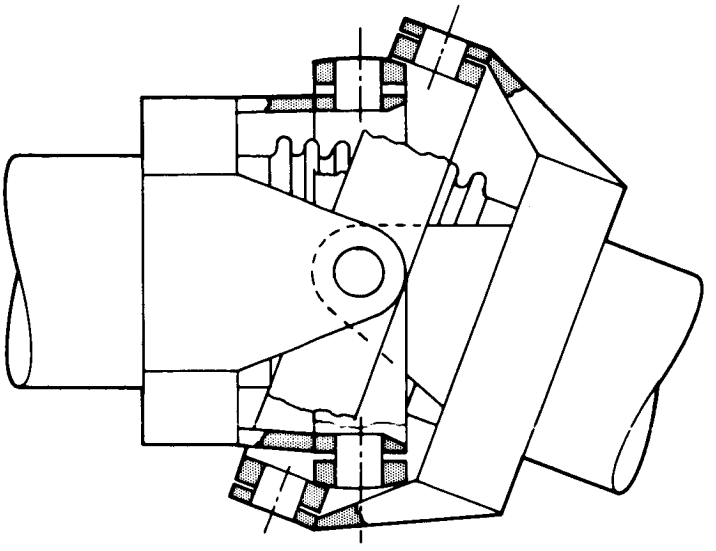

FIGURE 12. FOUR-LUG GIMBAL JOINT CONCEPT

the total load, therefore, being distributed into the flange at four points (every 90 degrees). Conservative analyses indicate that the section modulus of the four-lug flange can be reduced to approximately one-half that of a two-lug flange for the same diameter and working pressure.

Bellows-Sealed Ball Joints

The concept of the bellows-sealed ball joint was advanced in various forms. Basically, this joint consists of a light shell restraining structure with angular deflections permitted by rotational surfaces in bearing contact. Most concepts envisioned spherical bearing surfaces, while one concept puts forth mutually perpendicular cylindrical surfaces (Fig. 13).

Advantages of the ball joint are:

- Lighter weight
- No induced torque in bellows similar to that produced by gimbal joints
- Less parts; therefore, more reliable and lower cost
- Uniformly distributed loads across the joint

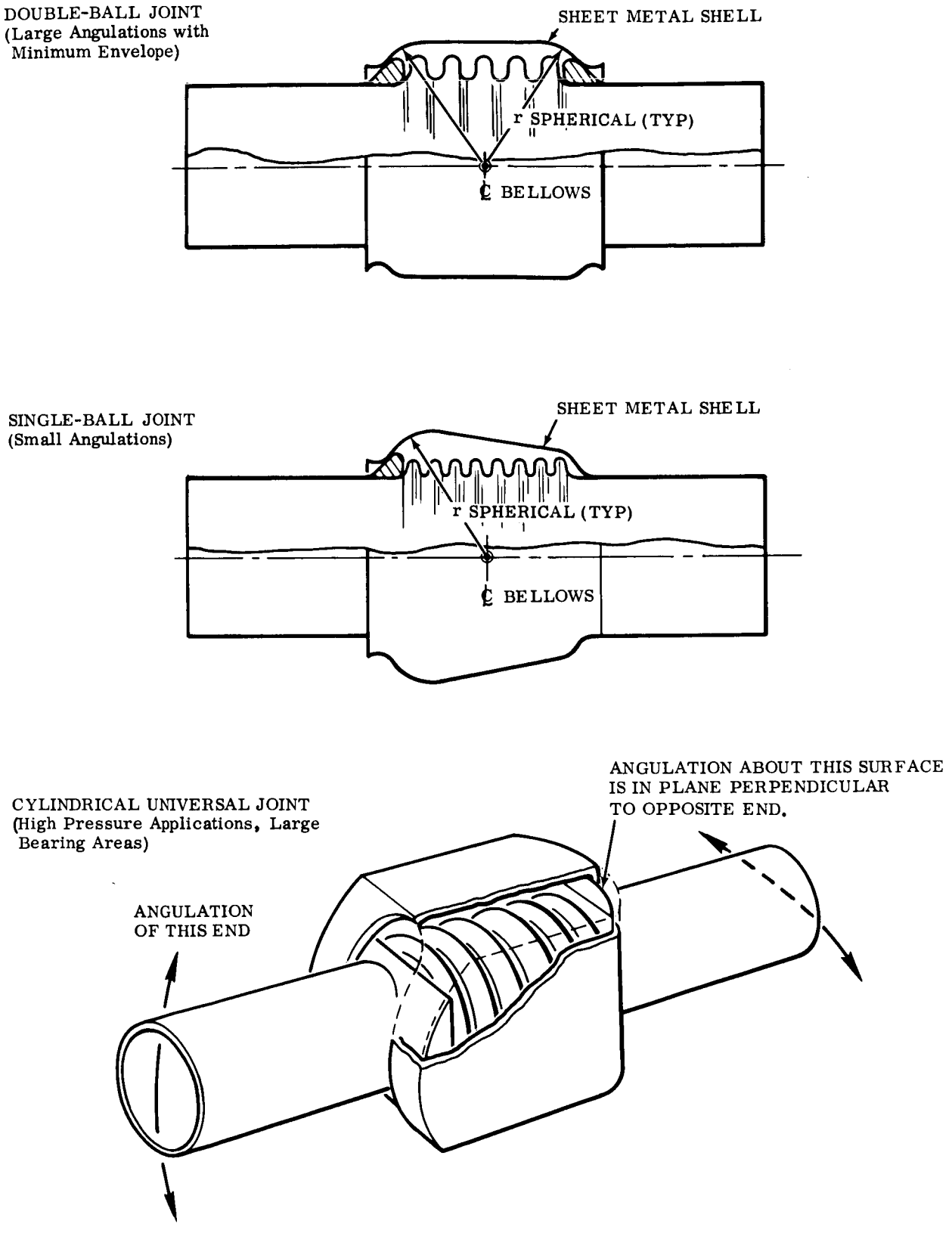


FIGURE 13. BALL JOINT CONCEPTS

Disadvantages are:

- Higher forces to angulate, since resisting moments are a function of radii about the center of the joint as opposed to relatively small pin radii of gimbal joints
- Inability to prevent torque from entering bellows due to system loading without the addition of other devices

The lighter weight of the unit is felt to be, by far, the greatest value of the ball joint; not only for the obvious space vehicle payload considerations, but from dynamic considerations of the ducting system itself. From this standpoint, the advantage of uniformly distributed loads across the joint into adjacent tubing is of particular value.

Continuing the discussion of dynamic considerations, the disadvantage of higher forces to angulate can be turned into an attractive feature. These higher forces are developed by large friction areas which can absorb considerably more dynamic energy than the pins in gimbal joints. It is conceivable that the bearing surfaces can be selected to match the damping needs of the entire ducting system. For example, consider a three flexible joint system typical of many Saturn vehicle flexible ducts. Reaction loads on attachment flanges and supports are most often developed by the joints which are adjacent to these points since their distances and, therefore, moments are the least. The center flexible joints contribute little in the way of reaction moment since the distance from these points is large. Since the center flexible joint also presents the largest unsupported mass in the system, a lightweight ball joint with high coefficient of friction contact surfaces would tend toward optimizing not just a joint, but the entire duct system. The end joints could be ball joints with low coefficient of friction surfaces or, if necessary, gimbal-type pin joints.

The ability to vary the surfaces of the ball joint is afforded by the amount of ball contact area which can be developed by relatively thin annular projected areas. For example an annular contact surface 3.50 inches inside diameter and 3.75 inches outside diameter (1/8 inch wide) contains 1.42 $in.^2$ of projected area. If the bellows mean diameter was 3.25 inches and the system working pressure equaled 100 psig, the bearing pressure on these contact surfaces would be only 585 psi.

One problem area in the design of a ball joint was the characteristics of various materials in sliding contact. Since the ball surfaces and structure would be

operating in a vacuum (the vacuum created by an insulating jacket or the vacuum of space), the surface characteristics under these conditions need to be known. Specifically the designer needs to know the:

- Number of cycles of sliding versus bearing pressures prior to galling in a vacuum
- Friction factor versus number of cycles in a vacuum

A preliminary study indicated that these data were not readily available; therefore, a testing program was inaugurated to provide this information.

## 4.6 BELLOWS INSTABILITY STUDY

Bellows instability, or squirm, is one of the limitations of a bellows which the designer must take into consideration when designing a flexible joint. Instability considerations generally limit the maximum length of the bellows and a minimum spring rate and therefore higher resulting deflection forces. In an attempt to increase the instability pressures, and/or reduce spring rate, the mechanism of squirm and the prevalent prediction techniques were reviewed. From this review, it was determined that the best way to improve bellows instability was to refine the prediction method to a point where the conservatisms used today, as a result of present prediction inaccuracies, were reduced to a much lower percentage of the pressure requirements. Since most flexible ducting systems are, in essence, tension systems whereby bellows expansion joints are restrained against axial deflection but must angulate, this instability becomes more critical since a bellows is prone to squirm at much lower pressure when angulated.

The conventional expression which was used to predict the critical squirm pressure, is given as:

$$P_{cr} = \frac{2\pi}{L} \times SR_A$$

where: $SR_A$ = computed axial spring rate of bellows

$L$ = length of bellows

None of the terms in the preceding equation take into account any stresses which exist in the bellows nor the relative strengths of the materials of constructions. The expressions for spring rate are a function of Young's modulus; however, the differences in critical squirm pressures for various materials have created much concern over the use of these expressions.

Most stainless steels and superalloys used as bellows materials have similar or identical Young's moduli. In the conventional instability expression, the critical instability pressure is directly proportional to the modulus of elasticity. Therefore, squirm predictions, using the conventional equation are accurate only while the stress state of the bellows remains within the elastic limit. Generally, in low cycle systems, the bellows stress at full angulation exceeds the material's yield strength. Therefore, once the compressive meridional membrane stress in the bellows exceeds the yield point, the elastic modulus no longer applies.

During this program, a fundamental hypothesis was confirmed regarding the relationship between material modulus of elasticity and critical squirm pressure. Testing carried out during this program has confirmed a previously conceived theory that critical squirm pressure in the plastic range is proportional to the tangent modulus of the stress-strain relationship. The conventional critical squirm pressure equation, has been modified by the ratio of tangent modulus over elastic modulus.

$$P_{cr} = \frac{2\pi}{L} SR_A (E_t/E)$$

Therefore, the expression now states that the critical squirm pressure is roughly proportional to the yield strength. This expression agrees with the test program results that indicated that Inconel 718 bellows will squirm at pressures approximately three times as high as the Type 321 stainless steel bellows.

The relative accuracies of the conventional instability expression versus the improved method for both Inconel 718 and Type 321 stainless steel bellows are shown in Figures 14 and 15. Since the spring rate term in the expression is being modified by the ratio $E_t/E$, we can now answer the question: Why does the spring rate of bellows vary with the increasing deflections? In the past, the load-to-deflect was assumed to be linear with the deflection.

During the program, 47 bellows of both materials and various configurations were tested. The bellows were 3-inch inside diameter, and ranged from 3.3 to 3.6 inches outside diameter. The number of convolutions were held constant at 10 per bellows. The specimens were of both single ply and two ply construction. All bellows were spring-rate tested prior to squirm testing, and squirm testing included bellows in the undeflected and deflected conditions up to 12 degrees angulation. A typical squirmed bellows is shown in Figure 16.

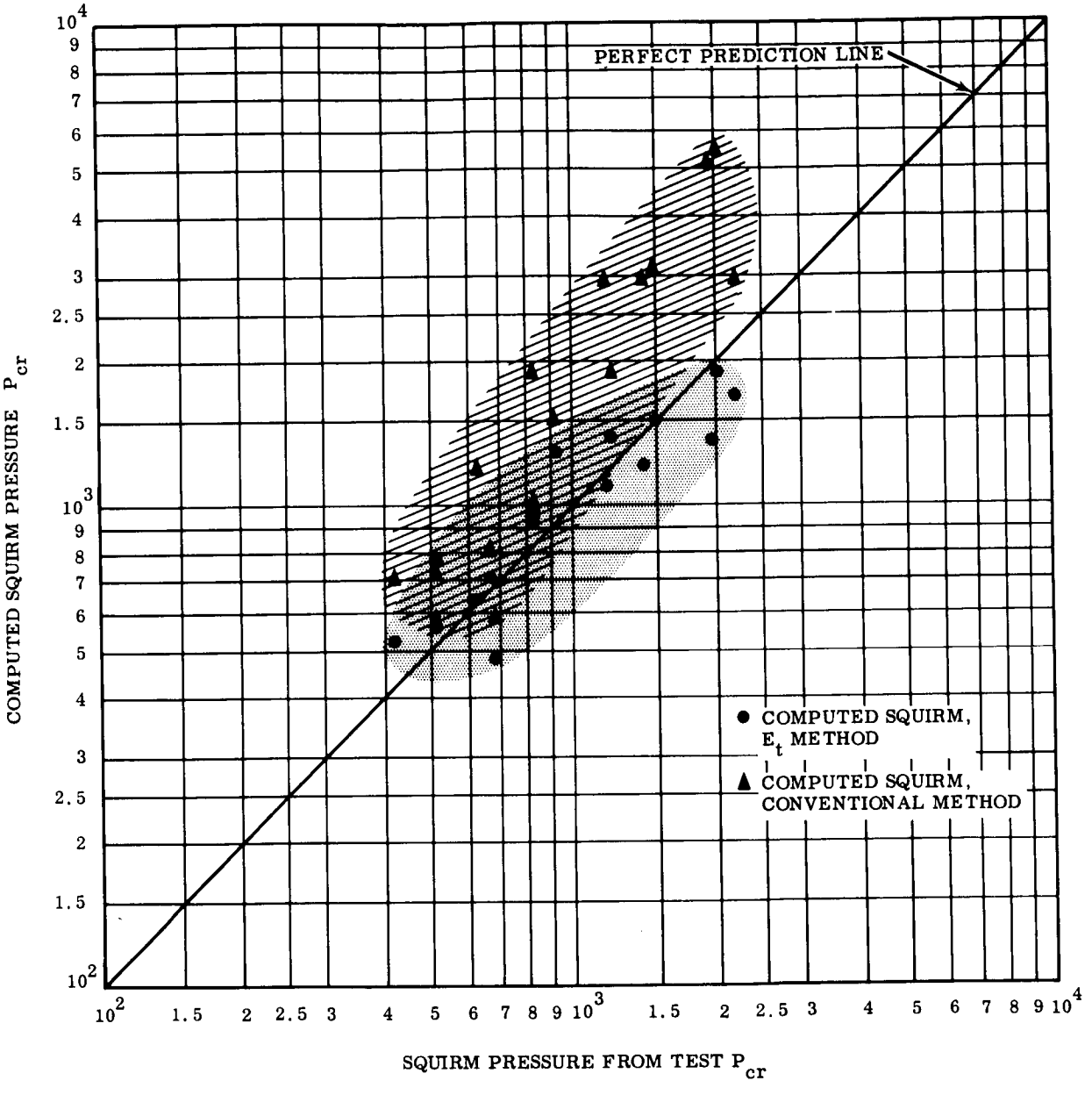


FIGURE 14. SQUIRM PRESSURE TEST OF INCONEL 718 BELLOWS

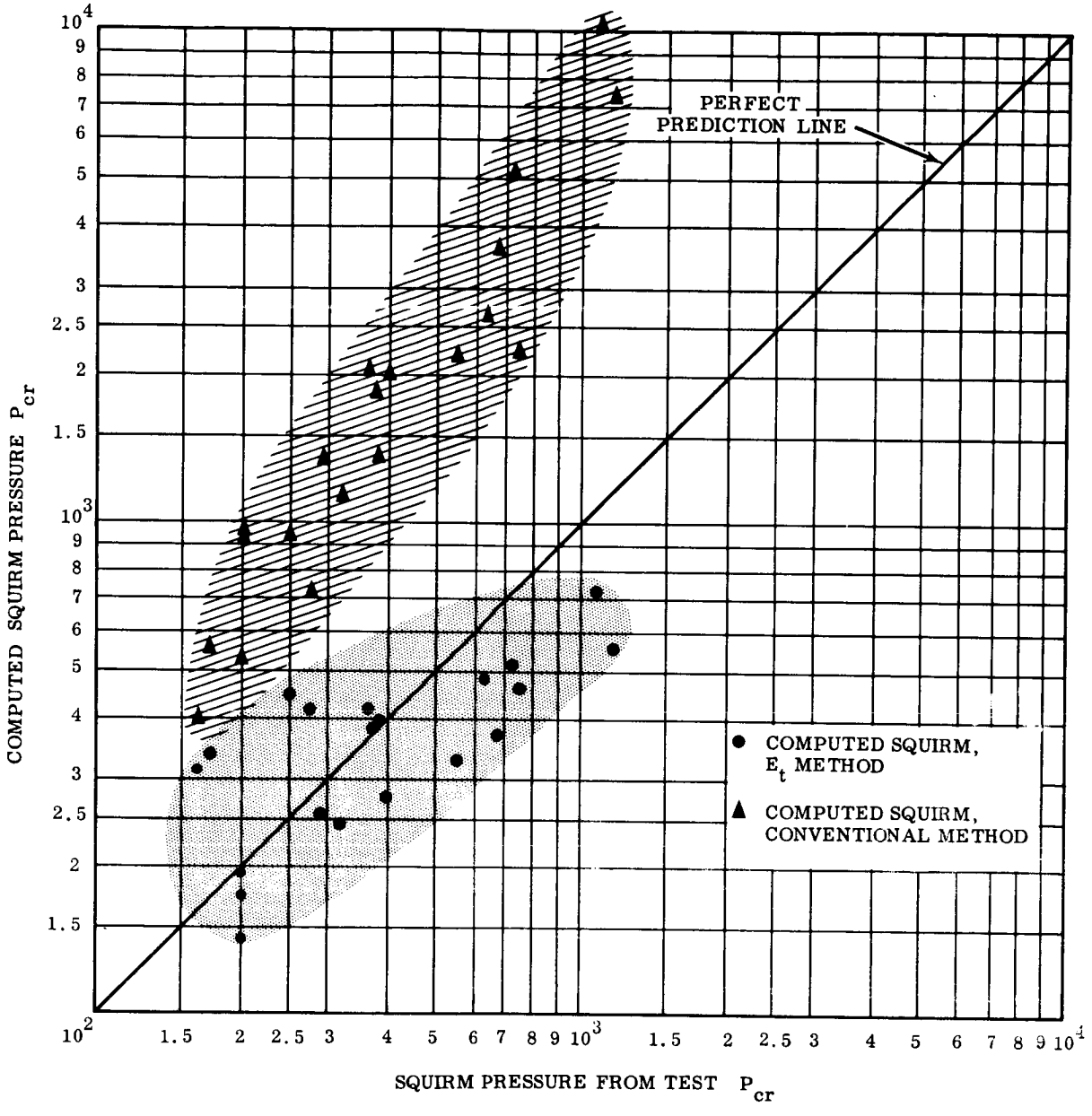


FIGURE 15. SQUIRM PRESSURE TEST OF TYPE 321 STAINLESS STEEL BELLOWS

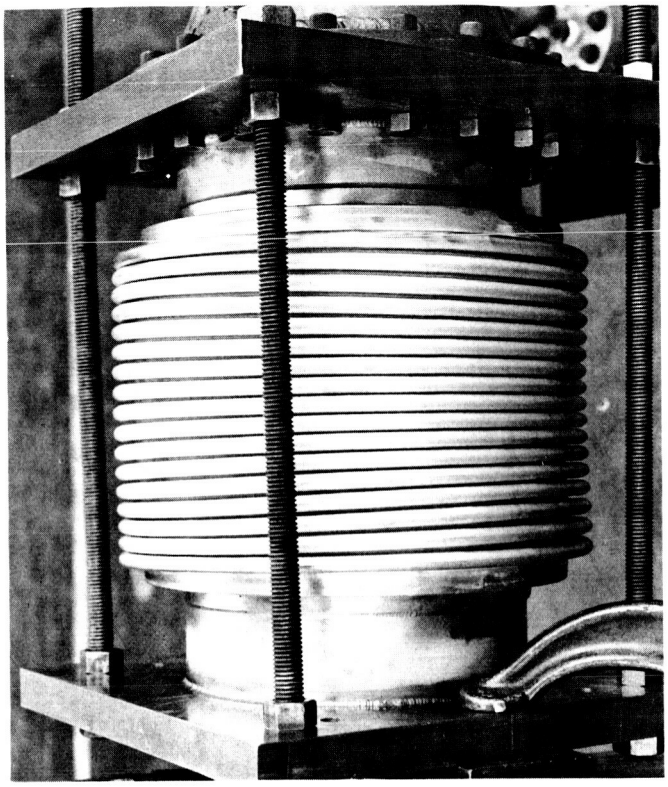

FIGURE 16.
TYPICAL SQUIRMED BELLOWS

Since bellows instability is similar in nature to a column compression failure, a reasonable conclusion to this effort would be to install bellows into flexible joints with tensile rather than compressive preloads. Under very high-pressure conditions, this might lead to the possibility of pretensioning bellows to a deflection equal to the compressive deflection during angulation. This idea, no doubt, will have to be modified by the total stress consideration. However, a compromise can be reached which will permit increasing the predicted bellows instability or the lowering of bellows spring forces.

Test procedures and data which were generated and used during this phase of the program are shown in Solar Engineering Report, M-1794, dated 19 August 1965, which is included as Appendix I.

## 4.7 BALL JOINT SURFACES FRICTION AND WEAR STUDY

To design ball joints for flight service, a knowledge is required of the change in the coefficient of friction of the sliding surfaces which occurs during repeated cycling. In addition, the designer must know the number of cycles which various material and surface combinations can be expected to withstand before seizing occurs or at least before the friction coefficient exceeds reasonable limits. Since the majority of motions

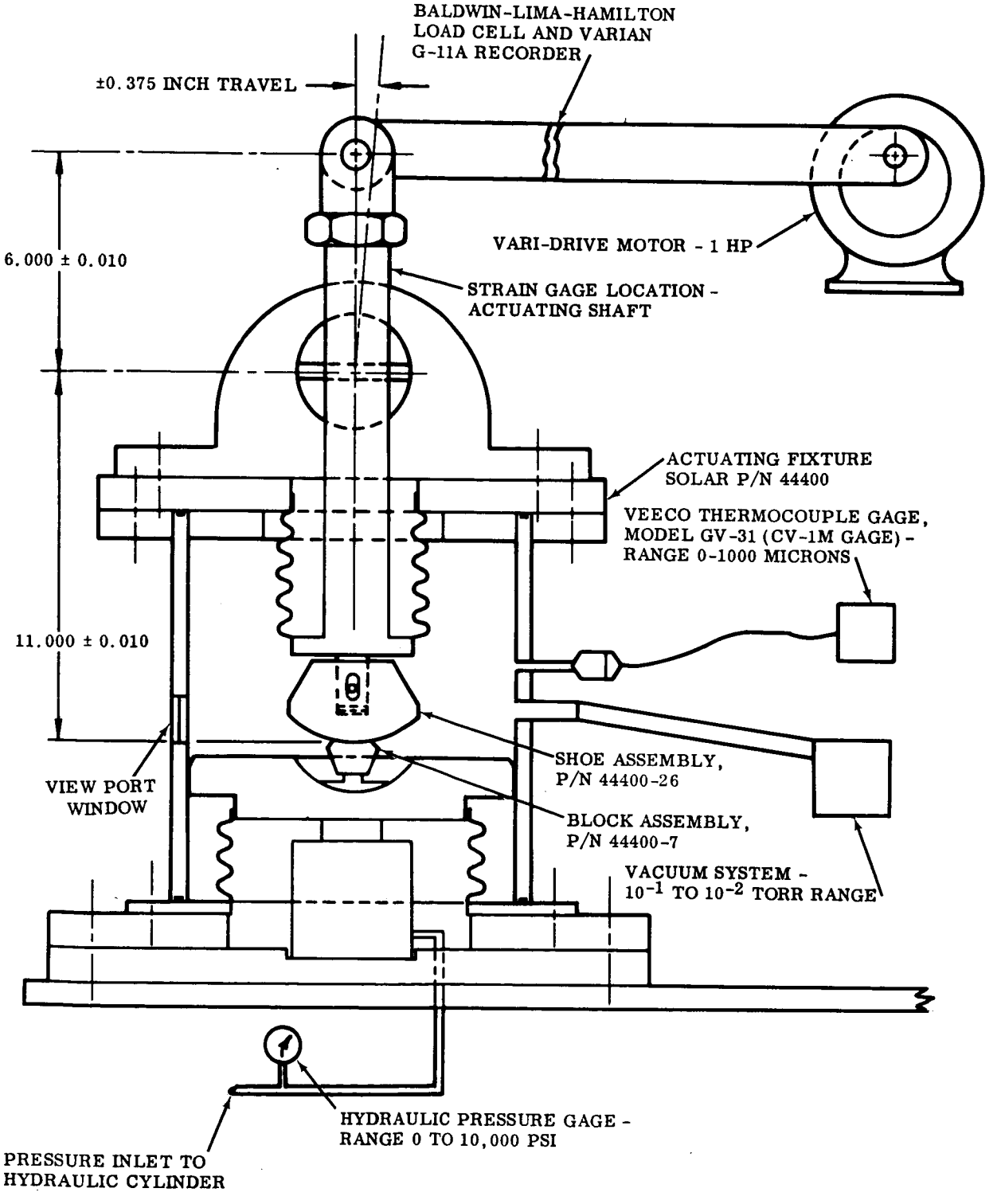


FIGURE 17. SCHEMATIC DIAGRAM OF CYCLE-PRESSURE TEST SETUP

of an upper stage, liquid hydrogen-fueled vehicle duct system would occur in the vacuum of space, the flexible joints would be operated in a vacuum or vacuum insulation of some type, therefore the environment in which the necessary data are gathered should include a vacuum. Toward this end, a test program was performed in which 22 test items with cylindrical contact surfaces were cycled in a vacuum to 10,000 cycles or seizing, whichever occurred first. During cycling, bearing pressures were varied to simulate various flexible joint internal pressure loads. A schematic of the test setup is shown in Figure 17; Figure 18 shows the actual equipment. The test procedure is included in this report as Appendix II.

In the desire to achieve conservative design data (i.e., to not produce data which, being based upon the ultimate in surface conditions, could not be achieved in production) the following ground rules were established:

- Contact surface radii were to be 6.00 ± 0.010 inches
- Surface finishes were to be 16 RMS

Figure 19 shows the test specimen configuration and dimensions. Table I lists the test specimens and Table II lists the test results. Figures 20 through 41 show the specimens at the completion of testing.

The specimens tested represented three groups of materials and material combinations:

- Common Ducting Materials. CRES Type 321 and Inconel 718 in contact with themselves and with each other, bare metal and dry lubricated. This is obviously the simplest and lowest cost system.
- Hard Facings. Metallic materials which have been developed to withstand sliding motion and prevent base metal failure such as:

  Hard Chrome Plate

  Haynes Stellate Alloy No. 12

  Asarcon 773 (continuous cast bronze bearing) by American Smelting and Refining Company (lubricated with molydisulfide coating)

  Super Oilite No. 16 (bronze) by Amplex Division, Chrysler Corporation (lubricated with molydisulfide coating)

- Low Friction Materials. Self-lubricating materials for high-cycle life and/or low-coefficient of friction.

  Teflon impregnated fibre glass (W. S. Shamban Company)

  Teflon impregnated bronze (Turcite B - W. S. Shamban Company)

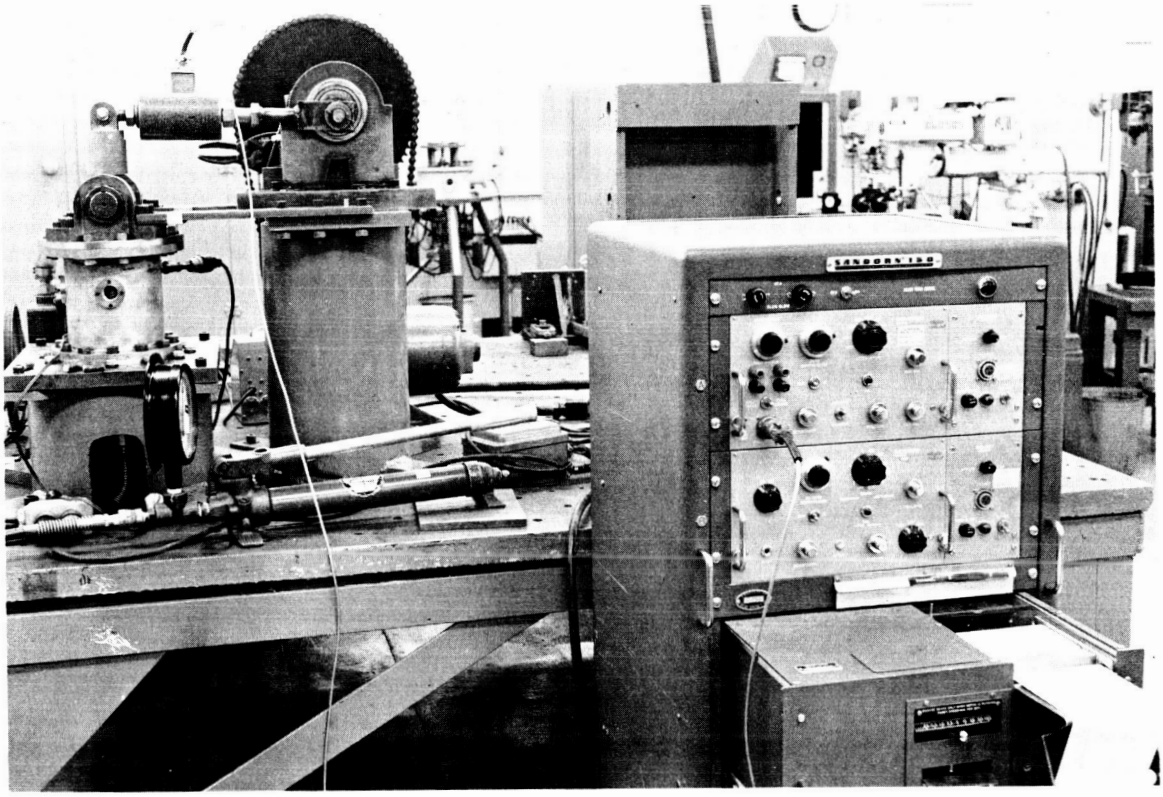

FIGURE 18. CYCLE-PRESSURE TEST SETUP

The materials in these groups had the common characteristics of:

- Compatibility with the materials of construction of the ducting system
- Compatibility with the fluids being transferred
- Compatibility with the manufacturing techniques employed in the fabrication of present $LH_2$ fluid transfer systems
- Compatibility with the cryogenic temperature and vacuum pressure environment
- No maintenance required after installation

At the test program inception, it was envisioned that bearing pressures in the order of those being felt by gimbal pins (approximately 20,000 psi) could be handled by the specimens. The equipment was, therefore, designed to impart normal loads capable of achieving these pressures. The earliest specimens, however, seized and cold-welded almost immediately under these loading conditions. The loads were then lowered to produce from 250 to 3,000 psi bearing pressures on the specimens.

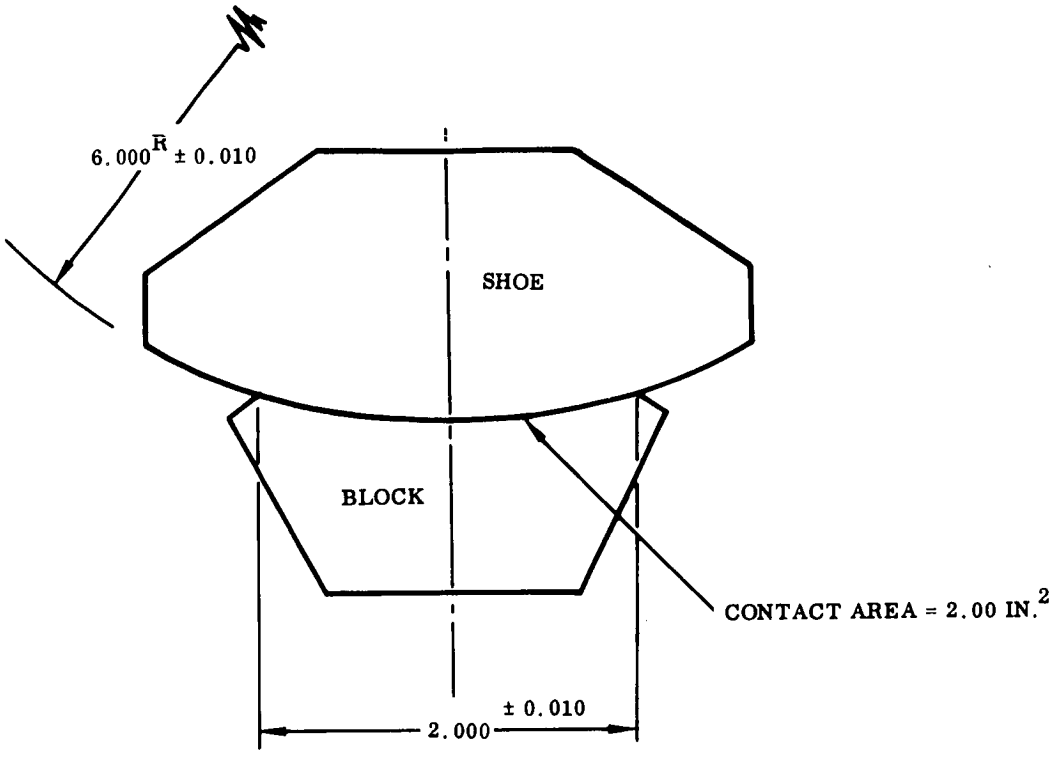


FIGURE 19. BALL JOINT TEST SPECIMEN CONFIGURATION AND DIMENSIONS

The study was self-limiting in that all testing was performed at 100 cycles per minute and arc deflections were held constant at ± 0.375 inches or ± 3.5 degrees. With these constants, the effect on surface life and change in friction factor as a function of surface velocities and accelerations could not be determined.

As indicated in Table II, most of the specimens experienced severe galling early in the cycling. Even with reduced bearing loads and dry film lubricants, breakdown of the surface was, in many instances, almost immediate. Part of this breakdown could be attributed to localized bearing pressures resulting from mismatch of the mating surfaces. This mismatch however, was within the tolerances to which the specimens were fabricated. To reiterate, these tolerances, primarily dimensional, were permissible as the low cost aspect and conservatism of the goal.

The lack of heat dissipation in the vacuum contributed to the surface failures. Some tests, which were halted and restarted at work shift changes, exhibited a return to low actuation forces, followed by a rapid increase to levels equal to those prior to the halting. From this lack of heat dissipation it can be assumed that the life of these surfaces would be extended if the flexible joints were subjected to cryogenic service.

# TABLE I

## FRICTION TEST SPECIMENS

| Test Item | Specimen Type | Test Specimen Description |
|---|---|---|
| -2 | -7 block | Passivate in accordance with MIL-S-5002 and dip in molydisulfide solution, Electrofilm 1005 (Electrofilm, Inc.) Material, Inconel 718 |
| | -26 shoe | 4 RMS surface finish. Material, Inconel 718 |
| -1 | -7 block | Passivate in accordance with MIL-S-5002 and dip in molydisulfide solution, Electrofilm 1005 (Electrofilm, Inc.). Material, Type 321 stainless steel |
| | -26 shoe | 4 RMS surface finish. Material, Type 321 stainless steel |
| -3 | -7 block | 16 RMS surface finish. Material, Inconel 718 |
| | -26 shoe | 16 RMS surface finish. Material, Inconel 718 |
| -6 | -7 block | 16 RMS surface finish. Material, Type 321 stainless steel |
| | -26 shoe | 16 RMS surface finish. Material, Type 321 stainless steel |
| -7 | -7 block | Passivate in accordance with MIL-S-5002 and dip in molydisulfide solution, Electrofilm 77S (Electrofilm, Inc.). Material, Type 321 stainless steel |
| | -26 shoe | 16 RMS surface finish. Material, Type 321 stainless steel |
| -8 | -7 block | Passivate in accordance with MIL-S-5002 and dip in molydisulfide solution, Electrofilm 77S (Electrofilm, Inc.). Material, Type 321 stainless steel |
| | -26 shoe | 16 RMS surface finish. Material, Inconel 718 |
| -9 | -7 block | 14 RMS surface finish. Material, Inconel 718 |
| | -26 shoe | Hard chrome plate in accordance with AMS-2406C and grind to RMS surface finish (0.015-inch plating thickness after grinding). Material, Type 321 stainless steel |
| -10 | -7 block | 14 RMS surface finish. Material, Type 321 stainless steel |
| | -26 shoe | Hard chrome plate in accordance with AMS-2406C and grind 16 RMS surface finish (0.015-inch plating thickness after grinding). Material, Type 321 stainless steel |
| -11 | -7 block | Coat with Haynes Stellite alloy 12. Grind to 16 RMS surface finish (0.06-inch thick after grinding). Material, Type 347 stainless steel |
| | -26 shoe | 16 RMS surface finish. Material, Type 321 stainless steel |
| -12 | -7 block | Coat with Haynes Stellite alloy 12. Grind to 16 RMS surface finish (0.06-inch thick after grinding). Material, Type 347 stainless steel |
| | -26 shoe | 16 RMS surface finish. Material, Inconel 718 |
| -13 | -7 block | Torch braze Asarcon 773 (American Smelting and Refining Co.) insert (width 0.99 to 1.00-inch by 0.12-inch thick) to -7 block. Dip in molydisulfide solution, Electrofilm 77S and cure 1 hour at 375 F. Material, Type 321 stainless steel |
| | -26 shoe | 16 RMS surface finish. Material, Type 321 stainless steel |
| -14 | -7 block | Torch braze Asarcon 773 (American Smelting and Refining Co.) insert (width 0.99 to 1.00-inch by 0.12-inch thick) to -7 block. Dip in molydisulfide solution, Electrofilm 77S and cure 1 hour at 375 F. Material, Type 321 stainless steel |
| | -26 shoe | 16 RMS surface finish. Material, Inconel 718 |
| -15 | -7 block | Torch braze Super-Oilite 16 (Amplex Division of Chrysler Corp.) insert (width 0.99 to 1.00-inch by 0.12-inch thick) to -7 block. Dip in molydisulfide solution, Electrofilm 77S and cure 1 hour at 375 F. Material, Type 321 stainless steel |
| | -26 shoe | 16 RMS surface finish. Material, Type 321 stainless steel |
| -16 | -7 block | Torch braze Super-Oilite 16 (Amplex Division of Chrysler Corp.) insert (width 0.99 to 1.00-inch by 0.12-inch thick) to -7 block. Dip in molydisulfide solution, Electrofilm 77S and cure 1 hour at 375 F. Material, Type 321 stainless steel |
| | -26 shoe | 16 RMS surface finish. Material, Inconel 718. |

TABLE I

FRICTION TEST SPECIMEN (Cont)

| Test Item | Specimen Type | Test Specimen Description |
|---|---|---|
| -17 | -7 block | Bond the Teflon-coated glass cloth (W. S. Shambam Co.)(0.014 inch thick) to -7 block (with bonding kit No. 2, Fluorocarbon Co.). Material, Type 321 stainless steel |
| | -26 shoe | 16 RMS surface finish. Material, Type 321 stainless steel |
| -18 | -7 block | Bond the Teflon-coated glass cloth (W. S. Shambam Co.)(0.014 inch thick) to -7 block (with bonding kit No. 2, Fluorocarbon Co.). Material, Type 321 stainless steel |
| | -26 shoe | 16 RMS surface finish. Material, Inconel 718 |
| -19 | -7 block | Passivate in accordance with MIL-S-5002 and dip in tungsten disulfide solution, Electro-film 2606 (Electrofilm, Inc.) and cure 2 hours at 180 F and 2 hours at 400 F. Material, Type 321 stainless steel |
| | -26 shoe | 16 RMS surface finish. Material, Type 321 stainless steel |
| -20 | -7 block | Passivate in accordance with MIL-S-5002 and dip in tungsten disulfide solution, Electro-film 2606 (Electrofilm, Inc.) and cure 4 hours at 180 F and 2 hours at 400 F. Material, Type 321 stainless steel |
| | -26 shoe | 16 RMS surface finish. Material, Inconel 718 |
| -21 | -7 block | Bond Turcite Type B insert (width 0.99 to 1.00 inch) to -7 block. Material, Type 321 stainless steel |
| | -26 shoe | 16 RMS surface finish. Material, Type 321 stainless steel |
| -22 | -7 block | Bond Turcite Type B insert (width 0.99 to 1.00 inch) to -7 block. Material, Type 321 stainless steel |
| | -26 shoe | 16 RMS surface finish. Material, Inconel 718 |

The best test results were achieved with Asarcon 773, Super-Oilite No. 16, and Teflon impregnated fibre glass against both Type 321 stainless steel and Inconel 718. Friction factor versus number of cycles curves for the preceeding bearing inserts are shown in Figures 42 through 47. As expected, the Teflon showed the lowest coefficient of friction and life spans up to 10,000 cycles. In the low cycle region (to 2000 cycles), steady or constantly changing coefficients were experienced with the other two materials. An exception to the lack of difference accountable to either the Type 321 stainless steel or Inconel 718 shoe materials were specimens No. 13 and 14 (Asarcon 773 against Type 321 stainless steel and Inconel 718, respectively). Specimen No. 14, even at higher bearing pressures, exhibited little or no galling at 10,000 cycles (Fig. 31). While Sanborn traces on specimen No. 13 indicated block surface failure at 2000 cycles, testing was continued to 10,000 cycles (Fig. 30).

TABLE II

FRICTION TEST RESULTS

| Test Item | Bearing Load (lb) | Breakaway Force (lb) | Actuation Force Range (Dynamic) | Total Number of Cycles | Remarks |
|---|---|---|---|---|---|
| -2 | 2000 | 1000 | 1500 to 4000 | 60 | Galling at approximately 15 cycles (Fig. 21) |
| -1 | 2000 | 600 | 5200 to 5600 | 134 | Immediate galling (Fig. 20) |
| -3 | 1000 | 640 | 4000 | 50 | Immediate galling |
| -6 | 1000<br>500 | 425<br>1200 | 425 to 4800<br>1600 to 2000 | 261<br>1950 | Immediate galling (Fig. 22, 23, 24)<br>Immediate galling |
| -7 | 2000 | 400 | 400 to 4000 (400 lb to 550 cycles) | 720 | Galling began at 550 cycles (Fig. 25) |
| -8 | 1000 | 155 | 400 to 4600 | 2982 | Rapid rise in actuation force at 1100 cycles (Fig. 26) |
| -9 | 500 | 400 | 400 to 1000 | 10,000 | Actuation force fluctuated between 800 and 1000 pounds after 800 cycles |
| -10 | 2000 | 2100 | 2100 to 4000 | 628 | Immediate galling (Fig. 27) |
| -11 | 2000 | 2000 | 2000 to 5200 | 16 | Immediate galling (Fig. 28) |
| -12 | 2000 | 1000 | 1000 to 4000 | 84 | Immediate galling (Fig. 29) |
| -13 | 2000 | 340 | 110 to 1900 | 10,000 | Galling began at 2000 cycles (Fig. 30) |
| -14 | 4000 | 230 | 200 to 1000 | 10,000 | Steady actuation force of 800 pounds from 2000 to 9500 cycles (Fig. 31) |
| -15 | 6000 | 550 | 550 to 3400 | 2594 | (Fig. 32) |
| -16 | 4000 | 350 | 350 to 2500 | 10,000 | Fluctuating actuating forces (Fig. 33) |
| -17 | 2000<br>4000 | 200<br>400 | 200 to 300<br>400 to 260 | 10,000<br>10,000 | (Fig. 34)<br>Load dropped to 260 at approximately 2000 cycles (Fig. 35) |
| -18 | 4000<br>6000 | 185<br>400 | 200 to 325<br>350 to 1220 | 10,000<br>2412 | (Fig. 36)<br>Galling at 2400 (Fig. 37) |
| -19 | 2000 | 270 | 500 to 3600 | 203 | Immediate galling (Fig. 38) |
| -20 | 2000 | 280 | 200 to 3200 | 261 | Immediate galling (Fig. 39) |
| -21 | 8000 | 500 | 550 to 1550 | 978 | Insert squeezed out from under block, causing metal to metal contact (Fig. 40) |
| -22 | 4000 | 200 | 200 | 504 | Test stopped. Material observed squeezing out sides of block (Fig. 41) |

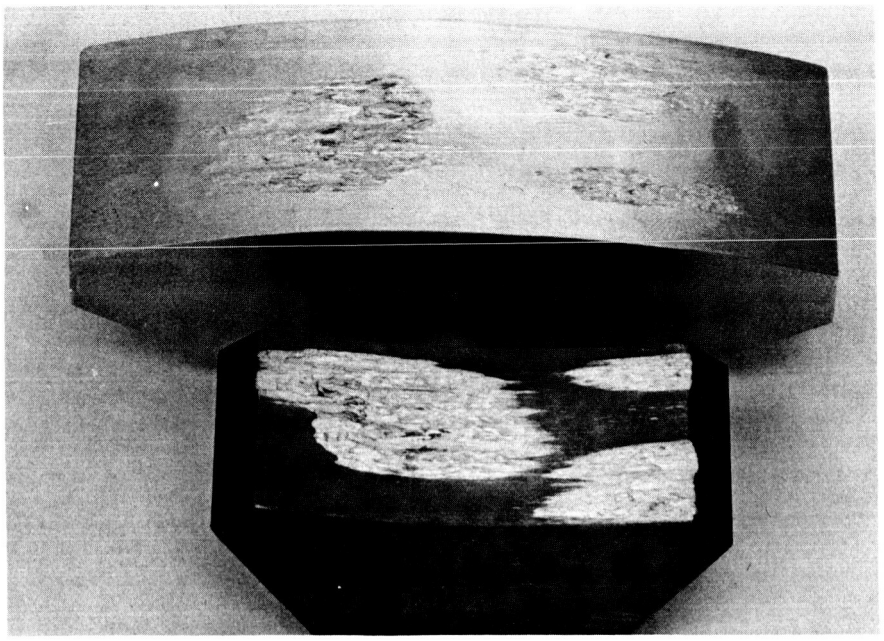

FIGURE 20. BALL JOINT TEST SPECIMEN TYPE - 1

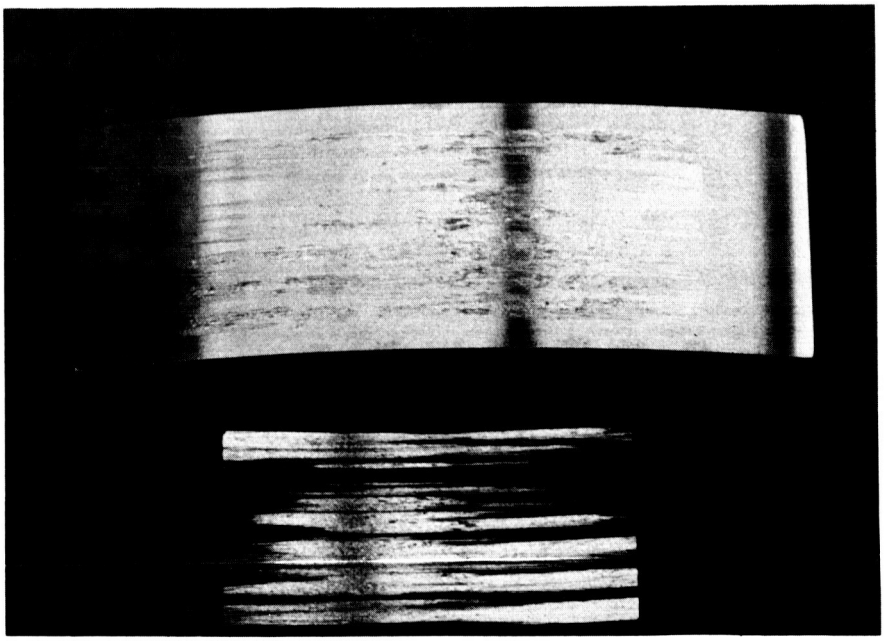

FIGURE 21. BALL JOINT TEST SPECIMEN TYPE - 2

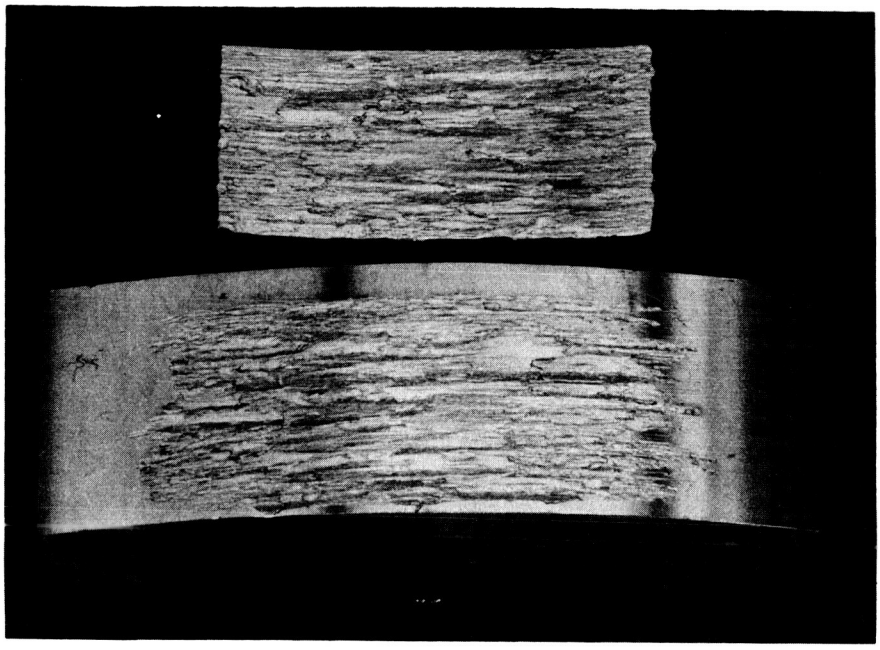

FIGURE 22. BALL JOINT TEST SPECIMEN TYPE - 6;
500 Pound Bearing Load, 1950 Cycles

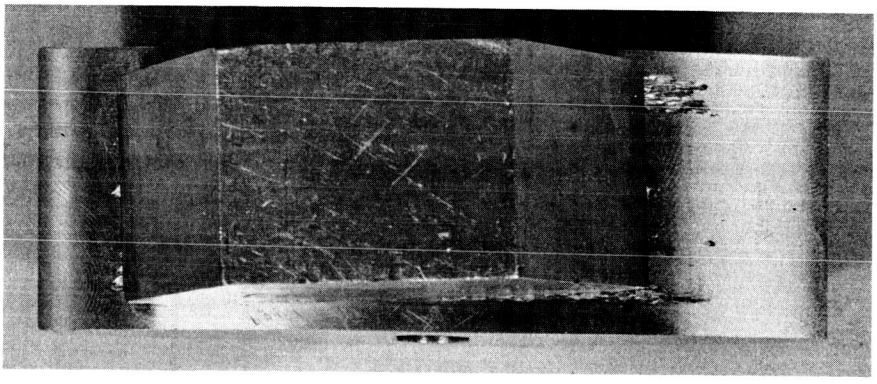

FIGURE 23. BALL JOINT TEST SPECIMEN TYPE - 6;
1000 Pound Bearing Load, Cold Welded
at 261 Cycles

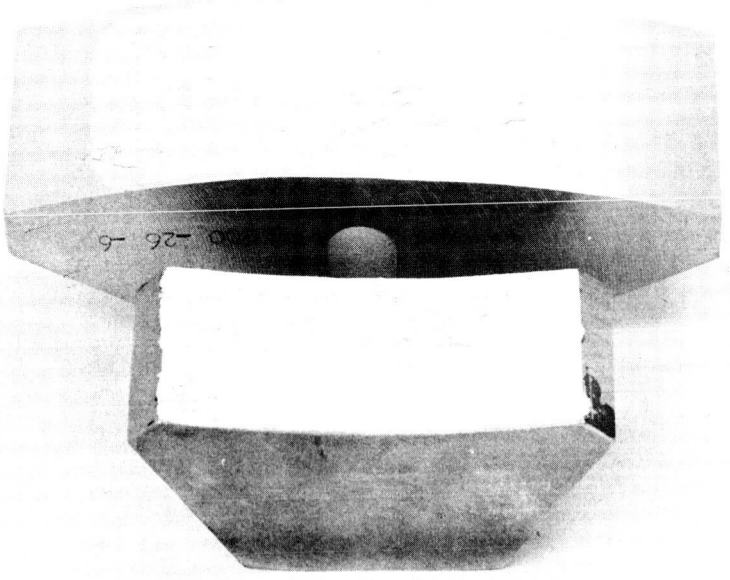

FIGURE 24. SPECIMEN SHOWN IN FIGURE 23 AFTER SEPARATION

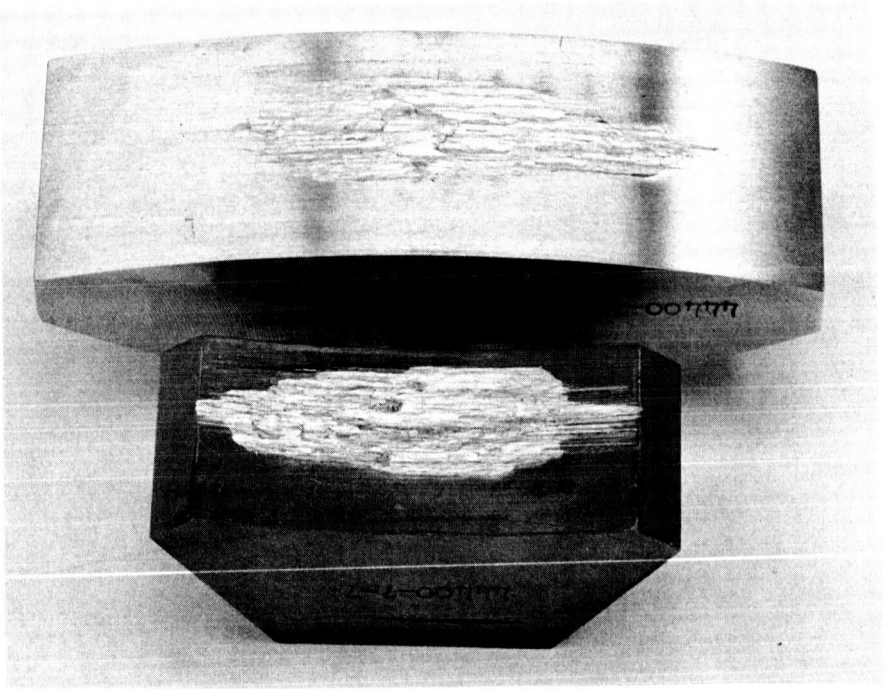

FIGURE 25. BALL JOINT TEST SPECIMEN TYPE - 7; 2000 Pound Bearing Load, 720 Cycles

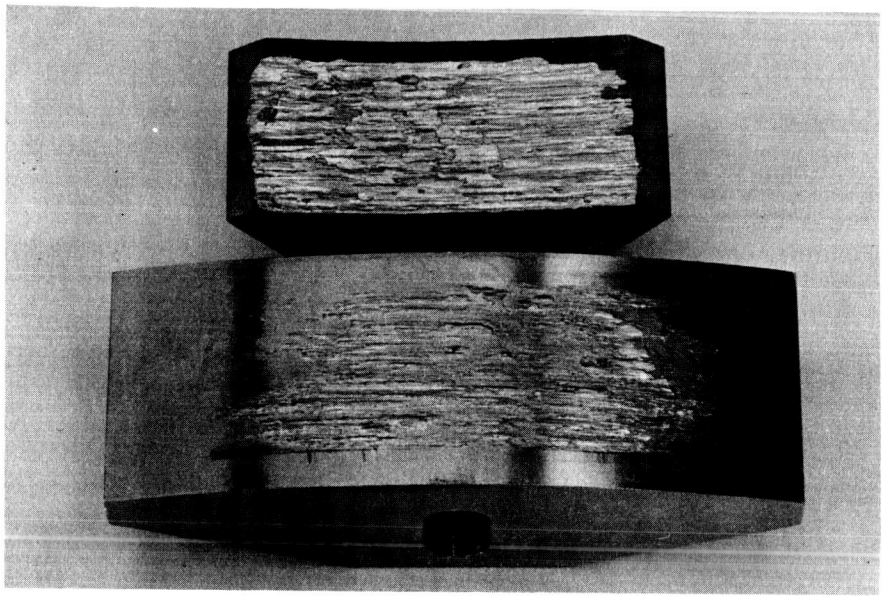

FIGURE 26. BALL JOINT TEST SPECIMEN TYPE - 8;
1000 Pound Bearing Load, 2982 Cycles

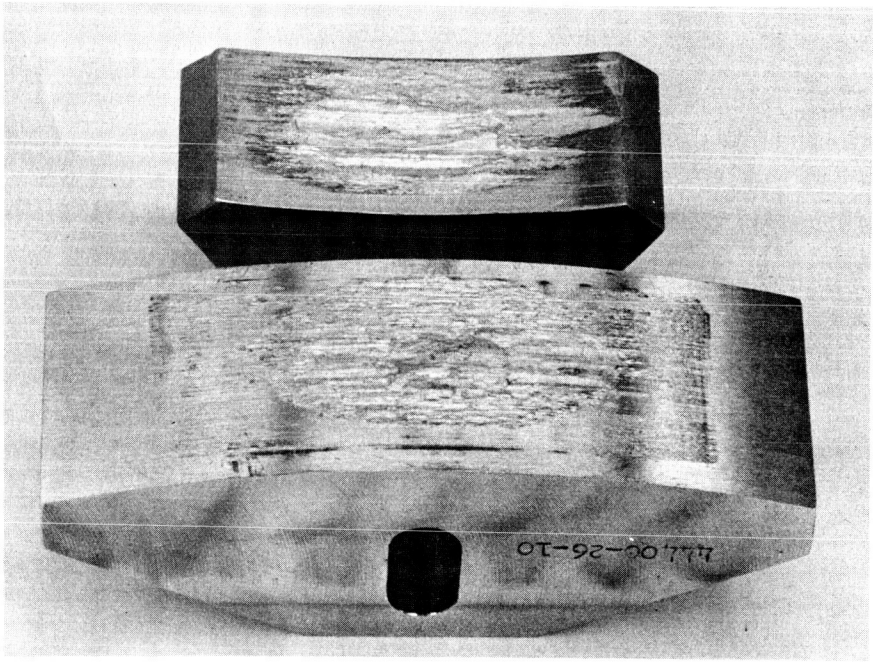

FIGURE 27. BALL JOINT TEST SPECIMEN TYPE - 10;
2000 Pound Bearing Load, 628 Cycles

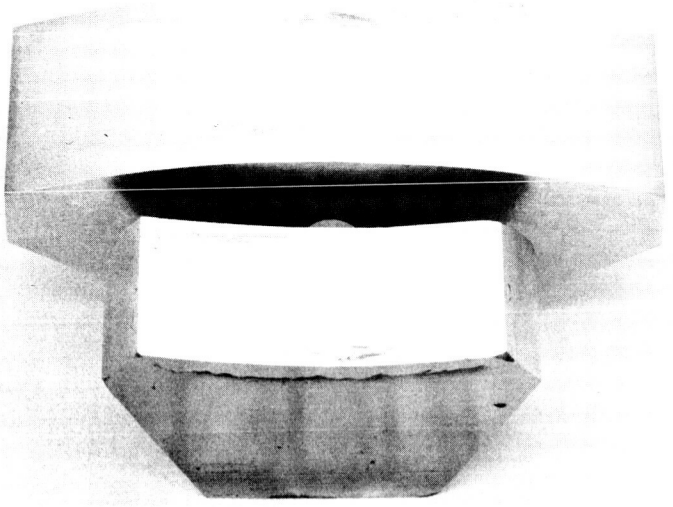

FIGURE 28. BALL JOINT TEST SPECIMEN TYPE - 11;
2000 Pound Bearing Load, 16 Cycles

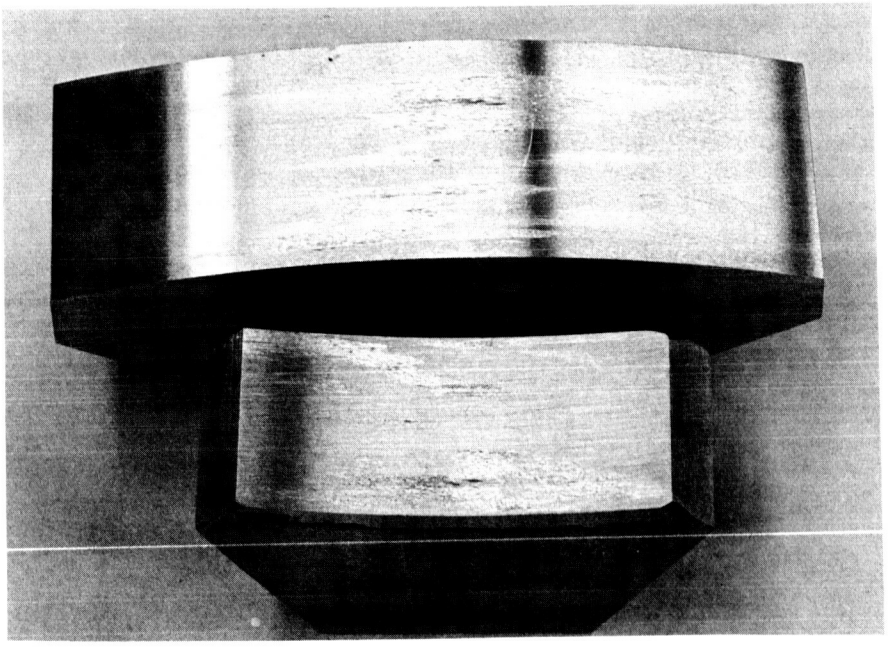

FIGURE 29. BALL JOINT TEST SPECIMEN TYPE - 12;
2000 Pound Bearing Load, 84 Cycles

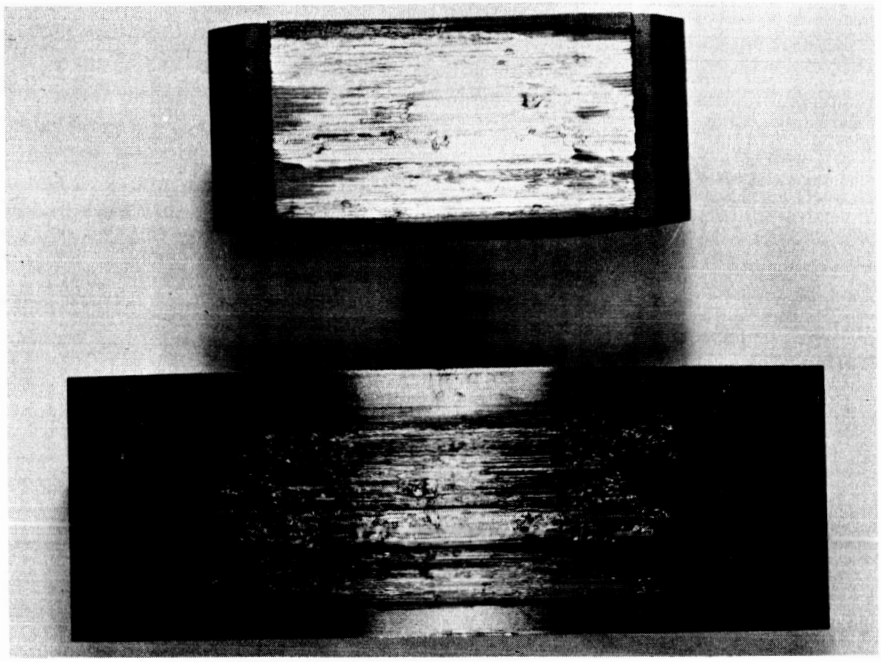

FIGURE 30. BALL JOINT TEST SPECIMEN TYPE - 13;
2000 Pound Bearing Load, 10,000 Cycles

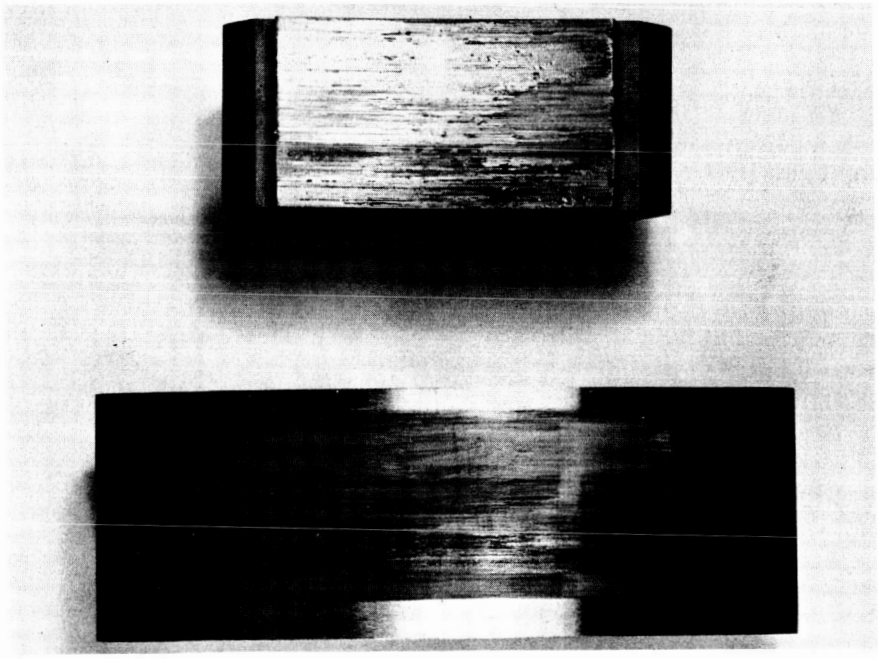

FIGURE 31. BALL JOINT TEST SPECIMEN TYPE - 14;
4000 Pound Bearing Load, 10,000 Cycles

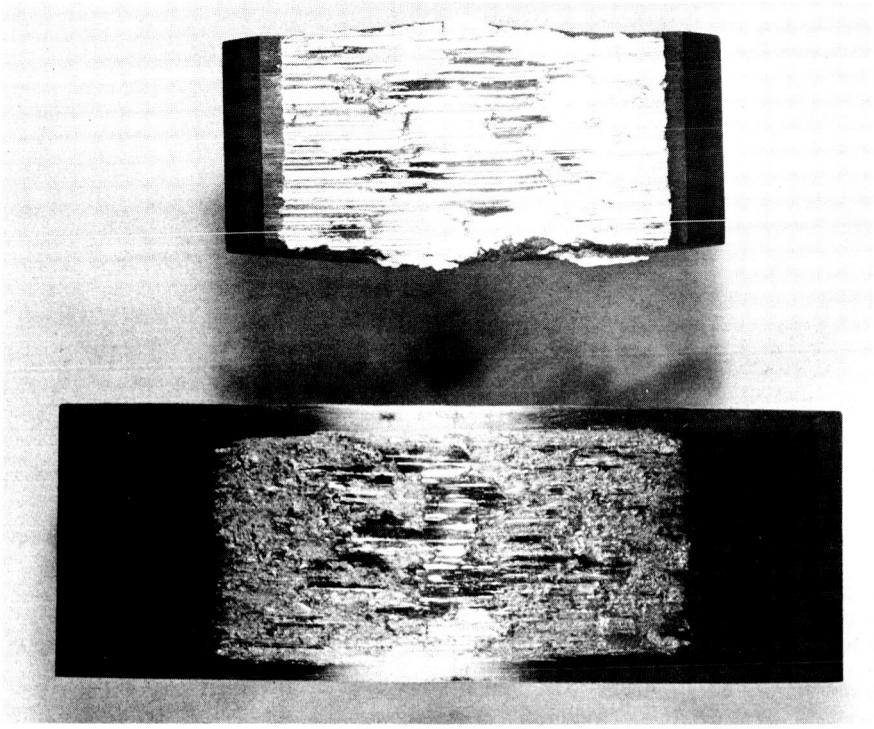

FIGURE 32. BALL JOINT TEST SPECIMEN TYPE - 15;
6000 Pound Bearing Load, 2594 Cycles

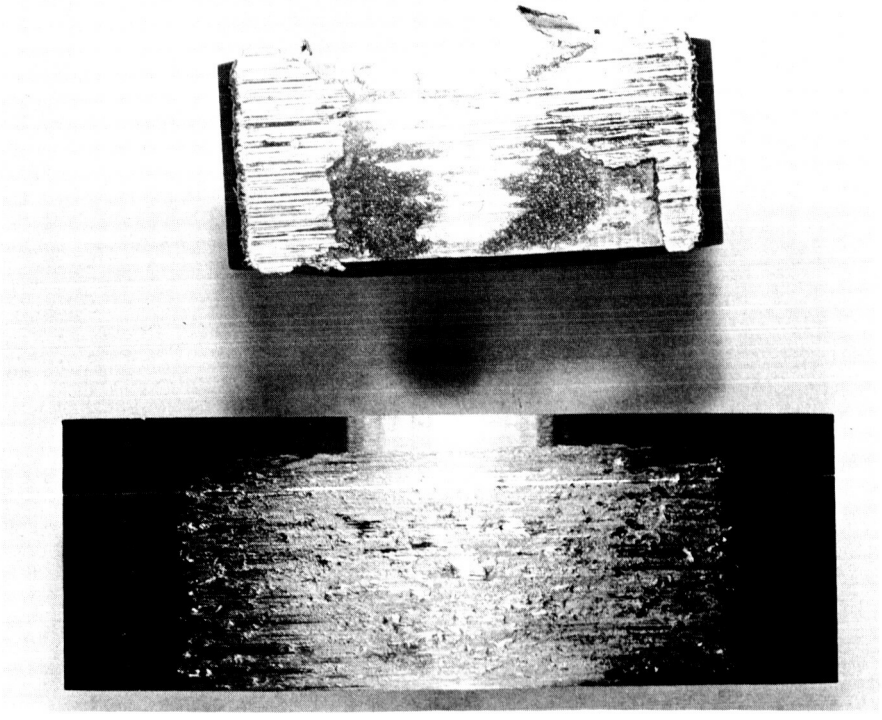

FIGURE 33. BALL JOINT TEST SPECIMEN TYPE - 16;
4000 Pound Bearing Load, 10,000 Cycles

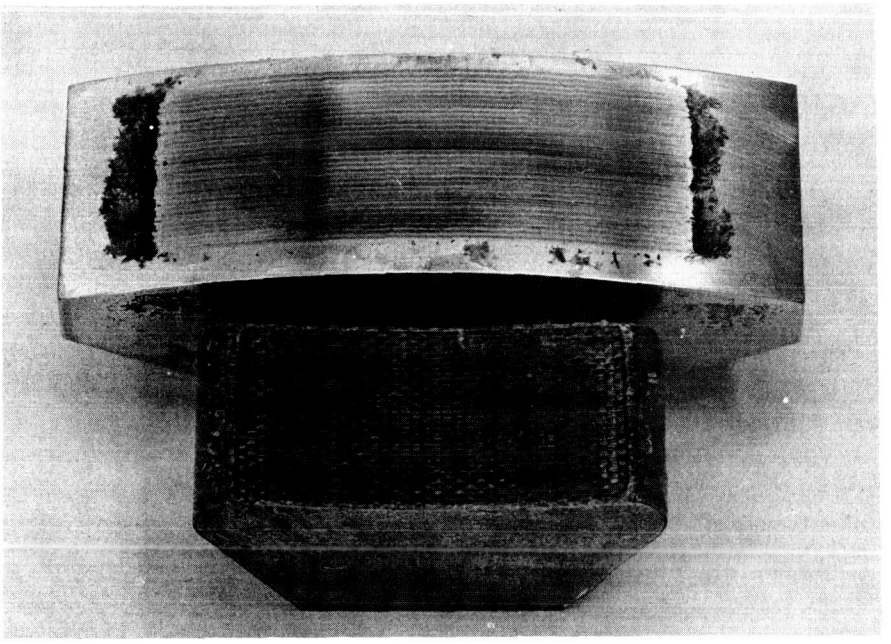

FIGURE 34. BALL JOINT TEST SPECIMEN TYPE - 17;
2000 Pound Bearing Load, 10,000 Cycles

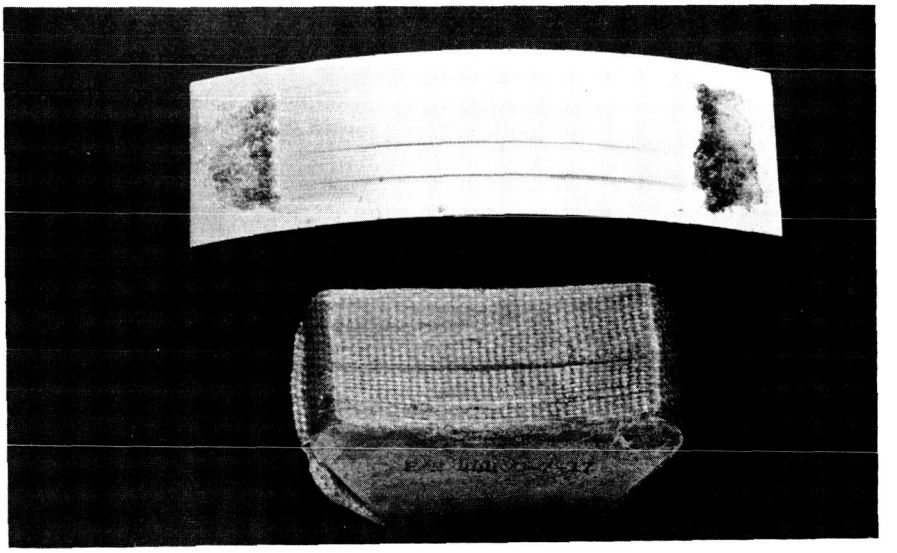

FIGURE 35. BALL JOINT TEST SPECIMEN TYPE - 17;
4000 Pound Bearing Load, 10,000 Cycles

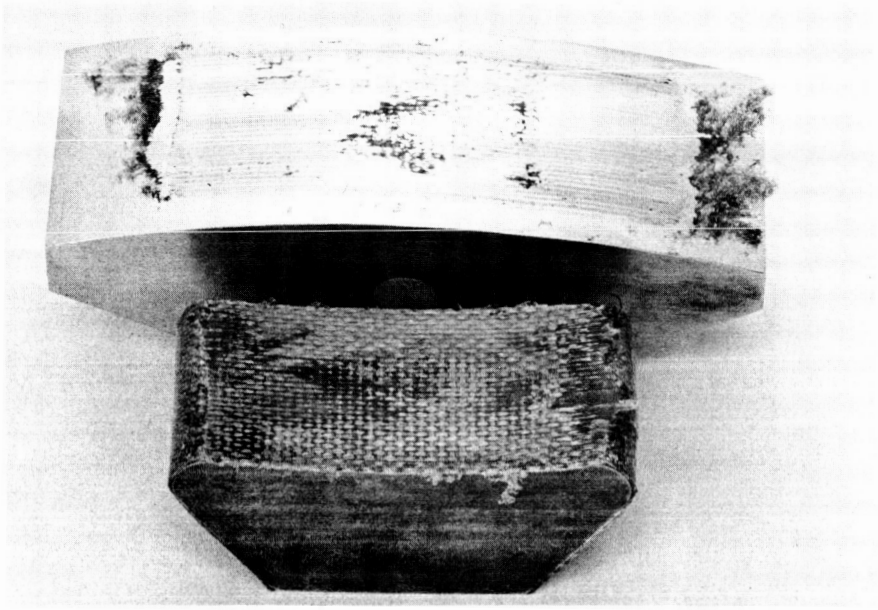

FIGURE 36. BALL JOINT TEST SPECIMEN TYPE - 18;
4000 Pound Bearing Load, 10,000 Cycles

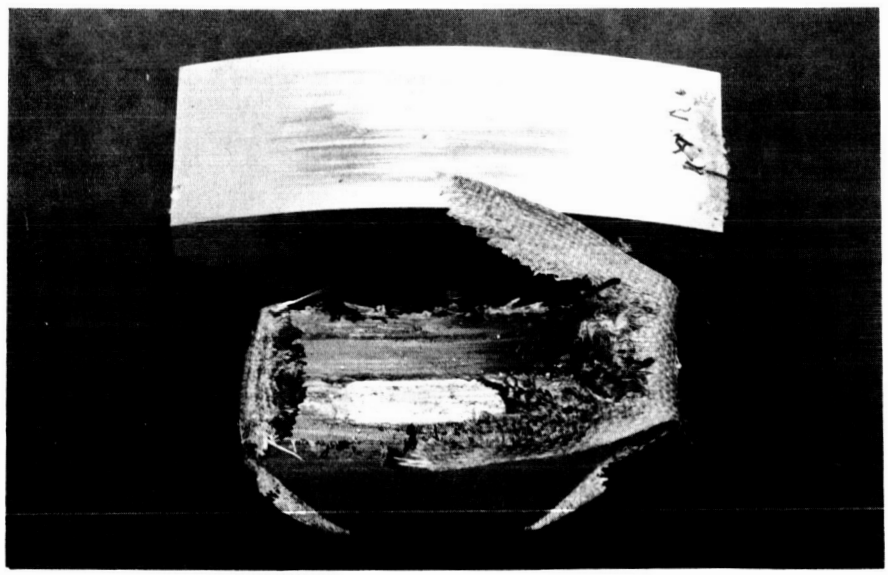

FIGURE 37. BALL JOINT TEST SPECIMEN TYPE – 18;
6000 Pound Bearing Load, 2412 Cycles

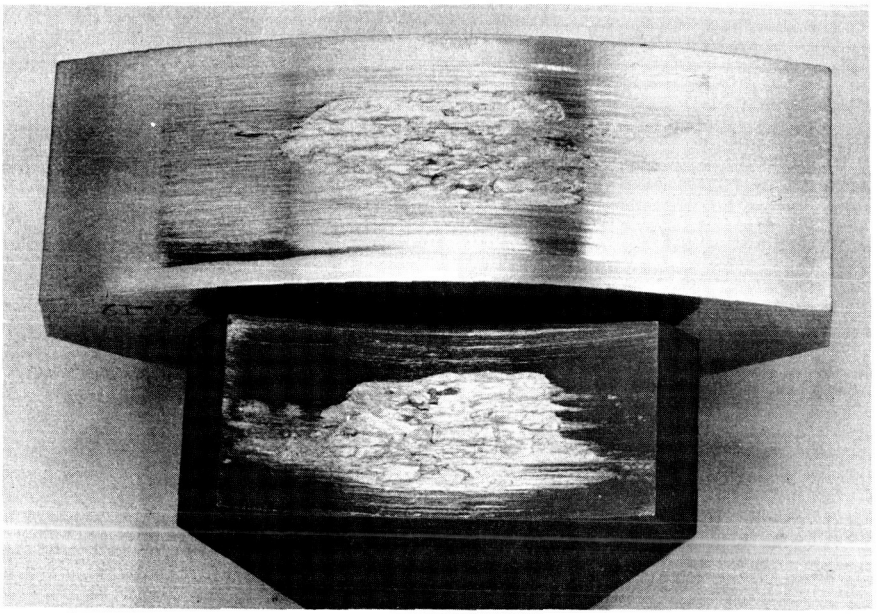

FIGURE 38. BALL JOINT TEST SPECIMEN TYPE - 19;
2000 Pound Bearing Load, 203 Cycles

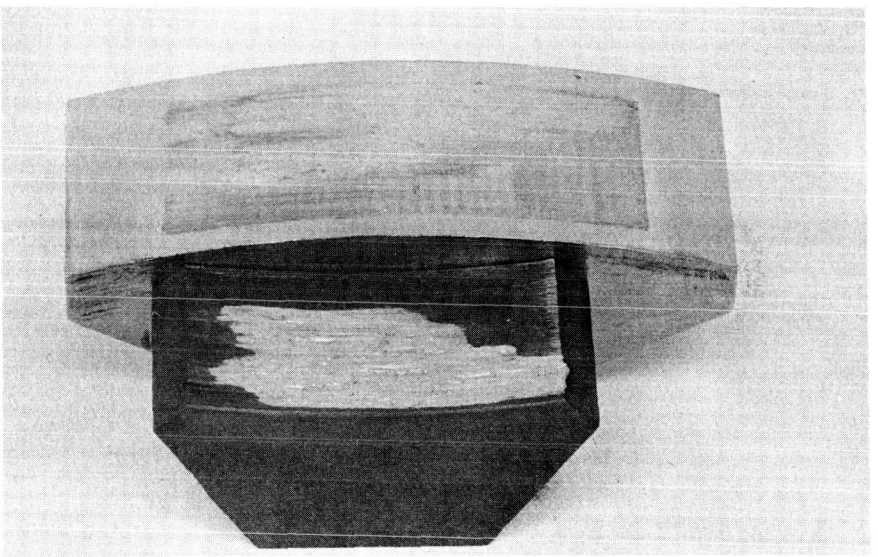

FIGURE 39. BALL JOINT TEST SPECIMEN TYPE - 20;
2000 Pound Bearing Load, 261 Cycles

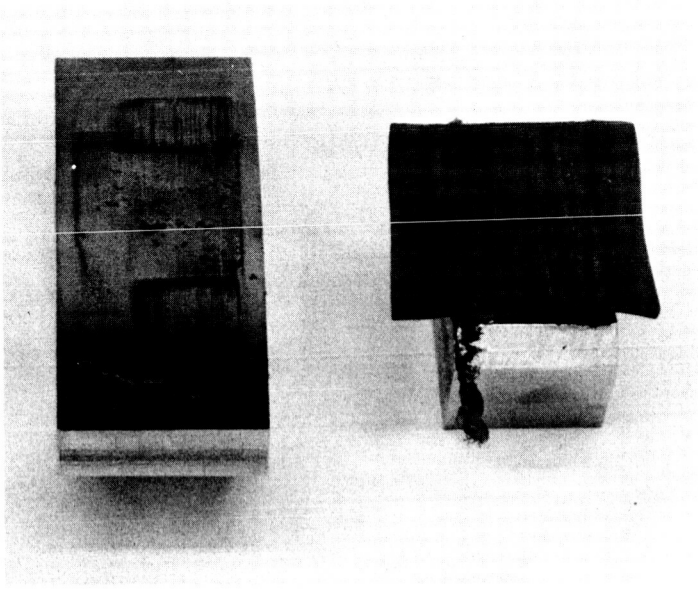

FIGURE 40. BALL JOINT TEST SPECIMEN TYPE - 21;
800 Pound Bearing Load, 978 Cycles

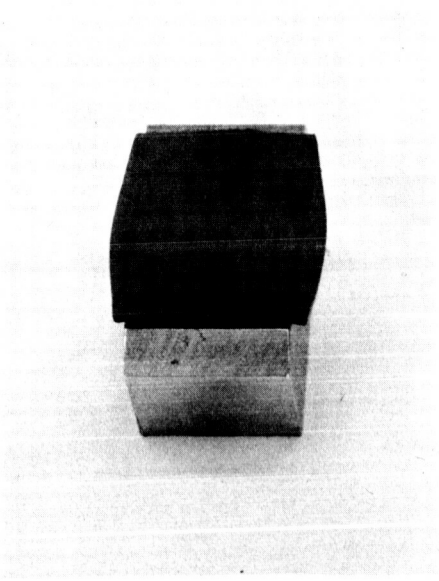

FIGURE 41.

BALL JOINT TEST SPECIMEN TYPE - 22;
4000 Pound Bearing Load, 504 Cycles

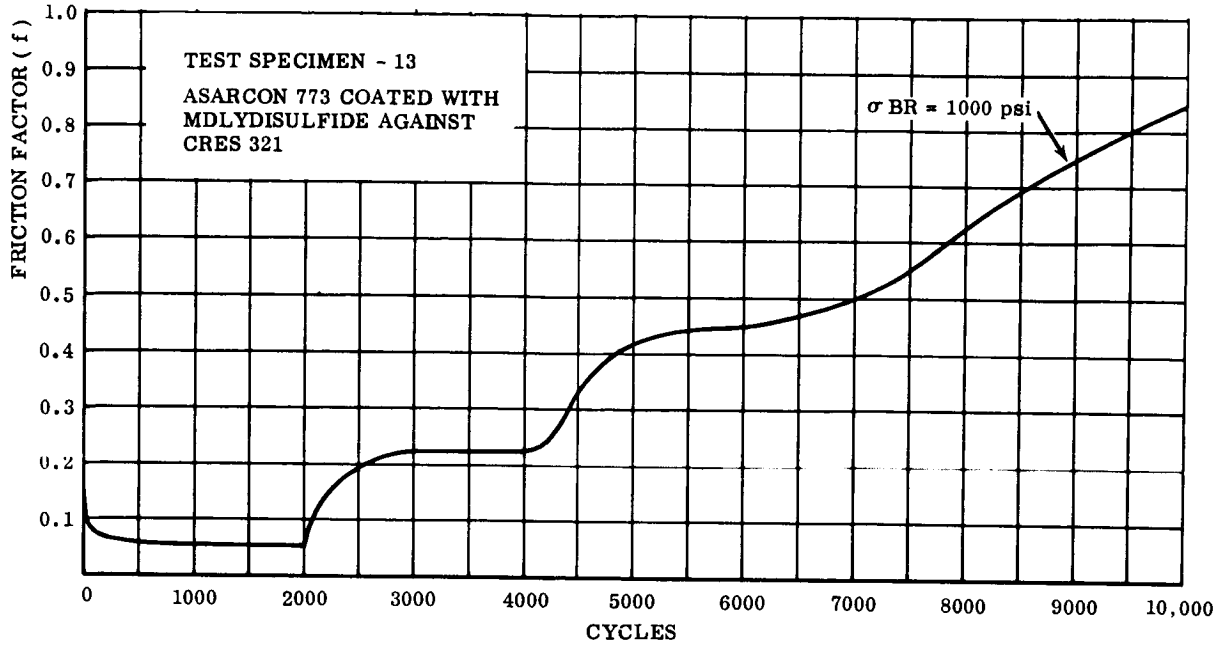


FIGURE 42. FRICTION FACTOR VERSUS CYCLES FOR TEST SPECIMEN - 13

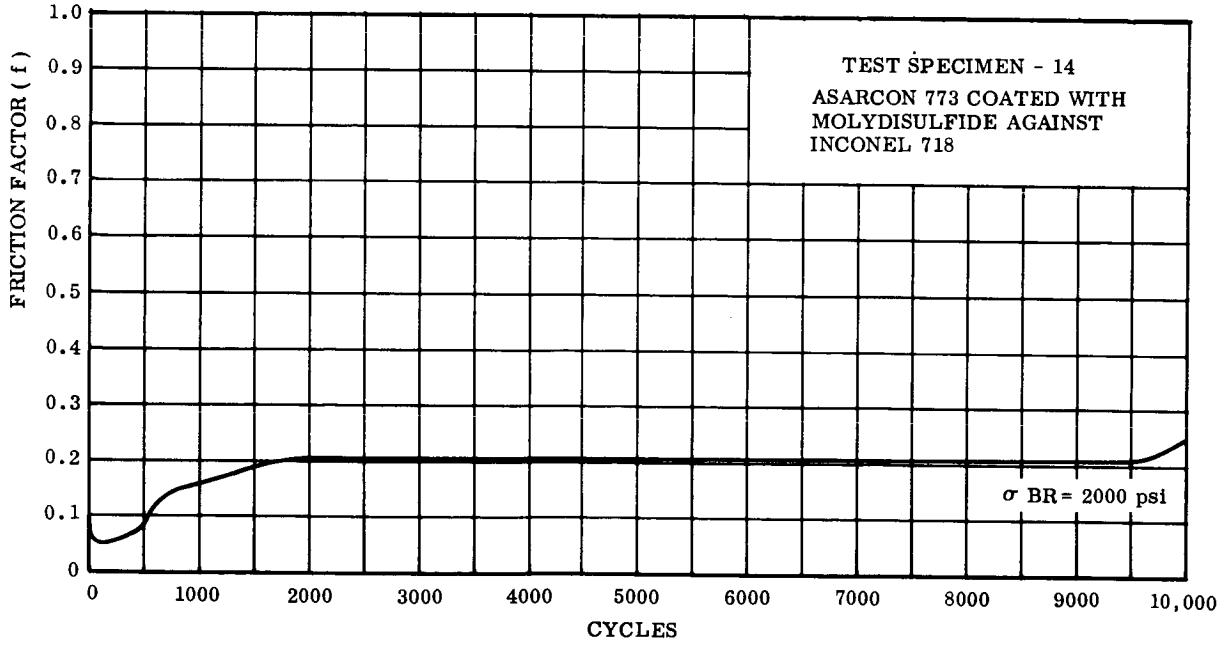


FIGURE 43. FRICTION FACTOR VERSUS CYCLES FOR TEST SPECIMEN - 14

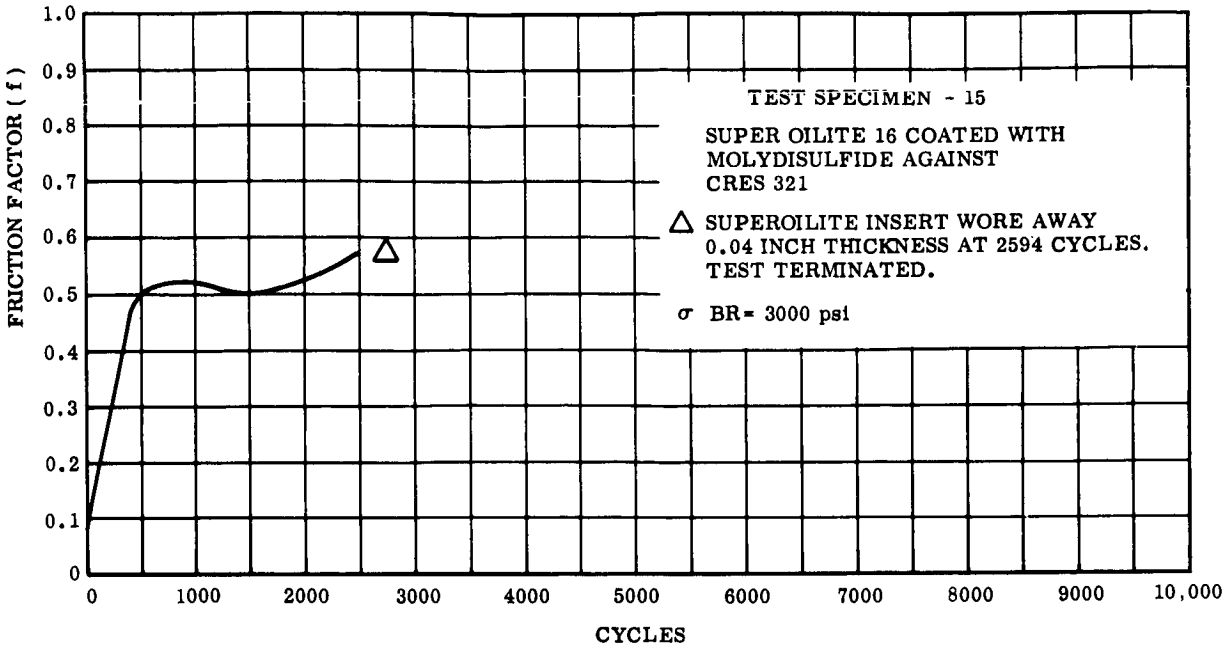


FIGURE 44. FRICTION FACTOR VERSUS CYCLES FOR TEST SPECIMEN - 15

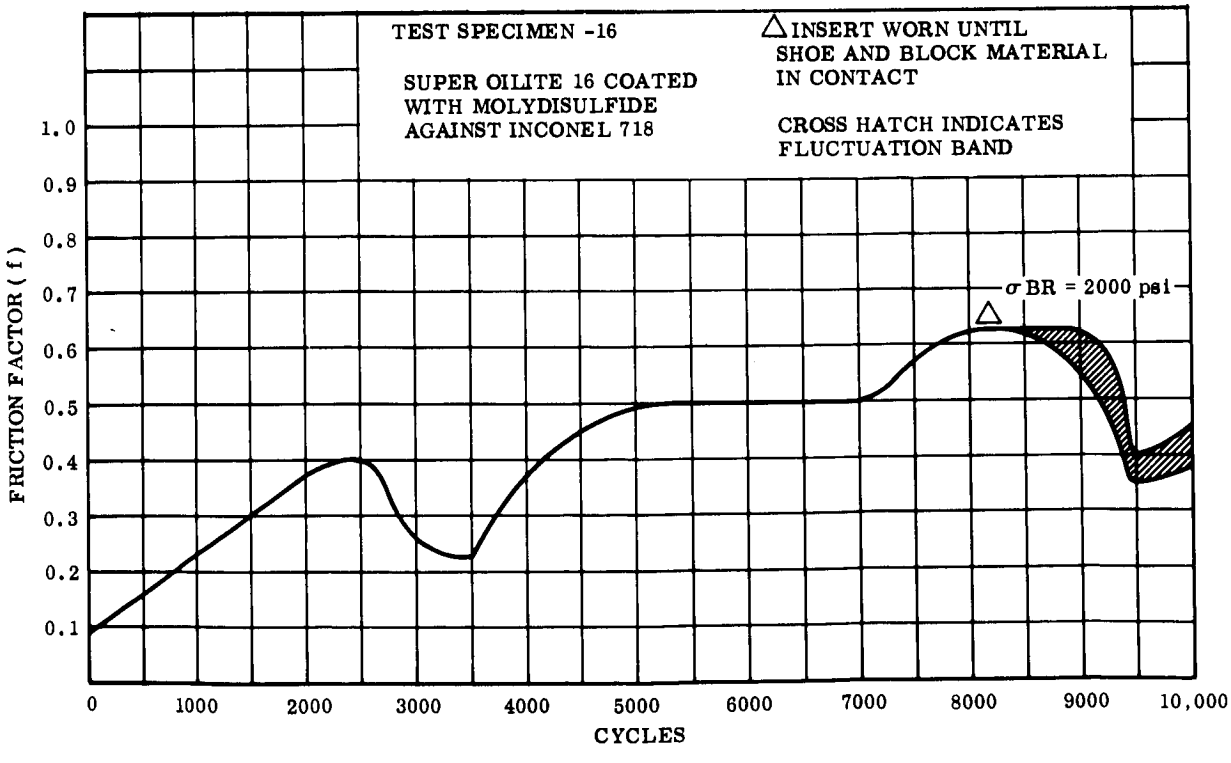


FIGURE 45. FRICTION FACTOR VERSUS CYCLES FOR TEST SPECIMEN - 16

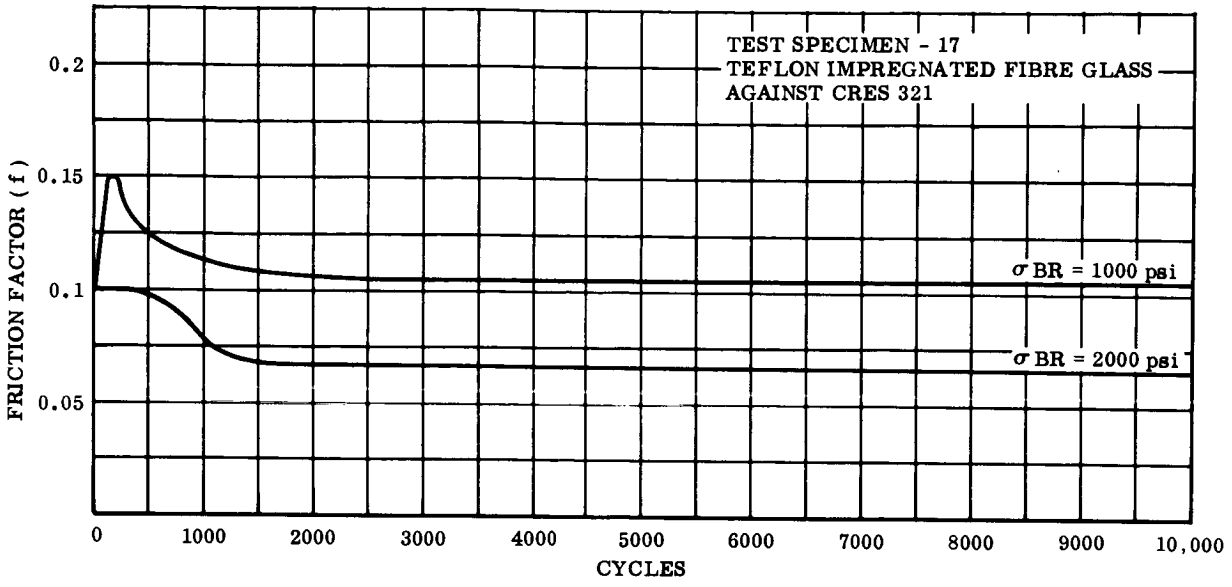


FIGURE 46. FRICTION FACTOR VERSUS CYCLES FOR TEST SPECIMEN - 17

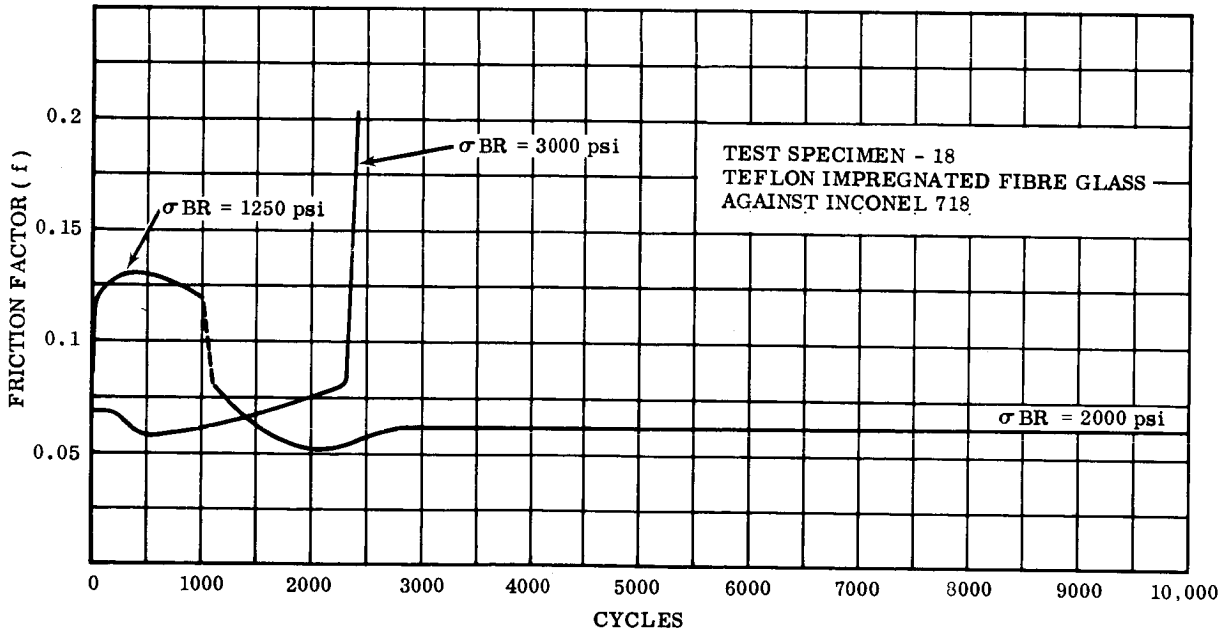


FIGURE 47. FRICTION FACTOR VERSUS CYCLES FOR TEST SPECIMEN - 18

# 5

## INSULATION

Liquid hydrogen ducting on the Saturn V vehicle are insulated with rigid metallic vacuum jackets. The scope of work in this contract dictated that insulation studies should not include this type of jacketing. A review of nonmetallic, nonrigid insulations used for tankage and other types of liquid hydrogen vessels and lines indicated that vacuum is still an important characteristic of an efficient insulation. The mission environment, which was envisioned for this study, was that of a vehicle required to restart its liquid hydrogen-fueled engines after relatively long periods of coasting in space. The heat leak to the fuel in the wetted lines during these coasting periods was assumed to be potentially higher than prior to lift-off and during launch. To meet this environment, an insulation is suggested (Fig. 48) which performs similar to some of the present tankage type insulations. This insulation consists of a heat-shrinkable Teflon tube which encapsulates a layer of Teflon wool similar to TEF-E-NUZ, a product of the W. S. Shamban Company. Inside the outer heat shrinkable Teflon tube would be a layer of aluminum foil acting as a radiation barrier. The ends of the heat-shrinkable Teflon tube would be sealed to the exterior of the liquid hydrogen duct adjacent to the flanges. The space containing the Teflon wool would be purged with a condensible gas such as carbon dioxide or nitrogen. During chill-down in ambient air, the condensible gas would create a vacuum within the heat-shrinkable Teflon tube causing atmospheric pressure to collapse the tube around the duct. While in atmosphere, this collapsed tube, which would compress the Teflon wool, would not be as efficient an insulation as a rigid vacuum jacket. However, as the vehicle leaves the atmosphere, the Teflon wool would have sufficient resiliency to spring the outer Teflon tube back to its original diameter thereby creating a vacuum jacket which would be highly efficient against heat sources such as the vehicle and the ambient temperature of space. The Teflon wool provides many, but long heat paths of high resistance from the inner tube to the radiation barrier. Being of small diameter filament, the stresses within the wool while compressed would not be high enough to permanently set the wool into a compacted condition.

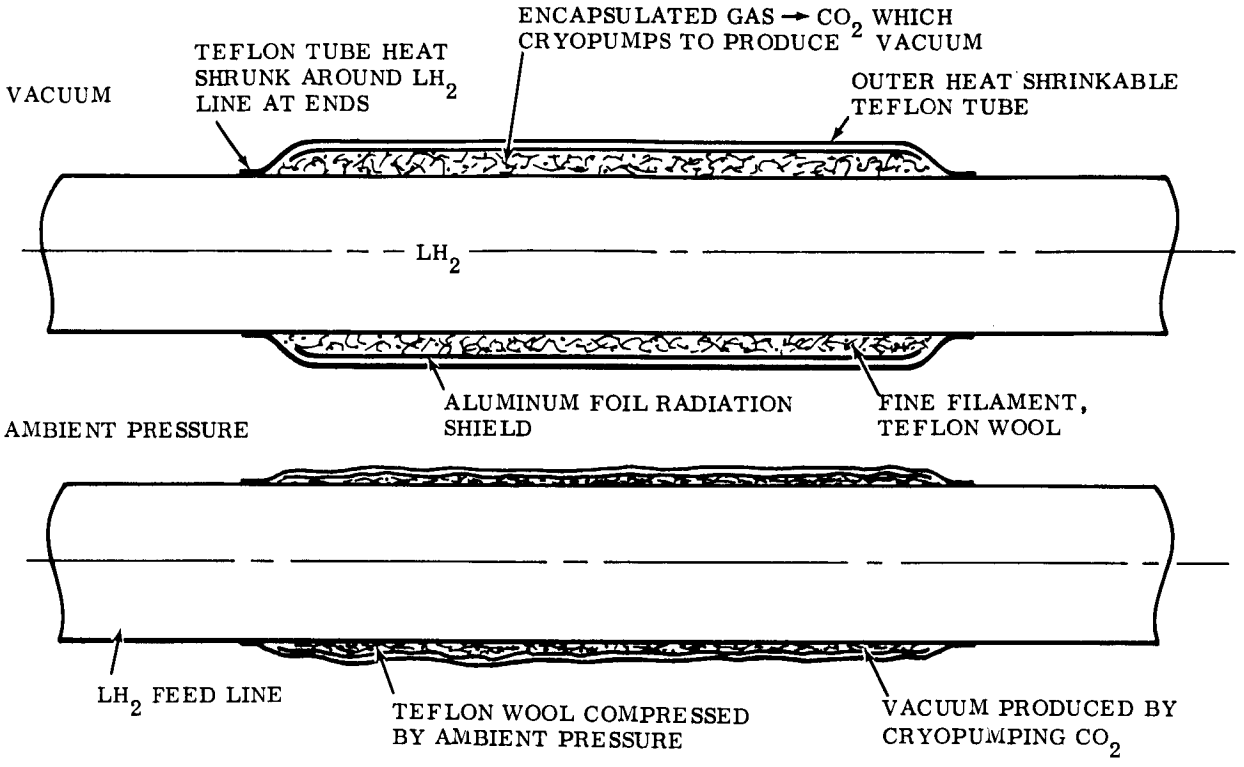


FIGURE 48. NONRIGID VACUUM INSULATION CONCEPT

# 6

## CONCLUSIONS AND RECOMMENDATIONS

The work attempted during this program was by no means intended to cover all the possible avenues of improvements in liquid hydrogen flexible ducting technology. The work that was done provides, in many instances, indications of areas of further fruitful effort.

Logically, we can conclude that the boltless flange concept, which consumed some of the effort in this program, has advantages over existing flanges and should be pursued in some future work. Practical problems still exist to its ultimate use in a flying system, such as the proper structural sealant material, but these are not considered to be insurmountable.

The weight of tubing in a flexible ducting system becomes important as system lengths increase. Materials of higher strength-to-density ratios than those which are being used today are presently available. However, little information exists as to these materials' ability to withstand the forces generated by a dynamic environment. It is recommended, therefore, that future work be devoted to analytical and empirical studies to more accurately predict the dynamic response of ducting systems and the ability of various materials to withstand these environments.

The flexible elbow described in Section III was presented as a concept. Future work should include analytical studies of the limits of this type of joint, and mechanical studies to determine the additional components which may be required for high-pressure applications. Trade-off studies based on weight, dynamic responses, and reliability should also be made to ascertain the usefulness of the concept. Empirical studies determining fabricability problems and performance characteristics should follow the analytical effort.

In this program, a number of flexible joint concepts were generated. Those which were pursued were felt to offer the greatest possible improvement in ducting systems. The low-profile gimbal joint and four-lug gimbal joint were basically novel applications of existing design techniques. The strength capability of the low-profile

gimbal concept was demonstrated during the program. The ability of the joint to withstand dynamic environments should be determined prior to any application of the concept. Weight and cost saving trade-offs on existing equipment should be made to demonstrate those areas where the fruits of this effort could be best applied.

Bellows-sealed ball joints seem to offer the most interesting area for further study. The implications of dynamically tuned ducting systems is interesting in light of the effort which went into the development of the large ducting systems being used on the Saturn V vehicle. The weight savings which can be achieved with use of the ball joint warrant additional studies and require development of anti-torque devices and lightweight rotational structures. The friction study which was conducted in this program and recorded in Section 4.7 attempted to establish a basis from which reliable designs could be made. The Teflon impregnated fibre glass offered the lowest coefficients of friction through the 10,000 cycle range. Most of the other specimens exhibited galling early in the cycling. However, the large amounts of bearing area which can be designed into ball-type joints offer the possibilities of reducing the bearing stresses far below those used in these tests thereby permitting the assumption that less sophisticated and less costly material combinations could be used. While cryogenic temperatures would enhance the cycling characteristics of most materials, experiments at these temperatures should be performed. Some test results indicate that lowering temperatures and providing heat sinks for dissipating frictional energy will greatly increase surface life. It is recommended, therefore, that this work be continued to include these untouched areas. In addition, this work did not answer the question as to the effect of surface velocities and accelerations attendant with different cycling rates and small excursions typical of dynamic responses.

The work on bellows squirm which was described in Section 4.6 was performed because squirm or instability is a design limit which tends to force specific minimums upon bellows spring rate and specific maximums on fatigue life. The inaccuracy of past analytical methods to predict critical squirm pressures resulted in higher than optimum spring rates. This work demonstrated the accuracy of the improvements made to predicting critical squirm pressure, which is based upon the realization that many bellows are operated above the plastic range of the material.

# APPENDIX I

## SOLAR ENGINEERING REPORT M-1794

## NASA BELLOWS SQUIRM PROGRAM

# ENGINEERING REPORT

NASA BELLOWS SQUIRM PROGRAM

REPORT M-1794 ISSUED 19 August 1965

**PREPARED BY**

D. T. Shen

D. T. Shen, Analytical Engineer

**APPROVED BY**

G. W. Bowers

G. W. Bowers, Group Engineer

H. T. Mischel

H. T. Mischel, Program Manager

CUSTOMER REF NAS8-11303

SOLAR REF 6-1612-7

SOLAR

A DIVISION OF INTERNATIONAL HARVESTER COMPANY
2200 PACIFIC HIGHWAY, SAN DIEGO, CALIFORNIA 92112

## SUMMARY

A series of convoluted metallic bellows were tested with internal pressure in an effort to prove the validity of a new analytical expression for critical squirm pressure in bellows. The expression had been discovered in recent space vehicle ducting programs at Solar, but test confirmation was needed to enable general application. Prior analytical method gave only approximate results. The new method was confirmed by the tests reported herein. The results show that critical squirm pressure for any bellows can be predicted within an accuracy of a few percent.

A total of forty-seven (47) bellows of two different materials and various configurations were tested. The two materials chosen were AISI type 321, an austenitic stainless steel; and Inconel 718, a high strength nickel base alloy. The bellows ranged in size from 3.3" to 3.6" outside diameter and all had 10 convolutions. Bellows of both single ply and two ply construction were tested. Generally, good agreement was found between the predicted and measured axial spring rate and critical pressure. Critical pressure ($P_{CR}$) was calculated using the expression:

$$P_{CR} = \frac{2\ SR_A}{L} \times \frac{E_t}{E}$$

where
- $SR_A$ = axial spring rate
- $L$ = axial length of bellows
- $E$ = elastic modulus
- $E_t$ = tangent modulus

It was also found that the critical pressure for Inconel 718 bellows is approximately 3 times that for AISI type 321 bellows of the same configuration.

# TABLE OF CONTENTS (CONT'D)

# TABLE OF CONTENTS (CONT'D)

SOLAR
A Division of International Harvester Company

ENGINEERING REPORT
NO. M-1794
DATE 8-19-65
PAGE 0 OF ____ PAGES
JOB NO. ____

SUBJECT: NASA BELLOWS SQUIRM PROGRAM
BY: D. SHEN

RESERVE THIS SPACE FOR BINDING.

## LIST OF SYMBOLS

| | | |
|---|---|---|
| $a$ | = | RADIUS OF CONVOLUTION, INCHES |
| $E$ | = | MODULUS OF ELASTICITY, PSI |
| $E_t$ | = | TANGENT MODULUS, PSI |
| $f_b$ | = | BENDING STRESS, PSI |
| $f_c$ | = | COMPRESSIVE MERIDIONAL MEMBRANE STRESS, PSI |
| $I$ | = | MOMENT OF INERTIA, $IN^4$ |
| I.D. | = | INSIDE DIAMETER, INCHES |
| $L$ | = | BELLOWS TEST LENGTH, INCHES |
| $l$ | = | FREE LENGTH OF BELLOWS, INCHES |
| $M$ | = | BENDING MOMENT, LB-IN |
| $N$ | = | NO. OF CONVOLUTIONS |
| $n$ | = | NO. OF PLIES |
| O.D. | = | OUTSIDE DIAMETER, INCHES |
| $P_{cr}$ | = | CRITICAL PRESSURE OR SQUIRM PRESSURE, PSI |
| $R$ | = | RADIUS, INCHES |
| $R_M$ | = | MEAN RADIUS OF BELLOWS, INCHES |
| $SR_A$ | = | AXIAL SPRING RATE, LB/IN |
| $t$ | = | THICKNESS PER PLY, INCHES |
| $\delta$ | = | AMOUNT OF EXTENSION OR COMPRESSION, INCHES |
| $\theta$ | = | ANGULATION, DEGREES |

SADI 1:38 REV. 2/64

# INTRODUCTION

INTERNAL PRESSURE INSTABILITY, SOMETIMES CALLED SQUIRM, CAN BE A SERIOUS PROBLEM FOR UNRESTRAINED BELLOWS IN A PRESSURIZED SYSTEM. THE PROBLEM MAY BECOME MORE COMPLICATED IF THE BELLOWS IS SUBJECTED TO EITHER AXIAL OR ANGULATED MOTIONS. THIS INSTABILITY PROBLEM WAS FIRST INVESTIGATED BY HARINGX IN REF. 2. SINCE THEN VERY FEW REPORTS HAVE BEEN WRITTEN IN RELATION TO THIS PROBLEM. RECENTLY ANDERSON (REF. 4) TRIED TO GATHER ALL AVAILABLE DATA AND ESTABLISH A DESIGN RECOMMENDATION FOR THE ASA CODE FOR PRESSURE PIPING. HE PROPOSED A SAFETY FACTOR OF 10 BE USED FOR MOST BELLOWS INSTABILITY DESIGNS. HE ALSO INDICATED THAT THERE IS NOT A PRACTICAL FORMULA THAT WILL CORRELATE CLOSELY WITH TEST RESULTS. THIS IS PROBABLY DUE TO LACK OF BOTH EXHAUSTIVE ANALYTICAL STUDY AND EXTENSIVE EXPERIMENTAL VERIFICATION.

IN THE CONVENTIONAL EQUATION, THE SQUIRM PRESSURE OR CRITICAL INSTABILITY PRESSURE IS DIRECTLY PROPORTIONAL TO MODULUS OF ELASTICITY E. SQUIRM PRESSURE PREDICTIONS USING THE CONVENTIONAL EQUATION ARE ACCURATE ONLY WHEN THE STRESS STATE OF THE BELLOWS REMAINS WITHIN THE ELASTIC LIMIT. ONCE THE COMPRESSIVE MERIDIONAL MEMBRANE STRESS IN THE BELLOWS BECOMES PLASTIC, THE ELASTIC MODULUS NO LONGER APPLIES, BUT NO PRIOR WORK HAS DEVELOPED

## INTRODUCTION (CONT'D)

A CORRECTION FACTOR OR A NEW FORMULA THAT WILL PREDICT WITH ANY REASONABLE ACCURACY THE BELLOWS SQUIRM BEHAVIOR IN THE PLASTIC RANGE.

IN RECENT DUCTING PROGRAMS AT SOLAR, THE AUTHOR CONCEIVED AND APPLIED THE USE OF THE TANGENT MODULUS AS A FACTOR IN THE SQUIRM PRESSURE EQUATION. THIS PARALLELS THE TREATMENT OF PRIMARY COLUMN INSTABILITY WHEREIN THE TANGENT MODULUS IS USED IN THE PLASTIC RANGE. IT APPEARED REASONABLE THAT THE SAME TREATMENT COULD BE APPLIED TO BELLOWS INSTABILITY AND A FEW TRIAL TESTS SUPPORTED THIS HYPOTHESIS. FOR FULL CONFIRMATION, A SERIES OF TESTS WERE THUS CARRIED OUT, USING TWO MATERIALS WITH ESSENTIALLY THE SAME ELASTIC MODULUS, BUT WITH WIDELY DIFFERENT ELASTIC LIMITS. THE TESTS AND THEIR RESULTS ARE REPORTED HEREIN.

THE BELLOWS SPECIMENS WERE MADE OF AISI 321 AND INCONEL 718 MATERIALS. THE GEOMETRY OF THE BELLOWS WAS LIMITED TO THE GENERAL CONVOLUTED CLASS WITH VARIATIONS IN SPAN HEIGHT, THICKNESS, RADIUS OF CONVOLUTION AND NUMBER OF PLIES. SQUIRM TESTS WERE CONDUCTED IN A STRAIGHT POSITION AS WELL AS IN AN ANGULATED POSITION, AND IN ALL CASES, THE TESTS WERE CONDUCTED AT ROOM TEMPERATURE.

## INTRODUCTION (CON'D)

IN THE REDUCTION & INTERPRETATION OF DATA, COMPARISONS WERE MADE BETWEEN COMPUTED AND MEASURED SPRING RATES AND SQUIRM PRESSURES. THE DIFFERENCE IN SQUIRM PRESSURES ON SIMILAR BELLOWS ARE ALSO PRESENTED AND DISCUSSED. THE SQUIRM TEST OF AN ANGULATED BELLOWS IS REPORTED AND COMPARED WITH THE ANALYTICAL PREDICTION.*

AN ATTEMPT WAS MADE TO DETERMINE THE EFFECT ON THE SQUIRM PRESSURE OF AXIALLY PRELOADING THE BELLOWS, BUT CERTAIN LIMITATIONS MADE THE RESULTS QUESTIONABLE. AN EXPLANATION ALSO WAS SOUGHT FOR THE NON-LINEARITY OF BELLOWS IN SPRING RATE TENSION AND COMPRESSION TESTS, BUT THE RESULTS WERE INCONCLUSIVE. IT HAS BEEN THOUGHT TO BE A TYPE OF SECONDARY INSTABILITY, BUT THIS HAS NOT BEEN PROVED YET.

* THE ANALYTICAL PREDICTION IS REFERRED TO THE CALCULATION OF BELLOWS SQUIRM BASED ON DWG. DIMENSIONS. THE PREDICTED VALUES CAN ALSO BE FOUND IN REF. 6

# METHOD OF ANALYSIS

IN ATTEMPTING TO DERIVE A SIMPLE SQUIRM PRESSURE EQUATION FOR BELLOWS, THE FOLLOWING ASSUMPTIONS ARE MADE:

1. THE BELLOWS ASSEMBLY BEHAVES LIKE A BEAM. THEREFORE BEAM THEORY WILL BE APPLIED IN THE DERIVATIONS.

2. FOR TWO-PLY BELLOWS, THE SPRING RATE OF THE INNER PLY IS ASSUMED TO BE THE SAME AS THE OUTER PLY.

3. THE MERIDIONAL BENDING STRESS DUE TO AXIAL COMPRESSION OR ANGULATED MOTIONS IS CONSIDERED DIRECTLY ADDITIVE TO THE MERIDIONAL COMPRESSIVE STRESS DUE TO INTERNAL PRESSURE. IN OTHER WORDS, THE MAXIMUM RESPECTIVE STRESSES ARE ASSUMED TO ACT AT THE SAME POINT, WHICH IS THE ROOT OF THE CONVOLUTION.

4. AXIAL SPRING RATE AND BENDING STRESS IN A BELLOWS ARE ASSUMED PROPORTIONAL TO MODULUS OF ELASTICITY $E$ IN THE ELASTIC RANGE AND TO THE TANGENT MODULUS $E_t$ IN THE PLASTIC RANGE.

# METHOD OF ANALYSIS

## CONVENTIONAL SQUIRM EQUATION

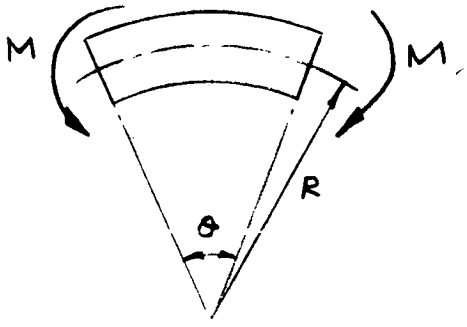


ASSUME THE BELLOWS BENDING LIKE A BEAM.

FROM BEAM THEORY, $\frac{M}{I} = \frac{E}{R}$

OR $EI = MR$

L, THE LENGTH OF BELLOWS $= R\theta$ $\quad \therefore R = \frac{L}{\theta}$

$\therefore (EI) = \frac{ML}{\theta}$ $\quad$ $\theta$, HERE, IS IN RADIANS

BUT $\frac{M}{\theta}$ = ANGULATION SPRING RATE OF BELLOWS (LB-IN/RADIAN)

$= SR_A \times \frac{R_m^2}{2}$ $\quad$ [REF. 1]

WHERE $SR_A$ = AXIAL SPRING RATE OF BELLOWS

$R_M$ = MEAN RADIUS OF BELLOWS

$(EI) = SR_A \times \frac{R_m^2}{2} L$ $\quad$ —(1)

THE CRITICAL LOAD FOR A STRUT WITH BOTH ENDS FIXED IS

$\frac{4\pi^2 (EI)}{L^2}$ $\quad$ —(2)

SUBSTITUDE (1) INTO (2) $\quad$ CRITICAL LOAD $= \frac{4\pi^2}{L^2} \times SR_A \times \frac{R_m^2}{2} \times L$

## METHOD OF ANALYSIS

### SQUIRM IN A STRAIGHT POSITION

$\therefore$ CRITICAL LOAD $= \frac{2\pi^2}{L} \times SR_A \times R_m^2$ — (3)

BUT CRITICAL LOAD = CRITICAL PRESSURE × AREA OF BELLOWS

$= P_{cr} \times \pi R_m^2$ — (4)

from (3) & (4)

$$P_{cr} = \frac{2\pi}{L} \times SR_A$$

CONVENTIONAL SQUIRM EQUATION — ELASTIC RANGE ONLY — (5)

AVERAGE CROSS-SECTIONAL AREA OF BELLOWS MATERIAL IS

$2\pi R_m t \times n$ WHERE $n$ = NO. OF PLIES

$\therefore$ COMPRESSIVE STRESS $f_c = \frac{\text{CRITICAL LOAD}}{2\pi R_m t\, n}$

SUBSTITUDE (3) INTO ABOVE $f_c = \frac{SR_A \times \pi R_m}{n t L}$ — (6)

FOR STRESS IN ELASTIC RANGE, $SR_A$ IS PROPORTIONAL TO $E$, THE YOUNG'S MODULUS. HOWEVER, IF STRESS IS IN PLASTIC RANGE $E_t$, THE TANGENT MODULUS HAS TO BE USED

i.e. $$f_c = \frac{SR_A \times \pi R_m}{n t L} \times \frac{E_t}{E}$$ — (7)

CONSEQUENTLY $P_{cr}$, SQUIRM PRESSURE $= \frac{2\pi}{L} \times SR_A \times \frac{E_t}{E}$ — (8)

## METHOD OF ANALYSIS

### SQUIRM IN AN ANGULATED POSITION

FOR BELLOWS PRESSURIZED IN AN ANGULATED POSITION, THE COMPRESSIVE BENDING STRESS MUST BE INCLUDED IN THE COMPRESSIVE STRESS, $f_c$ EQUATION.

LET THE BENDING STRESS BE $f_b$

FROM (7)

$$\text{TOTAL } f_c = \left[\frac{SR_A \times \pi R_m}{n t L} + f_b\right] \times \frac{E_t}{E} \qquad -(9)$$

AND $P_{cr}$, SQUIRM PRESSURE $= \frac{2\pi}{L} \times SR_A \times \frac{E_t}{E}$

THE CALCULATION OF SQUIRM PRESSURE IS AS FOLLOWS: (ANGULATED)

(i) CALCULATE $SR_A$ & $f_b$ USING CONVENTIONAL METHOD

(ii) USING A COMPRESSIVE STRESS - TANGENT MODULUS CURVE, $E_t$ CAN BE OBTAINED FROM EQUATION (9)

(iii) WITH $E_t$ KNOWN, $P_{cr}$ THE SQUIRM PRESSURE CAN BE COMPUTED.

IN THIS PRESENT REPORT, IBM PROGRM BASED ON REF. 5 IS EMPLOYED TO CALCULATE $SR_A$ & $f_b$.

SEE APPENDIX A & APPENDIX B FOR SAMPLE CALCULATIONS.

# DEVELOPMENT TEST DESCRIPTION

FORTY-SEVEN (47) CONVOLUTED BELLOWS, SOLAR PART NUMBER 9101 THROUGH 9126, WERE MANUFACTURED FROM INCONEL 718 (A HIGH STRENGTH NICKEL BASE ALLOY) AND AISI 321 STAINLESS STEEL. GEOMETRICAL VARIATIONS INCLUDE WALL THICKNESS, SPAN HEIGHT, CONVOLUTION RADIUS, NUMBER OF PLIES AND FREE LENGTH.

A SKETCH OF A TYPICAL TEST SPECIMEN IS SHOWN ON THE FOLLOWING PAGE. A LIST OF THE TEST SPECIMENS AND THEIR IDENTIFICATION NUMBER AND DRAWING DIMENSIONS CAN BE FOUND ON PAGE 10.

FOR DETAIL TEST SET-UP, TEST EQUIPMENT AND TEST PROCEDURES, PART OF REF. 8 IS INCLUDED IN APPENDIX E FOR REFERENCE.

# GEOMETRY OF TEST SPECIMEN

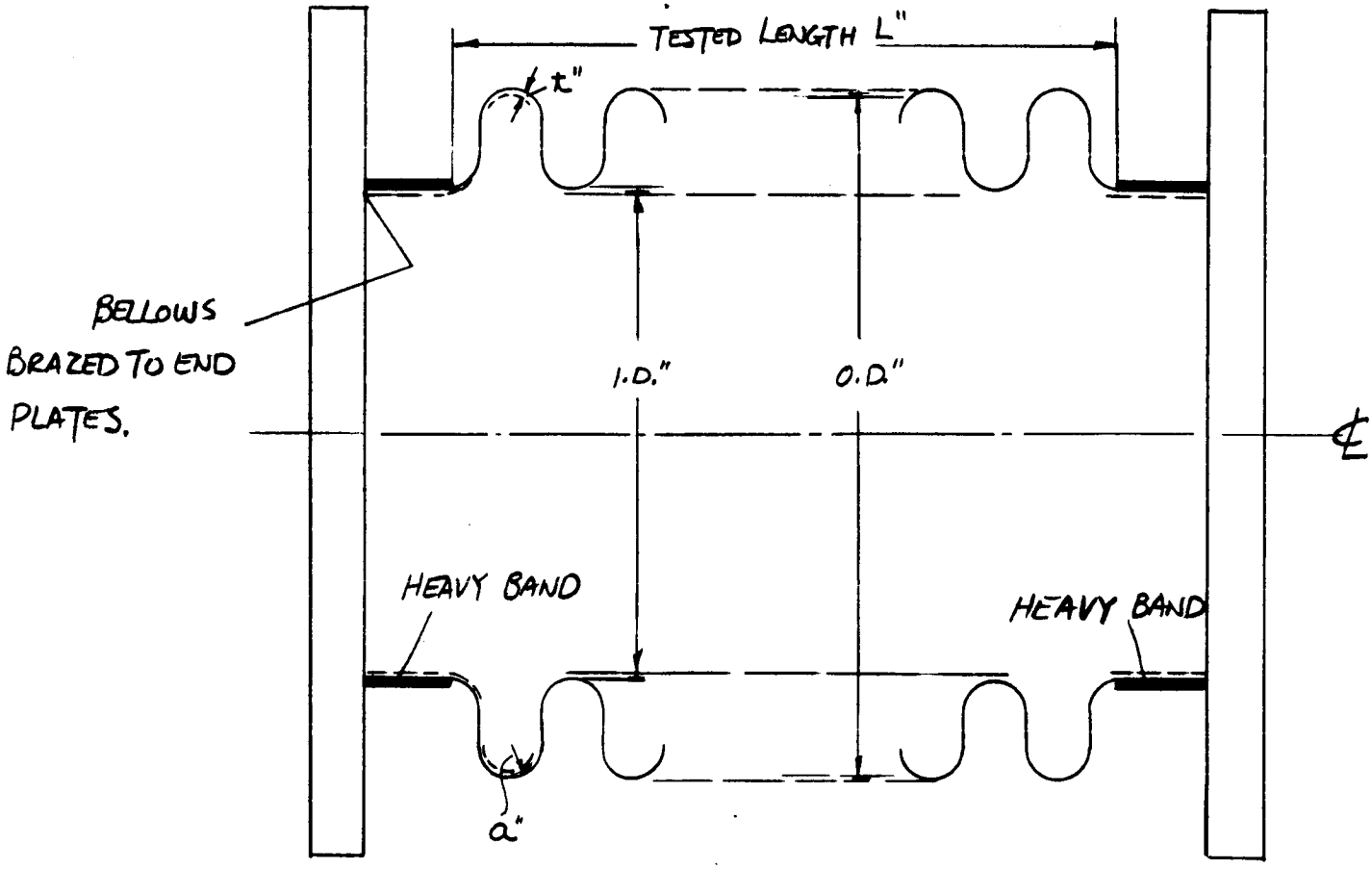


$n$ = NO. OF PLIES
$N$ = NO. OF CONVOLUTIONS = 10
$t$ = THICKNESS PER PLY
O.D. = OUTSIDE DIAMETER
I.D. = INSIDE DIAMETER
$a$ = RADIUS OF CONVOLUTION
$L$ = TESTED LENGTH.

NOTE THAT $a$, I.D. & O.D. ARE MEASURED TO THE MID-PLANE OF PLY. (FOR 2-PLY BELLOWS, $a$, I.D. & O.D. ARE MEASURED TO THE PLANE BETWEEN PLIES)

SOLAR
A Division of International Harvester Company

ENGINEERING REPORT
NO. M-1794
DATE 8-19-65
PAGE 10 OF ____ PAGES
JOB NO. ____

SUBJECT: NASA BELLOWS SQUIRM PROGRAM
BY: D. SHEN

## LIST OF TEST SPECIMENS AND THEIR DRAWING DIMENSIONS

I. D. = 2.91"  L" = SEE TEST LENGTH IN RESULT APPENDIX D

N = 10

| O.D." | a" | t" (n) | DRAWING NO. & SPECIMEN NO. | |
|---|---|---|---|---|
| | | | AISI 321 | INCONEL 718 |
| 3.3 | 0.074 | 0.010 (1) | 9101-1, 9101-2 | 9102-1, 9102-2 |
| 3.3 | 0.074 | 0.010 (2) | 9103 | |
| 3.3 | 0.074 | 0.012 (1) | 9104-1, 9104-2 | 9105-1, 9105-2 |
| 3.3 | 0.074 | 0.012 (2) | 9106 | |
| 3.3 | 0.057 | 0.010 (1) | 9107-1, 9107-2 | |
| 3.3 | 0.057 | 0.012 (1) | 9108-1, 9108-2, 9108-3 | |
| 3.4 | 0.074 | 0.010 (1) | 9109 | |
| 3.4 | 0.074 | 0.012 (1) | 9111-1, 9111-2 | 9112-1, 9112-2 |
| 3.4 | 0.057 | 0.010 (1) | 9113-1, 9113-2, 9113-3 | 9114-1, 9114-2 |
| 3.4 | 0.057 | 0.010 (2) | 9115 | |
| 3.4 | 0.057 | 0.012 (1) | 9116-1, 9116-2 | |
| 3.6 | 0.074 | 0.010 (1) | 9117 | 9118-1, 9118-2 |
| 3.6 | 0.074 | 0.010 (2) | 9119 | |
| 3.6 | 0.074 | 0.012 (1) | 9120-1, 9120-2 | 9121-1, 9121-2 |
| 3.6 | 0.057 | 0.010 (1) | 9122-1, 9122-2 | 9123-1, 9123-2, 9123-3 |
| 3.6 | 0.057 | 0.010 (2) | 9124 | |
| 3.6 | 0.057 | 0.012 (1) | 9125-1, 9125-2, 9125-3 | 9126-1, 9126-2 |

RESERVE THIS SPACE FOR BINDING.

SADI 138 REV. 2/64

## TEST DESCRIPTION – MATERIAL PROPERTIES.

STANDARD TEST COUPONS WERE CUT FROM SAME SHEET AS THE BELLOWS, AND THE CUTTING DIRECTION WAS AT RANDOM. THE INCONEL 718 COUPONS WERE HEAT TREATED WITH THE INCONEL 718 BELLOWS. THE AISI 321 BELLOWS ARE IN AN ANNEALED CONDITION, AS ARE THE RESPECTIVE COUPONS. A TOTAL OF TWENTY FOUR (24) COUPONS WERE TESTED

FOR REFERENCE PURPOSES, ONE PAIR EACH OF INCONEL 718 AND AISI 321 COUPONS WERE CUT AT 90 DEGREES TO EACH OTHER. THE INCONEL 718 COUPONS WENT THROUGH THE SAME HEAT TREATMENT AS THE BELLOWS AND ALL WERE TENSILE TESTED. THE CORRESPONDING STRESS–STRAIN CURVES ARE SHOWN ON PAGES C-2 & C-3.

SOLAR
A Division of International Harvester Company

ENGINEERING REPORT
NO. M-1799
DATE 8-19-65
PAGE 12 OF ____ PAGES
JOB NO. ____

SUBJECT: NASA BELLOWS SQUIRM PROGRAM
BY: D. SHEN

RESERVE THIS SPACE FOR BINDING.

# TEST DISCRIPTION

## SPRING RATE TEST

COMPRESSION AND TENSION SPRING RATE TESTS WERE PERFORMED ON ALL BELLOWS AS THEY CAME OFF BELLOWS FORMING MACHINE IN THE AS-MANUFACTURED CONDITION, AND AGAIN AFTER BEING DEFORMED TO SPECIFIED LENGTH (AFTER-SIZING CONDITION).

A TYPICAL LOAD-DEFLECTION CURVE IS ILLUSTRATED AT RIGHT.

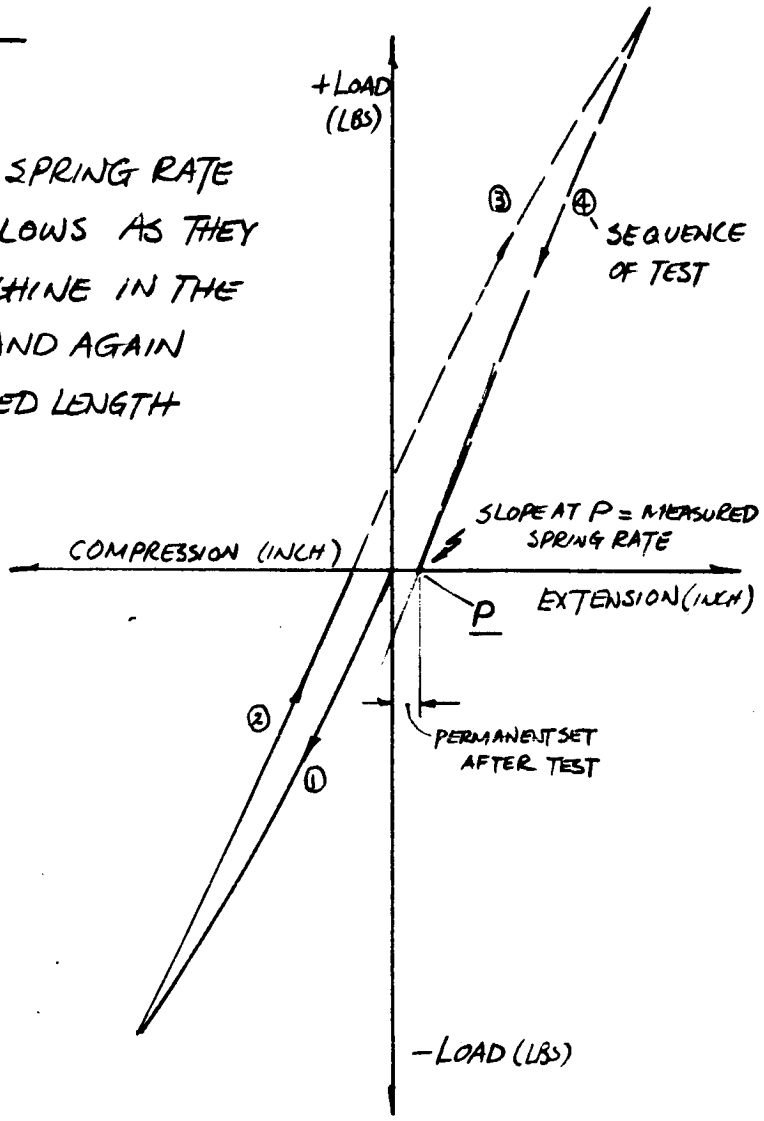


TYPICAL LOAD-DEFLECTION CURVE

SADI 138 REV. 2/64

# TEST DESCRIPTION

## SQUIRM PRESSURE TEST

THE BELLOWS WERE PRESSURIZED BY A HYDRAULIC PUMP. THE PRESSURE WAS CONTROLLED IN SUCH A WAY THAT THE RATE OF PRESSURE RISE WAS NEARLY CONSTANT. A SLIGHT PRESSURE DROP DURING THE RISE PERIOD USUALLY WAS AN INDICATION OF INSTABILITY. THIS PRESSURE DROP COULD EASILY BE NOTED ON THE STRIP RECORDER. (SEE P. 37 FOR A TYPICAL CHART)

DUE TO A MISUNDERSTANDING, THE TEST BELLOWS WERE MANUFACTURED WITH LONG UNSUPPORTED ENDS. THIS RESULTED IN TWO BELLOWS BEING TESTED WITHOUT OBTAINING THE TRUE SQUIRM SINCE THE UNSUPPORTED CYLINDRICAL ENDS OF THE BELLOWS BULGED DRASTICALLY. LIGHT SHEET METAL BANDS WERE THEN USED TO STIFFEN THE ENDS. AFTER NINE (9) MORE BELLOWS WERE SQUIRM TESTED, IT WAS DECIDED THAT THE TIGHTENING DEVICE OF THE LIGHT SHEET METAL BAND WAS SIMPLY NOT ADEQUATE; BULGING OF THE ENDS STILL EXISTS THOUGH MUCH LESS SEVERE. MACHINED BANDS WERE THEN MADE AND USED ON THE REST OF THE BELLOWS TO BE SQUIRM TESTED. EACH MACHINED BAND CONSISTED OF TWO SPLIT RINGS WHICH WERE BOLTED AT EACH CYLINDRICAL END SECTION OF THE BELLOWS. THE RESULTS OF THE TWO BELLOWS TESTED WITH NO BANDS AND THE NINE WITH LIGHT SHEET METAL BANDS WERE TREATED IN A SEPARATE SECTION. (SEE P. 19, 25 & 26)

## TEST DESCRIPTION

### SQUIRM PRESSURE TEST (CONT'D)

IT WAS UNFORTUNATE THAT ALL BELLOWS PLANNED TO BE SQUIRM TESTED AT AN EXTENDED OR COMPRESSED LENGTH (PRE-STRESSED) WERE IN THIS GROUP.

NOTE: FOR ALL PREDICTED SQUIRM BASED ON DRAWING DIMENSION, SEE PROPOSED WORK IN REF. 6.

## RESULTS - SPRING RATES

BOTH THE SPRING RATE AND BENDING STRESS (USED IN SQUIRM PRESSURE CALCULATION) DUE TO DEFLECTION & ANGULATION ARE COMPUTED BY SOLAR PROGRAM 224. THIS PROGRAM IS BASED ON THE ARTICLE 'ANALYSIS OF U-SHAPE EXPANSION BELLOWS' WRITTEN BY LAUPA & WEIL. (REF. 5) UNLESS OTHERWISE NOTED, THE INPUT USED ARE AVERAGE MEASURED DIMENSIONS.

THE SPRING RATE OF A BELLOWS IS DETERMINED FROM THE LOAD-DEFLECTION CURVE OF THE PARTICULAR BELLOWS. THE SLOPE AT THE END POINT OF EACH LOAD DEFLECTION CURVE IS CHOSEN TO BE THE SPRING RATE OF THAT BELLOWS, AS SHOWN ON PAGE 12. COMPUTED AND MEASURED SPRING RATE COMPARISONS ARE TABULATED SEPARATELY FOR AISI 321 BELLOWS AND INCONEL 718 BELLOWS ON PAGES 20 & 22.

FROM THE TEST RESULTS, IN GENERAL, THE SPRING RATE TENDS TO BECOME LOWER IN THE SECOND SPRING RATE TEST. IT ALSO SHOWS THAT INCONEL 718 BELLOWS SEEMS TO GIVE BETTER CORRELATION THAN THE AISI 321 BELLOWS.

## RESULTS - SQUIRM PRESSURE (BELOWS TESTED WITH MACHINED BANDS)

IN ORDER TO COMPUTE THE THEORETICAL SQUIRM PRESSURE, THE TANGENT MODULUS $E_t$ MUST BE KNOWN. THE TANGENT MODULUS CURVES, IN THIS REPORT, ARE CONSTRUCTED FROM THE STRESS-STRAIN CURVES OF THE TEST COUPONS.

SINCE THE TEST COUPONS HAD BEEN CUT AT RANDOM FROM THE SHEETS, IT WAS SUSPECTED THAT DUE TO ANISTROPY THERE WOULD BE A MARKED DIFFERENCE IN THE STRESS-STRAIN CURVES FOR THE TWO PRINCIPAL DIRECTIONS, LONGITUDINAL AND TRANSVERSE. FOR INCONEL 718, THE CURVES ARE SEGREGATED INTO TWO GROUPS BY VIRTUE OF THE SLOPE OF THE TANGENT MODULUS CURVE. THEY ARE IDENTIFIED AS GROUPS A AND B AS SHOWN ON PAGE C-4. THE AISI 321 STRESS-STRAIN CURVES, HOWEVER, SEEM TO DEPEND PRIMARILY ON THE TEST COUPON THICKNESS. THE THICKER SPECIMEN GIVES A HIGHER STRESS THAN THE THINNER SPECIMEN AT THE SAME STRAIN LEVEL IN THE PLASTIC REGION. THE COMPUTED RANGE OF BELLOWS SQUIRM PRESSURE BASED ON MEASURED DIMENSIONS IS TABULATED IN COMPARISON FORM ON PAGES 21 AND 23 FOR INCONEL 718 AND AISI 321 RESPECTIVELY.

PRIOR TO THE DEVELOPMENT TEST, SQUIRM PRESSURES BASED ON DRAWING DIMENSIONS OF THE TEST SPECIMENS

## RESULTS - SQUIRM PRESSURE (CONT'D)

WERE COMPUTED TO PREDICT EACH BELLOWS INSTABILITY. (SEE REF 6 ) THE TANGENT MODULUS CURVES FOR INCONEL 718 AND AISI 321 USED IN THIS CASE ARE ACTUAL PUBLISHED DATA AS INDICATED ON PAGE C-1. THESE PREDICTED SQUIRM PRESSURES ARE ALSO TABULATED WITH THE ACTUAL TEST RESULTS ON PAGES 21 & 23.

THE PREDICTED RESULTS BASED ON DRAWING DIMENSIONS OF INCONEL 718 BELLOWS ALL FALL WITHIN THE RANGE OF 0.694 AND 1.48 TIMES THE ACTUAL TEST VALUE. THE MINIMUM COMPUTED SQUIRM PRESSURE FOR INCONEL 718 BELLOWS BASED ON MEASURED DIMENSION IN MOST CASES ARE LOWER OR ABOUT EQUAL TO THE TESTED VALUES. [EXCEPT ONE OUT OF TOTAL SIXTEEN BELLOWS, WHICH HAD A PREDICTED SQUIRM PRESSURE 19.4 % HIGHER THAN THE ACTUAL TEST VALUE.]

THE AISI 321 BELLOWS, HOWEVER, DO NOT GIVE AS PREDICTABLE RESULTS AS THE INCONEL 718 BELLOWS. IN SIXTEEN OUT OF THE TWENTY BELLOWS TESTED, THE PREDICTED SQUIRM PRESSURES BASED ON DRAWING DIMENSIONS ARE SOMEWHAT LOWER OR COMPARABLE TO THE TEST VALUES. THE REMAINING FOUR (4) BELLOWS ALL HAVE HIGH COMPUTED VALUES, THE MAXIMUM BEING TWICE THE TESTED VALUE. THE SAME FOUR BELLOWS ALSO GIVE HIGHER MINIMUM COMPUTED SQUIRM PRESSURES WHEN ACTUAL MEASURED DIMENSIONS ARE USED.

## RESULTS - SQUIRM PRESSURE (CONT'D)

THE OVERALL TEST RESULTS INDICATE THAT NONE OF THE PREDICTED SQUIRM VALUES, NOR THE COMPUTED MINIMUM SQUIRM EXCEEDS MORE THAN TWICE THE TEST VALUE - AN OVERALL RESULT WHICH IS CONSIDERED TO BE QUITE GOOD SINCE EVEN IN THE BUCKLING OF SHELLS, SUCH AGREEMENT BETWEEN TEST DATA AND PREDICTED VALUE WOULD HAVE BEEN CONSIDERED ACCEPTABLE. ASIDE FROM THIS OVERALL PICTURE, THE MOST SIGNIFICANT RESULT IN THIS DEVELOPMENT PROGRAM IS THAT FOR BELLOWS OF IDENTICAL DRAWING DIMENSIONS THE INCONEL 718 BELLOWS HAS THREE (3) TIMES THE SQUIRM PRESSURE OF AISI 321 BELLOWS. A TABLE OF COMPARISON, INCLUDING THE PREDICTED VALUES IS SHOWN OF PAGE 24. THE REMARKABLE CONSISTENCY OF THE COMPARATIVE RESULTS COMLETELY CONTRADICTS THE CONVENTIONAL SQUIRM PRESSURE FORMULA $\frac{2\pi SR_A}{L}$ WHERE $SR_A$ IS PROPORTIONAL TO E.

## RESULTS - SQUIRM PRESSURE ( BELLOWS TESTED WITH OR WITHOUT LIGHT BANDS )

THE RESULTS OF THE MISTREATED GROUP OF BELLOWS TESTED WITH OR WITHOUT LIGHT SHEET METAL BANDS ARE TABULATED ON PAGES 25 & 26. IF RESULTS OF THE TWO TEST SPECIMENS WITHOUT BANDS ARE VOIDED, SEVEN OF THE NINE PREDICTED VALUES FALL WITHIN THE RANGE OF 0.586 AND 1.083 TIMES THE TEST VALUES WHILE THE REMAINING TWO ARE ABOUT TWICE THE TEST SQUIRM PRESSURES. IT HAS TO BE POINTED OUT THAT THE PREDICTED SQUIRM PRESSURE CALCULATION DO NOT INCLUDE THE EFFECT OF PRESTRESSING DUE TO PRE-DEFORMATION $\delta$.

THE EFFECT OF PRE-DEFORMATION ON INSTABILITY CAN BE BEST ILLUSTRATED IN TABLE OF COMPARISON SHOWN ON PAGE 26. WHILE A POSITIVE STATEMENT CAN NOT BE MADE DUE TO LIMITED TEST RESULTS, IT HAS TO BE NOTED THAT CONVENTIONAL SQUIRM PRESSURE FORMULA $2\pi SR_A/L$ DOES NOT QUITE HOLD TRUE HERE (IN CASE OF CONSTANT $SR_A$) IF INITIAL STRESS IS TO BE APPLIED.

SOLAR
A Division of International Harvester Company

ENGINEERING REPORT
NO. M-1794
DATE 8-19-65
PAGE 20 OF ____ PAGES
JOB NO. ____

SUBJECT: NASA BELLOWS SQUIRM PROGRAM
BY: D. SHEN

RESERVE THIS SPACE FOR BINDING.

# COMPARISON OF COMPUTED & TESTED SPRING RATES (INC. 718 BELLOWS)

| ITEM | O.D." / I.D." | a" | t"(n) | COMPUTED * SPRING RATE (LB/IN) | SPRING RATE AS MANUFACTURED | SPRING RATE AFTER SIZING |
|---|---|---|---|---|---|---|
| 9102-1 | 3.285 / 2.924 | 0.06975 | 0.01 (1) | 1473 | — | 1,180.0 |
| 9102-2 | 3.29 / 2.921 | 0.0705 | 0.01 (1) | 1,395 | 1,500.0 | 1.025.0 |
| 9105-1 | 3.276 / 2.923 | 0.0715 | 0.012 (1) | 2,574 | 2,000.0 | 2,000.0 |
| 9105-2 | 3.279 / 2.917 | 0.069 | 0.012 (1) | 2,404 | 2,220.0 | 2,260.0 |
| 9112-1 | 3.373 / 2.923 | 0.069 | 0.012 (1) | 1,377 | 1,380.0 | 1,356.0 |
| 9112-2 | 3.372 / 2.923 | 0.0685 | 0.012 (1) | 1,384 | 1250.0 | 1,290.0 |
| 9114-1 | 3.389 / 2.905 | 0.058 | 0.01 (1) | 681.7 | 740.0 | 548.0 |
| 9114-2 | 3.392 / 2.908 | 0.058 | 0.01 (1) | 682.3 | 715.0 | 500.0 |
| 9118-1 | 3.616 / 2.918 | 0.077 | 0.01 (1) | 269.3 | 312.0 | 263.0 |
| 9118-2 | 3.596 / 2.903 | 0.0795 | 0.01 (1) | 276.6 | 332.0 | 241.0 |
| 9121-1 | 3.59 / 2.908 | 0.0692 | 0.0125 (1) | 468 | 465.0 | 416.0 |
| 9121-2 | 3.57 / 2.905 | 0.068 | 0.0125 (1) | 561.3 | 526.0 | 410.0 |
| 9123-1 | 3.597 / 2.899 | 0.067 | 0.01 (1) | 261.9 | 263.0 | 196.0 |
| 9123-2 | 3.6 / 2.898 | 0.0675 | 0.01 (1) | 258.1 | 294.0 | 177.0 |
| 9126-1 | 3.5675 / 2.895 | 0.0662 | 0.0125 (1) | 544.8 | 596.0 | 416.0 |
| 9126-2 | 3.566 / 2.898 | 0.064 | 0.01 (1) | 293.3 | 312.0 | 227.0 |
| | | | | | | |
| | | | | | | |
| | | | | | | |
| | | | | | | |
| | | | | | | |

* BASED ON MEASURED DIMENSIONS SHOWN ON THIS PAGE.

SABI 138 REV. 2/64

SOLAR
A Division of International Harvester Company

ENGINEERING REPORT
NO. M-1794
DATE 8-19-65
PAGE 21 OF ____ PAGES
JOB NO. ____

SUBJECT: NASA BELLOWS SQUIRM PROGRAM
BY: D. SHEN

RESERVE THIS SPACE FOR BINDING.

## INCONEL 718 BELLOWS

THE FOLLOWING TABLE SHOWS THE COMPARISON OF CALCULATED AND TESTED SQUIRM PRESSURES.

| | SQUIRM PRESSURES (PSI) | | | | |
|---|---|---|---|---|---|
| ITEM | CALCULATED SQUIRM BASED ON DRAWING DIM. | TESTED SQUIRM | CALC. SQUIRM BASED ON ACTUAL DIM. | | NOTE |
| | | | RANGE - GROUP A† | RANGE - GROUP B† | |
| 9102-1 | 1500 | 1498 | 1462 - 1982 | 1420 - 1970 | - |
| 9102-2 | 1100 | 1183 | 1112 - 1505 | 1012 - 1403 | ANGULATED |
| 9105-1 | 1900 | 2000 | 2017 - 2740 | 1832 - 2540 | - |
| 9105-2 | 1360 | 1960 | 1368 - 1862 | 1197 - 1654 | ANGULATED |
| 9112-1 | 1700 | 2200 | 1723 - 2218 | 1860 - 2545 | - |
| 9112-2 | 1210 | 1408 | 1107 - 1703 | 1186 - 1643 | ANGULATED |
| 9114-1 | 1390 | 1200 | 1272 - 1688 | 1477 - 1880 | - |
| 9114-2 | 958 | 830 | 905 - 1242 | 891 - 1230 | ANGULATED |
| 9118-1 | 552 | 516 | 536 - 571 | 496 - 581 | - |
| 9118-2 | 483 | 680 | 388 - 527 | 462 - 588 | *ANGULATED |
| 9121-1 | 983 | 830 | 848 - 993 | 861 - 1010 | - |
| 9121-2 | 637 | 625 | 614 - 824 | 618 - 852 | *ANGULATED |
| 9123-1 | 763 | 515 | 616 - 721 | 626 - 733 | - |
| 9123-2 | 525 | 420 | 436 - 577 | 483 - 654 | *ANGULATED |
| 9126-1 | 1300 | 910 | 930 - 1231 | 1036 - 1410 | - |
| 9126-2 | 717 | 662 | 441 - 588 | 454 - 626 | *ANGULATED |

* 12 DEGREES ANGULATION; OTHERS ARE ANGULATED 6 DEGREES

† SEE P. 16 & C-4 FOR EXPLANATION.

DI 138 REV. 2/64

SOLAR
A Division of International Harvester Company

ENGINEERING REPORT
NO. M-1794
DATE 8-19-65
PAGE 22 OF ____ PAGES
JOB NO. ____

SUBJECT: NASA BELLOWS SQUIRM PROGRAM
BY: D. SHEN

RESERVE THIS SPACE FOR BINDING.

## COMPARISON OF COMPUTED & TESTED SPRING RATES (AISI 321 BELLOWS)

| ITEM | O.D." / I.D." | a" | t"(n) | COMPUTED * SPRING RATE (LB/IN) | SPRING RATE AS MANUFACTURED | SPRING RATE AFTER SIZING |
|---|---|---|---|---|---|---|
| 9101-2 | 3.31 / 2.932 | 0.0705 | 0.009(1) | 940.7 | 670.0 | 625.0 |
| 9103 | 3.297 / 2.9416 | 0.066 | 0.0105(2) | 3,423 | 2,000.0 | 2360.0 |
| 9104-2 | 3.29 / 2.923 | 0.0675 | 0.011(1) | 1,729 | 1,330.0 | 1250.0 |
| 9106 | 3.281 / 2.942 | 0.065 | 0.0115(2) | 4,818 | 2,000.0 | 2610.0 |
| 9109 | 3.402 / 2.933 | 0.0645 | 0.009(4) | 525.2 | 513.0 | – |
| 9111-1 | 3.378 / 2.931 | 0.067 | 0.011(1) | 1,042 | 910.0 | 976.0 |
| 9111-2 | 3.377 / 2.929 | 0.0655 | 0.011(1) | 1,035 | 851.0 | 1,050.0 |
| 9113-1 | 3.383 / 2.906 | 0.058 | 0.009(1) | 497 | 335.0 | 317.0 |
| 9113-2 | 3.386 / 2.908 | 0.0575 | 0.009(1) | 494.7 | 500.0 | 334.0 |
| 9115 | 3.39 / 2.922 | 0.0575 | 0.011(2) | 1,867 | 1010.0 | 755.0 |
| 9116-1 | 3.366 / 2.905 | 0.0595 | 0.011(1) | 961.3 | 740.0 | 625.0 |
| 9117 | 3.607 / 2.912 | 0.0655 | 0.009(1) | 187 | 208.0 | 175.0 |
| 9119 | 3.569 / 2.935 | 0.082 | 0.011(2) | 871.9 | – | 417.0 |
| 9120-1 | 3.601 / 2.914 | 0.0635 | 0.011(1) | 341.1 | 263.0 | 294.0 |
| 9120-2 | 3.598 / 2.913 | 0.0635 | 0.012(1) | 441.7 | 278.0 | 274.0 |
| 9122-1 | 3.589 / 2.90 | 0.056 | 0.009(1) | 199.7 | 128.0 | 119.0 |
| 9122-2 | 3.59 / 2.899 | 0.058 | 0.009(1) | 188.8 | 135.0 | 114.0 |
| 9124 | 3.586 / 2.923 | 0.069 | 0.011(2) | 749.2 | 477.0 | 260.0 |
| 9125-1 | 3.581 / 2.898 | 0.0625 | 0.011(1) | 345.2 | – | 204.0 |
| 9125-2 | 3.591 / 2.899 | 0.06 | 0.011(1) | 335 | 313.0 | 210.0 |
| | | | | | | |

* BASED ON MEASURED DIMENSIONS SHOWN ON THIS PAGE.

SOLAR
A Division of International Harvester Company

ENGINEERING REPORT
NO. M-1794
DATE 8-19-65
PAGE 23 OF ____ PAGES
JOB NO. ____

SUBJECT: NASA BELLOWS SQUIRM PROGRAM
BY: D. SHEN

RESERVE THIS SPACE FOR BINDING.

## AISI 321 BELLOWS

THE FOLLOWING TABLE SHOWS THE COMPARISON OF CALCULATED AND TESTED SQUIRM PRESSURES.

| ITEM | SQUIRM PRESSURES (PSI) | | | |
|---|---|---|---|---|
| | CALCULATED SQUIRM BASED ON DWG DIM. | TESTED SQUIRM | CALCULATED SQUIRM RANGE BASED ON ACTUAL DIM | NOTE |
| 9101-2 | 276 | 397 | 221-244 | ANGULATED |
| 9103 | 552 | 1,145 | 703-748 | |
| 9104-2 | 365 | 668 | 373-395 | |
| 9106 | 730 | 1,082 | 763-819 | |
| 9109 | 247 | 320 | 158-170 | ANGULATED |
| 9111-1 | 468 | 745 | 459-483 | - |
| 9111-2 | 324 | 550 | 324-340 | ANGULATED |
| 9113-1 | 391 | 380 | 319-339 | - |
| 9113-2 | 252 | 290 | 199-211 | ANGULATED |
| 9115 | 504 | 730 | 678-712 | ANGULATED |
| 9116-1 | 480 | 638 | 462-496 | - |
| 9117 | 312 | 162 | 237-257 | - |
| 9119 | 384 | 375 | 438-454 | ANGULATED |
| 9120-1 | 416 | 277 | 331-347 | - |
| 9120-2 | 176 | 200 | 188-196 | *ANGULATED |
| 9122-1 | 336 | 170 | 233-248 | - |
| 9122-2 | 142 | 200 | 113-119 | *ANGULATED |
| 9124 | 414 | 365 | 334-350 | ANGULATED |
| 9125-1 | 440 | 250 | 327-340 | - |
| 9125-2 | 192 | 200 | 189-198 | *ANGULATED |

* 12° ANGULATION; OTHERS 6° ANGULATION

SADI 130 REV. 2/64

SOLAR
A Division of International Harvester Company

ENGINEERING REPORT
NO. M-1794
DATE 8-19-65
PAGE 24 OF ____ PAGES
JOB NO. ____

SUBJECT: NASA BELLOWS SQUIRM PROGRAM
BY: D. SHEN

# COMPARISON OF SQUIRM PRESSURES FOR INCONEL 718 & S/S 321 BELLOWS OF SAME DRAWING DIMENSIONS

THE FOLLOWING TABLE GIVES THE COMPARISON OF SQUIRM PRESSURES OF INCONEL 718 & S/S 321 BELLOWS MANUFACTURED FROM THE SAME DRAWING AND TESTED UNDER THE SAME CONDITIONS. THE COMPARISON OF CALCULATED SQUIRM PRESSURES BASED ON MEASURED DIMENSIONS IS NOT INCLUDED.

| | ITEM NO | | ANGULATION (DEGREES) | CALCULATED SQUIRM BASED ON DWG. DIM. | | TESTED SQUIRM | | INC. 718 / AISI 321 | |
|---|---|---|---|---|---|---|---|---|---|
| | S/S 321 | INC. 718 | | S/S 321 | INC. 718 | S/S 321 | INC 718 | CALC. | TEST |
| | 9101-2 | 9102-2 | 6 | 276 | 1100 | 397 | 1183 | 3.99 | 2.98 |
| | 9104-2 | 9105-2 | 6 | 365 | 1360 | 668 | 1960 | 3.73 | 2.93 |
| | 9111-1 | 9112-1 | 0 | 468 | 1700 | 745 | 2200 | 3.63 | 2.95 |
| | 9111-2 | 9112-2 | 6 | 324 | 1210 | 550 | 1408 | 3.73 | 2.56 |
| | 9113-1 | 9114-1 | 0 | 391 | 1390 | 380 | 1200 | 3.56 | 3.16 |
| | 9113-2 | 9114-2 | 6 | 252 | 958 | 290 | 830 | 3.81 | 2.86 |
| | 9117 | 9118-1 | 0 | 312 | 552 | 162 | 516 | 1.77 | 3.19 |
| | 9120-1 | 9121-1 | 0 | 416 | 983 | 277 | 830 | 2.36 | 3.0 |
| | 9120-2 | 9121-2 | 12 | 176 | 637 | 200 | 625 | 3.62 | 3.12 |
| | 9122-1 | 9123-1 | 0 | 336 | 763 | 170 | 515 | 2.26 | 3.03 |
| * | 9122-2 | 9123-2 | 12 | 142 | 525 | 200 | 420 | 3.7 | 2.1 |
| * | 9125-1 | 9126-1 | 0 | 440 | 1300 | 250 | 910 | 2.96 | 3.64 |
| | 9125-2 | 9126-2 | 12 | 192 | 717 | 200 | 662 | 3.74 | 3.31 |

* EXCEPT THOSE MARKED, INCONEL 718 BELLOWS APPROXIMATELY 3 TIMES THE SQUIRM PRESSURE OF THOSE MADE OF S/S 321

RESERVE THIS SPACE FOR BINDING.

SADI 13H REV. 2/64

SOLAR
A Division of International Harvester Company

ENGINEERING REPORT
NO. M-1794
DATE 8-19-65
PAGE 25 OF ____ PAGES
JOB NO. ____

SUBJECT: NASA BELLOWS SQUIRM PROGRAM
BY: D. SHEN

RESERVE THIS SPACE FOR BINDING.

## BELLOWS WITH AND WITHOUT LIGHT BANDS

COMPARISON OF COMPUTED AND TESTED SQUIRM PRESSURES.

N, NO. OF CONVOLUTIONS = 10

| ITEM | TESTED SQUIRM(PSI) | COMPUTED SQUIRM BASED ON DWG DIMENSIONS (PSI) | RANGE OF COMPUTED SQUIRM BASED ON MEAS. DIM. (PSI) | NOTE | $\delta$" |
|---|---|---|---|---|---|
| 9101-1 | 520 | 411 | 335-362 | ENDS BULGED | ≈0 |
| 9104-1 | 760 | 511 | 530-555 | ENDS BULGED | ≈0 |
| 9109-1 | 560 | 420 | 368-397 | ENDS BULGED | ≈0 |
| 9107-2 | 490 | 420 | 345-366 | NO BAND, SEVERE BULGING | +0.5 |
| 9108-1 | 900 | 527 | 547-575 | ENDS BULGED | ≈0 |
| 9108-2 | 270 | 527 | 296-316 | ENDS MISALIGNED | -0.5 |
| 9108-3 | 300 | 527 | 296-316 | NO BAND, ENDS BULGED | -0.5 |
| 9113-3 | 480 | 391 | 323-340 | LITTLE BULGING | +0.5 |
| 9116-2 | 648 | 480 | 261-277 | LITTLE BULGING | -0.5 |
| 9125-3 | 200 | 440 | 163-171 | ALMOST NO BULGING | -0.5 |
| * 9123-3 | 705 | 763 | 469-723 | ALMOST NO BULGING | +0.5 |

* MADE OF INCONEL 718, ALL OTHERS AISI 321.

SADI 138 REV. 2/64

SOLAR
A Division of International Harvester Company

ENGINEERING REPORT
NO. M-1794
DATE 8-19-65
PAGE 26 OF ____ PAGES
JOB NO. ____

SUBJECT: NASA BELLOWS SQUIRM PROGRAM
BY: D SHEN

RESERVE THIS SPACE FOR BINDING.

## COMPARISON OF SQUIRM PRESSURES WITH OR WITHOUT PRE-DEFORMATION FOR BELLOWS OF SAME DRAWING DIMENSIONS

THE FOLLOWING TABLE GIVES THE COMPARISON OF SQUIRM PRESSURES FOR BELLOWS OF SAME MATERIAL AND DRAWING DIMENSIONS EXCEPT DIFFERENT TESTED FREE LENGTH. THE -2 OR -3 BELLOWS IS APPROX.* $\delta$" LONGER OR SHORTER THAN -1 BELLOWS. $\delta$ IS APPLIED TO THE BELLOWS PRIOR TO THE SQUIRM TEST.

| ITEM | +PREDICTED SQUIRM PSI | TESTED SQUIRM PSI | $\delta$" | L" * |
|---|---|---|---|---|
| 9108-1 | 527 | 900 | 0 | 2.28" |
| 9108-2 | | 270 | -0.5" | 1.888" |
| 9113-1 | 391 | 380 | 0 | 2.28" |
| 9113-3 | | 480 | +0.5" | 2.877" |
| 9116-1 | 480 | 638 | 0 | 2.28" |
| 9116-2 | | 648 | -0.5" | 1.901" |
| 9123-1 | 763 | 515 | 0 | 2.28" |
| 9123-3 | | 705 | +0.5" | 3.353" |
| 9125-1 | 440 | 250 | 0 | 2.28" |
| 9125-3 | | 200 | -0.5" | 2.433" |

* $L" = \ell" + \delta"$ WHERE $L$ = TESTED LENGTH $\ell"$ = FREE LENGTH. $L$ IN MOST CASES, DEPENDS ON $\ell$. FOR $\delta = 0$ BELLOWS, THE SPECIMEN WILL BE DEFORMED TO $L"$ REGARDLESS OF $\ell"$.

\+ EFFECT OF $\delta$ IS NOT INCLUDED IN PREDICTED SQUIRM CALCULATIONS

DI 138 REV. 2/64

## DISCUSSION - SPRING RATE

A TYPICAL LOAD-DEFLECTION LOOP IS ILLUSTRATED AT RIGHT. THE ARROW HEADS AND THE NUMERALS IN CIRCLES INDICATE THE SEQUENCE OF TEST PROCESS. THE SOLID LINES ARE TYPICAL FOR MOST OF THE SPRING RATE TESTS WHILE THE DOTTED LINE COMPLETES THE UNFAMILIAR HALF OF THE SPRING RATE TEST LOOP. HOWEVER, THE GENERAL LOAD-DEFLECTION CURVE SHOWN (FOR THE GENERAL CONVOLUTED BELLOWS CLASS) MAY NOT HOLD TRUE IF THE TEST SEQUENCE IS REVERSED. SOME OF THE TEST OBSERVATIONS OF THIS DEVELOPMENT PROGRAM CAN BE NOTED BELOW:

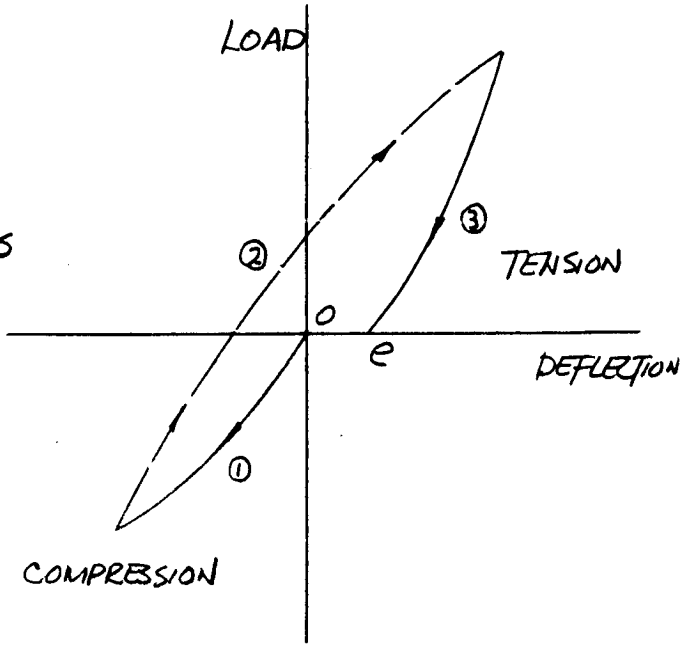


LOAD-DEFLECTION LOOP OF A SPRING RATE TEST OF BELLOWS

(a) GENERALLY, THE AXIAL SPRING RATE *SRA IN TENSION EXCEEDS THAT IN COMPRESSION. HOWEVER, THE OPPOSITE IS NOTED ON SOME RARE OCCASIONS.

* THE AXIAL SPRING RATE OF A BELLOWS AT A GIVEN LOAD OR DEFLECTION IS MERELY THE SLOPE OF THE CURVE AT THAT POINT.

## DISCUSSION - SPRING RATE (CONT'D)

(b) THE END POINT e USUALLY ENDS UP WITH A SHALLOWER SLOPE THAN THAT OF THE STARTING POINT O.

(c) THE AXIAL SPRING RATE IN AFTER-SIZING CONDITION IS IN GENERAL, LOWER THAN THAT IN AS-MANUFACTURED CONDITION. THE REASON MAY BE EXPLAINED BY (d)

(d) THE PERMANENT SET AFTER BELLOWS EXTENSION TEST ALWAYS EXCEEDS THAT AFTER COMPRESSION TEST. (IF, AMOUNT OF EXTENSION = AMOUNT OF COMPRESSION)

(e) IN ALMOST ALL CASES, THE COMPUTED SPRING RATE FROM REF. 5 GIVES HIGHER VALUES THAN THE TEST RESULT.

(f) WHEN COMPARING WITH THE COMPUTED SPRING RATES FROM REF. 5, THE INCONEL 7/8 BELLOWS TEST RESULTS EXHIBIT GOOD CORRELATION WHILE THE AISI 321 BELLOWS RESULTS VARY QUITE A LOT.

(g) ALL THE 2-PLY BELLOWS BEING TESTED IN THIS PROGRAM GIVE MUCH LOWER SPRING RATE THAN COMPUTED. THIS MAY BE ATTRIBUTED TO THE FACT THAT THE INNER PLY OF THE BELLOWS IS ASSUMED TO HAVE THE SAME SPRING RATE AS THE OUTER PLY IN COMPUTATION.

(CONT'D)

## DISCUSSION - SPRING RATE (CONT'D)

(L) UNSUCCESSFUL ATTEMPTS WERE MADE TO INVESTIGATE LINEARITY AND NON-LINEARITY OF BELLOWS SPRING RATE. LACK OF INTENSIVE STUDY ON EFFECT OF HOOP STRESS UPON EXTENDED OR COMPRESSED BELLOWS SPRING RATE IS CONSIDERED DIRECTLY RESPONSIBLE FOR THIS FAILURE.

NOTE: SEE PAGE 39 FOR PLOT OF COMPUTED SPRING RATE VERSUS TESTED SPRING RATE FOR INCONEL 718 & AISI 321 BELLOWS

## DISCUSSION - TANGENT MODULUS $E_t$

THE INTRODUCTION OF TANGENT MODULUS INTO THE PRESENT CONVENTIONAL SQUIRM PRESSURE FORMULA DEFINITELY IMPROVES THE CORRELATION OF ANALYTICAL PREDICTION WITH THE TEST RESULT (IN A GENERAL CONVOLUTED CLASS). THE AVAILABILITY OF A COMPRESSIVE TANGENT MODULUS CURVE FOR A CERTAIN MATERIAL POSES AN IMMEDIATE PROBLEM. IT HAS BEEN DEMONSTRATED IN THIS REPORT THAT IF AN ESTABLISHED COMPRESSIVE STRESS STRAIN CURVE IS AVAILABLE, TANGENT MODULUS CURVE CAN BE CONSTRUCTED WITH SUFFICIENT ACCURACY. WHEN COMPRESSIVE STRESS STRAIN CURVE IS NOT AVAILABLE, A TENSILE STRESS-STRAIN CUURE SEEMS TO BE ADEQUATE IN SOME CASES.

SINCE BELLOWS ARE FORMED FROM ROLLED SHEET, IT MAY BE REMARKED THAT THE PROCESS OF ROLLING FREQUENTLY PRODUCES A DEFINITE ORIENTATION OF CRYSTALS; THUS THE SHEET IS SAID TO BE ANISOTROPIC - WHICH MEANS THAT THE ELASTIC PROPERTIES ARE DIFFERENT IN DIFFERENT DIRECTIONS. IN THIS PRESENT DEVELOPMENT TEST, BELLOWS AS WELL AS TEST COUPONS WERE CUT AT RANDOM. THE STRESS-STRAIN CURVES, CONSEQUENTLY THE TANGENT MODULUS CURVES. RESULT IN A QUITE WIDE SPREAD AS SHOWN ON PAGES C-4 TO C-6.

DISCUSSION - TANGENT MODULUS $E_t$ (CONT'D)

THE GENERAL SIMILARITY OF SOME INCONEL 718 CURVE SHAPES MAY NOT IMPLY THAT THE CORRESPONDING TEST COUPONS ARE CUT IN THE SAME DIRECTION, BUT THEY DO SUGGEST THIS POSSIBILITY. AS INDICATED ON PAGES C-2 & C-3 (TENSILE TEST OF COUPONS CUT AT 90 DEGREES TO EACH OTHER), A NEGLIGIBLE CHANGE IN ELASTIC PROPERTIES FOR AISI 321 IS INDICATED BY THE TEST RESULTS, WHILE INCONEL 718 SHOWS A MARKED DIFFERENCE (ANISOTROPY). IT IS INTERESTING TO NOTE THAT ALMOST ALL THE TEST RESULTS OF INCONEL 718 BELLOWS APPEAR TO BE VERY CLOSE TO EITHER EXTREMES OF THE COMPUTED GROUPS AS SHOWN ON PAGE 21. (FOR EXPLANATION OF GROUPS, SEE PAGES 16 & C-4) THIS, OF COURSE, IS NOT TRUE IN THE CASE OF AISI 321 BELLOWS.

SOLAR
A Division of International Harvester Company

ENGINEERING REPORT
NO. M-1794
DATE 8-19-65
PAGE 32 OF ____ PAGES
JOB NO. ____

SUBJECT: NASA BELLOWS SQUIRM PROGRAM
BY: D. SHEN

## DISCUSSION - SQUIRM PRESSURE

FOR BELLOWS TESTED IN THE STRAIGHT POSITION AND AT 6 DEGREES ANGULATION, SQUIRM WAS VISIBLE AND IN ALL CASES COINCIDED WITH THE PRESSURE DROP NOTED ON THE STRIP RECORDER. A TYPICAL EXAMPLE OF THIS PRESSURE DROP IS SHOWN ON PAGE 37. THE MOVEMENT OF A CONVOLUTION TOWARDS ANOTHER, FOLLOWED BY OUT-FOLDING OF THE INNER CONVOLUTION IS THE USUAL SIGN OF BELLOWS INSTABILITY. FOR SOME INCONEL 718 BELLOWS, THEY SPRUNG RIGHT BACK TO THE ORIGINAL SHAPE IF THE INTERNAL PRESSURE WAS BLED OFF IMMEDIATELY AFTER THE SIGN OF INSTABILITY OCCURRED.

BELLOWS TESTED AT 12 DEGREES ANGULATION BEHAVED RATHER DIFFERENTLY DURING SQUIRM PRESSURE TEST. THE PRONOUNCED SQUIRM DEFINED SPECIALLY FOR THE 12-DEGREE-ANGULATED BELLOWS CAN BE DESCRIBED AS FOLLOWS. THE CONVOLUTIONS ON BOTH ENDS OF THE CONVEX SIDE OF THE BELLOWS GRADUALLY GROUP TOGETHER WHILE THE FEW MIDDLE CONVOLUTIONS ON THE OPPOSITE SIDE ALSO SLOWLY TOUCH EACH OTHER. (SEE SKETCH ON NEXT PAGE) THE POINT OF INSTABILITY IS DECIDED AS THE PRESSURE AT WHICH PERMANENT DEFORMATION REMAINS AFTER THE PRESSURE IS RELEASED.

(CONT'D)

## DISCUSSION – SQUIRM PRESSURE (CONT'D)

AS INDICATED IN THE SQUIRM EQUATION, THE CRITICAL PRESSURE IS DIRECTLY PROPORTIONAL TO THE AXIAL SPRING RATE AS WELL AS THE TANGENT MODULUS. AND IN RECOGNIZING THE ACTUAL SPRING RATE BEING MOSTLY LOWER THAN THE COMPUTED SPRING RATE WHICH IS USED IN PREDICTING THE SQUIRM PRESSURE OF A BELLOWS, IT IS NECESSARY TO INVESTIGATE THE EFFECT OF SPRING RATE UPON THE COMPUTED SQUIRM PRESSURE. THE THREE EXAMPLES OF SQUIRM PRESSURE CALCULATION IN APPENDIX A ARE BASED ON COMPUTED AXIAL SPRING RATES. THE SAME THREE EXAMPLES ARE REWORKED WITH MEASURED SPRING RATES IN APPENDIX B. IT CAN BE SEEN IN THE CALCULATION THAT THE CHANGE OF AXIAL SPRING RATE CHANGES THE TOTAL COMPRESSIVE STRESS AS WELL AS THE TANGENT MODULUS $E_t$. AS SHOWN OF PAGE 38, THE RESULTS OF THE THREE EXAMPLES INDICATE THAT A MAXIMUM CHANGE OF 59.6 % IN SPRING RATE ONLY RESULTS IN A MAXIMUM CHANGE OF 10.78 % IN THE CALCULATED SQUIRM PRESSURE. THE REASON BEHIND THIS IS THAT A DECREASE IN SPRING RATE ACCOMPANIES AN INCREASE IN TANGENT MODULUS, AND VICE VERSA. THUS IT APPEARS THAT THE VARIATION OF SPRING RATE IS RELATIVELY IMMATERIAL AS FAR AS SQUIRM PRESSURE CALCULATION IS CONCERNED IN THE

(CONT'D)

## DISCUSSION- SQUIRM PRESSURE (CONT'D)

INELASTIC REGION. HOWEVER, IT SHOULD BE MENTIONED THAT THE ABOVE STATEMENT IS BASED ON THE PRESENT SQUIRM PRESSURE FORMULA AND THE THREE EXAMPLES CITED WITHIN THE SCOPE OF THIS DEVELOPMENT PROGRAM.

THE OVERALL RESULT OF THIS PROGRAM CAN BE CONSIDERED QUITE SATISFACTORY. THERE ARE A FEW REASONS THAT MAY EXPLAIN THE UNPREDICTABILITY OF THE INCONEL 718 AND AISI 321 BELLOWS OTHER THAN SOME REFINED CONSIDERATIONS OF THE PRESENT MODIFIED SQUIRM PRESSURE FORMULA. THE REASONS ARE AS FOLLOWS.

(a) THE STRESS-STRAIN CURVES OF THE COUPONS ARE OBTAINED FROM THE TENSILE TEST INSTEAD OF FROM A COMPRESSIVE TEST.

(b) INCONEL 718 GIVES A RELATIVELY CONSTANT MODULUS OF ELASTICITY WHEREAS AISI 321 EXHIBITS A LINEAR PROPERTY OVER ONLY A VERY SMALL RANGE.

(c) IT IS DIFFICULT TO OBTAIN ACCURATE MODULUS DATA FROM THE LOAD-DEFLECTIVE CURVES DIRECTLY PRODUCED BY THE PLOTTER CONNECTED WITH THE TENSILE MACHINE.

(d) MINOR ERRORS ARE BOUND TO EXIST IN MANUAL CONSTRUCTION OF TANGENT MODULUS CURVES FROM THE STRESS-STRAIN DATA.

(CONT'D)

## DISCUSSION - SQUIRM PRESSURE (CONT'D)

(e) THE BIGGEST SINGLE FACTOR IS THE INCONSISTENCY IN BELLOWS GEOMETRY FROM CONVOLUTION TO CONVOLUTION. SLIGHT VARIATIONS IN SPAN HEIGHT, RADIUS, THICKNESS ETC., CAN MAKE SOME DIFFERENCE IN THE FINAL TEST RESULTS.

NOTE: SEE PAGES 40 & 41 FOR PLOT OF COMPUTED SQUIRM VERSES MEASURED SQUIRM PRESSURE FOR INCONEL 718 AND AISI 321 BELLOWS.

SOLAR
A Division of International Harvester Company

ENGINEERING REPORT
NO. M-1794
DATE 8-19-65
PAGE 37 OF ____ PAGES
JOB NO. ____

SUBJECT: NASA BELLOWS SQUIRM PROGRAM
BY: D SHEN

RESERVE THIS SPACE FOR BINDING.

## TEST DESCRIPTION - INDICATION OF SQUIRM

THE FOLLOWING PICTURE IS TAKEN FROM THE STRIP RECORDER SHOWING THE SQUIRM INDICATION OF 9102-2 TEST SPECIMEN. THE PRESSURE DROP COINCIDES WITH THE VISUAL SQUIRM AT 1,183 psi.

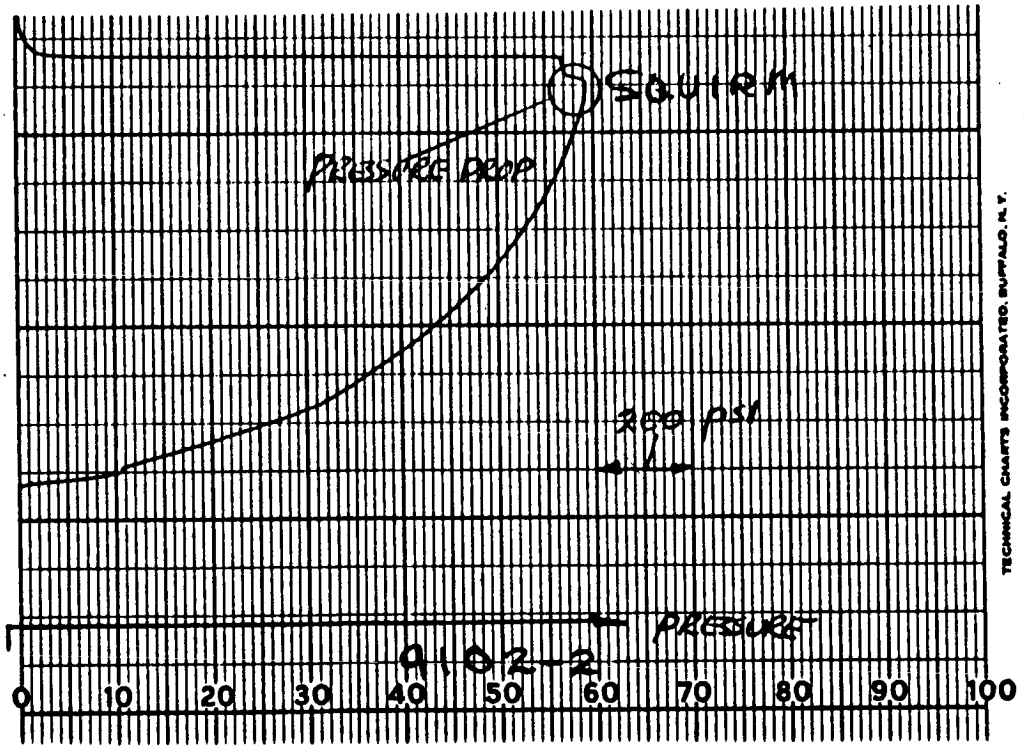


TYPICAL INDICATION OF SQUIRM - THE PRESSURE DROP

SI 138 REV. 2/64

# COMPUTED SPRING RATE vs TESTED SPRING RATE

## for INC. 718 & AISI 321 BELLOWS

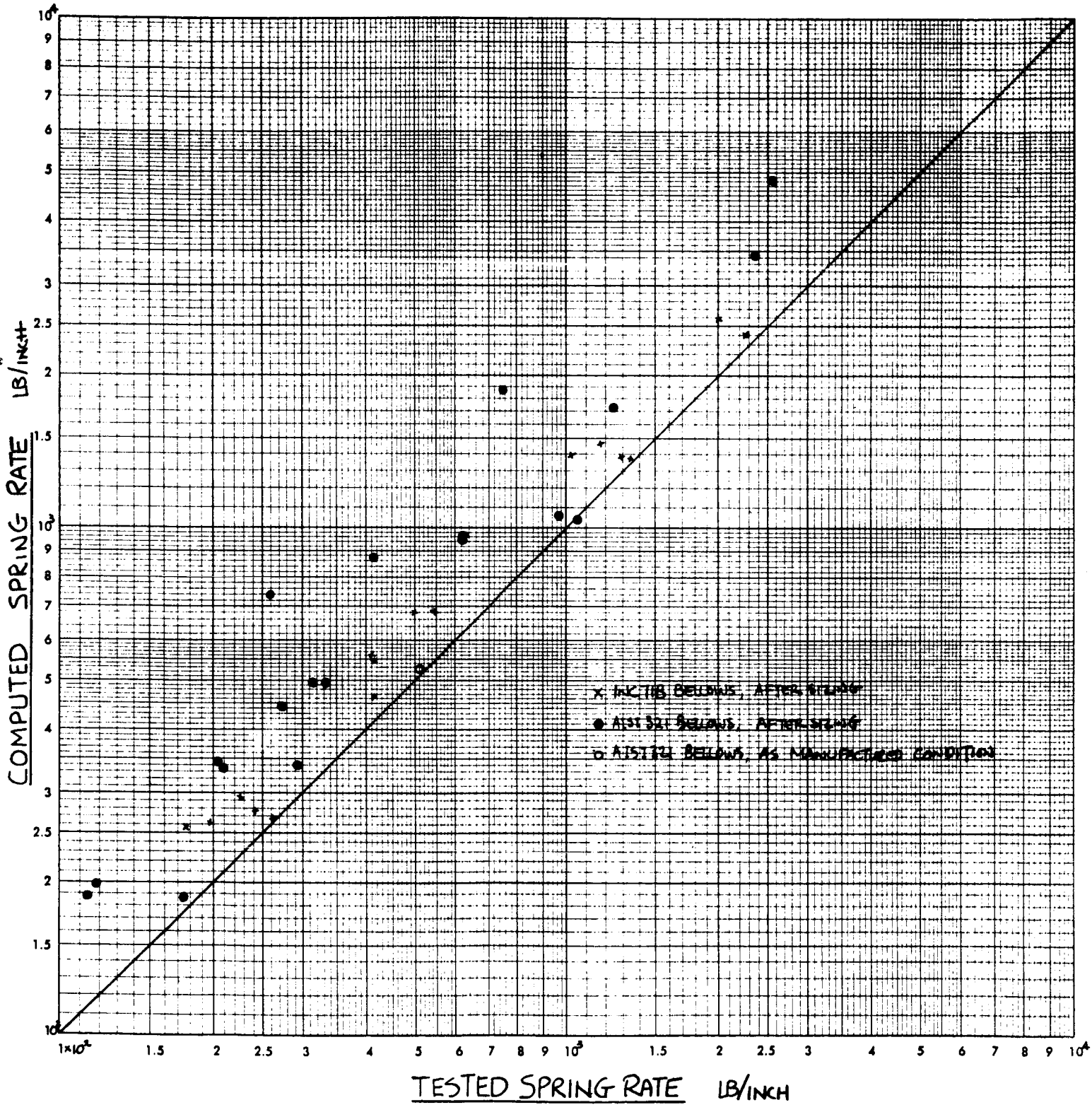


BY D. SHEN

# COMPUTED SQUIRM PRESSURE Vs MEASURED SQUIRM PRESSURE FOR INCONEL 718 BELLOWS



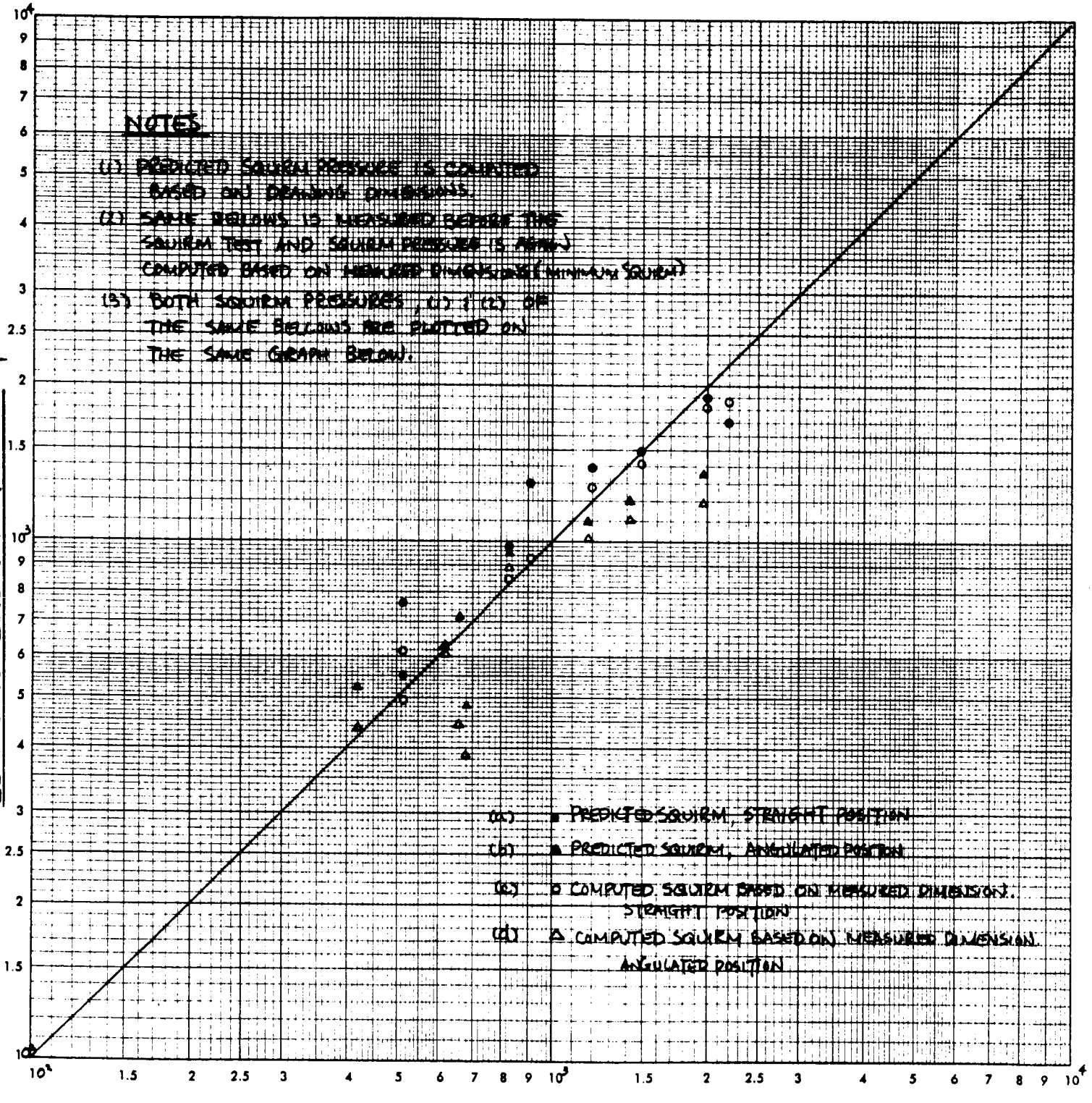


by D.SIHEN

# COMPUTED SQUIRM PRESSURE Vs TESTED SQUIRM PRESSURE

## FOR AISI 321 BELLOWS

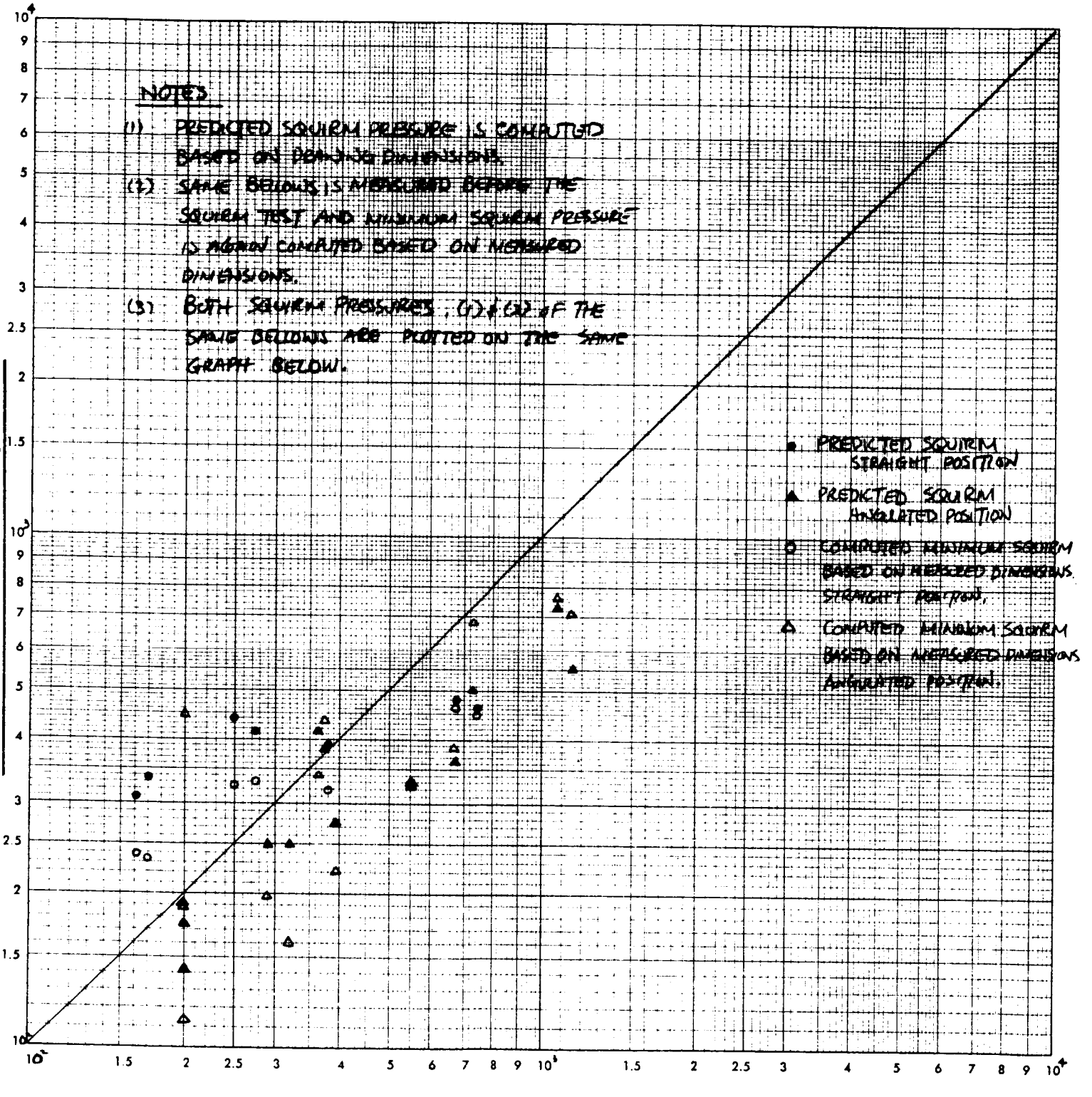


By P. STIEV

## CONCLUSIONS AND RECOMMENDATIONS

FROM THE RESULTS PRESENTED, THE FOLLOWING CONCLUSIONS AND RECOMMENTIONS ARE NOTED:

(a) THE OVERALL RESULTS PROVIDE NECESSARY CONFIDENCE IN USING THE MODIFIED SQUIRM PRESSURE EQUATION $P_{cr} = 2\pi SR_A E_t/E \cdot L$

(b) IT APPEARS THAT THE PROPOSED METHOD TO PREDICT BELLOWS SQUIRM IN AN ANGULATED POSITION GIVES SATISFACTORY CORRELATION WITH TEST RESULTS.

(c) THE VARIATION IN COMPUTED AND MEASURED AXIAL SPRING RATES OF A BELLOWS DOES NOT SEEM TO EFFECT THE OUTCOME OF THE COMPUTED SQUIRM PRESSURE FOR BELLOWS IN THE INELASTIC REGION.

(d) THE SQUIRM PRESSURE OF AN INCONEL 718 BELLOWS CAN BE CONSIDERED 3 TIMES THAT OF AN AISI 321 BELLOWS IF THEY ARE IN THE INELASTIC REGION.

(e) BASED ON THIS STUDY, SAFETY FACTORS OF AT LEAST 2 FOR AISI 321 BELLOWS AND 1.5 FOR INCONEL 718 BELLOWS ARE RECOMMENTED FOR THE COMPUTED SQUIRM PRESSURE. [LIMIT TO GENERAL CONVOLUTED CLASS]

(f) THE TANGENT MODULI CURVES FOR INCONEL 718 AND AISI 321 ON PAGE C-1 CAN BE USED FOR SQUIRM PRESSURE PREDICTIONS PROVIDED THE SAFETY FACTORS IN (e) ARE USED

(CONT'D)

## CONCLUSIONS AND RECOMMENDATIONS (CONT'D)

(g) PRESTRESSING THE BELLOWS BY EXTENSION OR COMPRESSION DOES SEEM TO CHANGE THE SQUIRM PRESSURE. HOWEVER, MORE AND BETTER-CONTROLLED TESTS HAVE TO BE CONDUCTED TO VERIFY THIS STATEMENT.

(h) AN IMMEDIATE INVESTIGATION OF THE INELASTIC BEHAVIOR OF INCONEL 718 AND AISI 321 IS RECOMMENDED. (SEE BOTTOM OF PAGE 33 FOR PROPOSED CLUE) THIS INVESTIGATION MAY PROVIDE BETTER UNDERSTANDING OF THE CONSISTENT CALCULATED AND TESTED SQUIRM PRESSURE RATIOS OF INCONEL 718 BELLOWS TO AISI 321 BELLOWS.

(i) A THOROUGH AND RIGOROUS ANALYTICAL STUDY SHOULD BE PERFORMED TO OBTAIN A BETTER UNDERSTANDING OF BELLOWS AND CONSEQUENTLY TO OBTAIN MORE ACCURATE SPRING RATE AND SQUIRM PRESSURE EXPRESSIONS. CHANGE OF SPRING RATE AS WELL AS SQUIRM PRESSURE DUE TO EXTENSION OF COMPRESSION OF A BELLOWS SHOULD ALSO BE ANALYTICALLY INVESTIGATED.

(j) SQUIRM PRESSURE TESTS FOR BELLOWS WITH VARIOUS GEOMETRICAL CONFIGURATIONS MUST BE PERFORMED TO OPTIMIZE THE SQUIRM DESIGN OF A BELLOWS.

(k) BELLOWS IN AN OFF-SET POSITION SHOULD BE ANALYZED AND SQUIRM PRESSURE TESTED.

## REFERENCES

1. 'BELLOWS DESIGN DATA' SOLAR REPORT ER-1049 BY H. LINDGREN & A. M. CVJETKOVIC

2. 'INSTABILITY OF BELLOWS SUBJECTED TO INTERNAL PRESSURE' BY J. A. HARINGX PHILIPS RESEARCH REPORT VOL 7, 1952 PP 189-196

3. 'AN INVESTIGATION OF THE EFFECT OF INTERNAL OR EXTERNAL PRESSURE ON THE BENDING CHARACTERISTICS OF AN ACTUATOR SYSTEM UTILIZING A BELLOWS'. BY P. SEIDE SPACE TECHNOLOGY LAB. REPORT NO. EM 8-25 DEC. 31, 1958

4 'ANALYSIS OF STRESSES IN BELLOWS' PART I BY W. F. ANDERSON. PRELIMINARY COPY, REPORT NAA-SR-4527 ATOMICS INTERNATIONAL. JULY, 1964.

5. SOLAR IBM PROGRAM NO. 224 BASED ON 'ANALYSIS OF U-SHAPED EXPANSION JOINTS' BY A. LAUPA & N.A. WEIL J.A.M. MARCH 1962 PP 115-123.

6. 'LIQUID HYDROGEN FLEXIBLE DUCTING TECHNOLOGY' PROGRESS REPORT 5 OF SOLAR REPORT ER 1473-5 BY H.T. MISCHEL, [COVERS PERIOD NOV. 1 TO NOV. 30, 1964.]

7. 'BELLOWS ANALYSIS' SOLAR REPORT M-1730 BY G. W. BOWERS & D. T. SHEN JAN. 1965.

8. 'DEVELOPEMENT TEST REPORT FOR 3" DIA. CONVOLUTED BELLOWS (DSK 9101-9126)' SOLAR REPORT 1490 BY S. BALL MAY, 1965.

9. METALS HDBK (ASM) 1948 EDITION p.14

SOLAR
A Division of International Harvester Company

ENGINEERING REPORT

SUBJECT: NASA BELLOWS SQUIRM PROGRAM

NO. M-1794

DATE 8-19-65

BY: D. SHEN

PAGE ____ OF ____ PAGES

JOB NO. ____

RESERVE THIS SPACE FOR BINDING.

# APPENDIX A

## TYPICAL SQUIRM PRESSURE CALCULATION

SADI 138 REV. 2/64

SOLAR
A Division of International Harvester Company

ENGINEERING REPORT
NO. M-1794
DATE 6-19-65
PAGE A-1 OF ____ PAGES
JOB NO. ____

SUBJECT: NASA BELLOWS SQUIRM PROGRAM
BY: D. SHEN

RESERVE THIS SPACE FOR BINDING.

## TYPICAL SQUIRM PRESSURE CALCULATION

THE FOLLOWING THREE SETS OF CALCULATIONS SERVE AS EXAMPLES OF COMPUTATION OF SQUIRM PRESSURES.

(a) BELLOWS 9103 (AISI 321)

$N = 10$ CONVOLUTIONS — $\delta$, DEFLECTION = +0.012" TENSION
$n = 2$ PLIES — $\theta$, ANGULATION = 6.0 DEGREES
$t = 0.0105$" PER PLY
O.D. = 3.297" — $a = 0.066$"
I.D. = 2.946" — $L = 2.96$"

FROM REF. 5 ; MERIDIONAL BENDING STRESS = |131,460 psi| DUE TO $\delta$ & $\theta$ $f_b$

$SR_A$, SPRING RATE = 3,423 LB/IN

$f_c$, TOTAL COMPRESSIVE STRESS = $\left(f_b + \frac{SR_A \pi R_M}{n t L}\right) \frac{E_t}{E}$

WHERE $\frac{SR_A \pi R_M}{n t L}$ IS COMPRESSIVE STRESS DUE TO INTERNAL PRESSURE
$f_b$ IS COMPRESSIVE BENDING STRESS DUE TO $\delta$ & $\theta$

$R_M = \frac{O.D. + I.D.}{4} = 1.5608$" — $E = 27.5 \times 10^6$ psi

$\therefore f_c = \left(131,460 + \frac{3423 \times 1.5608\,\pi}{2 \times 0.0105 \times 2.96}\right) \frac{E_t}{E}$

$= 14,570 \times 10^{-6}\, E_t$ psi

ADI 138 REV. 2/64

# TYPICAL SQUIRM PRESSURE CALCULATION

(a) BELLOWS 9103 (CONT'D)

WITH $f_c = 14{,}570 \times 10^{-6} E_t$ psi

BY TRIAL & ERROR OF PICKING $E_t$ TO SATISFY $f_c$ CORRESPONDING TO GRAPH SHOWN ON P. C-5, RANGE OF $E_t$ CAN BE FOUND TO BE $2.66 \times 10^6$ TO $2.83 \times 10^6$ psi

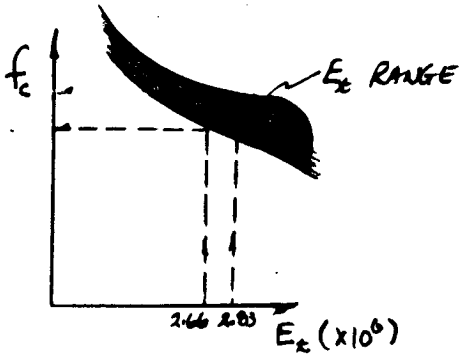


$f_c$ Vs $E_t$ GRAPH

$\therefore P_{cr}$, SQUIRM PRESSURE $= \frac{2\pi SR_A}{L} \times \frac{E_t}{E}$

$= \frac{2\pi \times 3423}{2.96} \times \frac{E_t}{27.5 \times 10^6}$ psi

THUS $P_{cr}$ IS FOUND TO BE WITHIN 703 psi & 748 psi

## TYPICAL SQUIRM PRESSURE CALCULATION

(b) BELLOWS 9106 (AISI 321)

$N = 10$ CONVOLUTIONS
$n = 2$ PLIES
$t = 0.0115"$ PER PLY
$O.D. = 3.281"$
$I.D. = 2.942"$

$\delta$, DEFLECTION $= +0.092"$
$\theta$, ANGULATION $= 6°$
$a = 0.065"$
$L = 2.96"$

FROM REF. 5 ; MERIDIONAL BENDING STRESS $f_b = |176,911 \text{ psi}|$ DUE TO $\delta$ & $\theta$

$SR_A$, SPRING RATE $= 4,818$ LB/IN

$$f_c, \text{ COMPRESSIVE STRESS} = \left(f_b + \frac{SR_A \pi R_M}{n t L}\right)\frac{E_t}{E}$$

$$= 19,000\, E_t$$

$R_M = \frac{O.D. + I.D.}{4} = 1.556"$

$E = 27.5 \times 10^6$

FROM GRAPH OF P. C-5

$E_t$ CAN BE FOUND IN THE RANGE OF $2.05 \times 10^6$ AND $2.2 \times 10^6$ psi

$\therefore P_{cr}$, SQUIRM PRESSURE $= \frac{2\pi SR_A}{L} \times \frac{E_t}{E}$

$$= \frac{2\pi \times 4818}{2.96} \times \frac{E_t}{27.5 \times 10^6} \text{ psi}$$

THUS $P_{cr}$ IS COMPUTED TO BE WITHIN 763 psi & 819 psi

SOLAR
A Division of International Harvester Company

ENGINEERING REPORT
NO. M-1794
DATE 8-19-65
PAGE A-4 OF ____ PAGES
JOB NO. ____

SUBJECT: NASA BELLOWS SQUIRM PROGRAM
BY: D. SHEN

RESERVE THIS SPACE FOR BINDING.

## TYPICAL SQUIRM PRESSURE CALCULATION

(C) BELLOWS 9115 (A151 321)

$N$ = 10 CONVOLUTIONS — $\delta$, DEFLECTION = ±0.022"
$n$ = 2 PLIES — $\theta$, ANGULATION = 6°
$t$ = 0.011"
O.D. = 3.39" — $a$ = 0.0575"
I.D. = 2.922" — $L$ = 2.28"

FROM REF. 5; MERIDIONAL BENDING STRESS $f_b$ = 102,157 psi DUE TO $\delta$ & $\theta$

$SR_A$, SPRING RATE = 1,867 LB/IN

$f_c$, COMPRESSIVE STRESS = $\left(f_b + \frac{SR_A \pi R_M}{n t L}\right) \frac{E_t}{E}$

$R_M = \frac{O.D. + I.D.}{4}$ = 1.578" = 10,400 $E_t$

$E = 27.5 \times 10^6$ psi

FROM GRAPH OF P. C-5
$E_t$ CAN BE FOUND IN THE RANGE OF $3.62 \times 10^6$ AND $3.8 \times 10^6$ psi

$P_{cr}$. SQUIRM PRESSURE = $\frac{2\pi SR_A}{L} \times \frac{E_t}{E}$

$= \frac{2\pi \times 1867}{2.28} \times \frac{E_t}{27.5 \times 10^6}$ psi

THUS $P_{cr}$ IS COMPUTED TO BE WITHIN 678 psi & 712 psi

SADI 138 REV. 2/64

SOLAR
A Division of International Harvester Company

ENGINEERING REPORT
NO. M-1794
DATE 8-19-65
PAGE ____ OF ____ PAGES
JOB NO. ____

SUBJECT: NASA BELLOWS SQUIRM PROGRAM
BY: D. SHEN

RESERVE THIS SPACE FOR BINDING.

# APPENDIX B

## EFFECT OF SPRING RATE UPON SQUIRM PRESSURE

THE COMPUTATION ILLUSTRATED IN THIS APPENDIX IS TO SHOW THAT VARIATION IN COMPUTED OR MEASURED SPRING RATE OF A BELLOWS DOES NOT AFFECT ITS COMPUTED SQUIRM PRESSURE APPRECIABLY.

SADI 138 REV. 2/64

SOLAR
A Division of International Harvester Company

ENGINEERING REPORT
NO. M-1794
DATE 8-19-63
PAGE B-1 OF ____ PAGES
JOB NO. ____

SUBJECT: NASA BELLOWS SQUIRM PROGRAM
BY: D. SHEN

RESERVE THIS SPACE FOR BINDING.

## EFFECT OF SLIGHT CHANGE OF SPRING RATE UPON COMPUTED SQUIRM PRESSURE

THE SQUIRM PRESSURE CALCULATION HAS BEEN BASED ON COMPUTED SPRING RATE. HOWEVER, IT HAS BEEN THE CASE THAT GENERALLY THE COMPUTED SPRING RATE IS HIGHER THAN THE TESTED SPRING RATE (IN THE ELASTIC RANGE). THE FOLLOWING THREE BELLOWS (SAME AS THOSE ON PAGES A1 TO A4) WILL EMPLOY TESTED SPRING RATES TO COMPUTE THE SQUIRM PRESSURES.

(a) BELLOWS 9103 (A1SI 321)

FROM PAGE 22 TESTED SPRING RATE = 2,360 LB/IN
COMPUTED SPRING RATE = 3,423 LB/IN

FROM PAGE A-1, $f_b$ DUE TO $\delta$ & $\theta$ = 131,460 psi BASED ON 3423 LB/IN

ASSUME $f_b$ IS PROPORTIONAL TO $SR_A$

$\therefore$ NEW $f_b = 131460 \times \frac{2360}{3423} = 90{,}600$ psi

USE SIMILAR PROCEDURE SHOWN ON PAGE A-1

$$f_c = \left(90{,}600 + \frac{2360 \times 1.5608\pi}{2 \times 0.0105 \times 2.96}\right) \frac{E_t}{E}$$

$$= 10{,}030\, E_t \times 10^{-6} \text{ psi}$$

RANGE OF $E_t$ = 3.74 TO 3.94 ($\times 10^6$)

$$P_{cr} = \frac{2\pi \times 2360}{2.96} \times \frac{E_t}{27.5 \times 10^6} \qquad \therefore \; 681 \leq P_{cr} \leq 718$$

SADI 138 REV. 2/64

SOLAR
A Division of International Harvester Company

ENGINEERING REPORT
NO. M-1794
DATE 8-19-65
PAGE B-2 OF ____ PAGES
JOB NO. ____

SUBJECT: NASA BELLOWS SQUIRM PROGRAM
BY: D. SHEN

RESERVE THIS SPACE FOR BINDING.

# EFFECT OF SLIGHT CHANGE OF SPRING RATE UPON COMPUTED SQUIRM PRESSURE

(b) BELLOWS 9106 (AISI 321) [SEE PAGE A-3 ]

FROM PAGE 22 TESTED $SR_A$ = 2610.0 LB/IN
COMPUTED $SR_A$ = 4818.0 LB/IN

$$\therefore \text{NEW } f_b = 176{,}911 \times \frac{2610}{4818} = 95{,}700 \text{ psi}$$

$$\therefore f_c = \left(95700 + \frac{2610 \times 1.556\pi}{2 \times 0.0115 \times 2.96}\right) \frac{E_t}{E}$$

$$= 10{,}300\, E_t \times 10^{-6} \text{ psi}$$

$\therefore$ RANGE OF $E_t$ = 3.66 TO 3.85 ($\times 10^6$)

$$P_{cr} = \frac{2\pi \times 2610}{2.96} \times \frac{E_t}{27.5 \times 10^6}$$

$$737 \leq P_{cr} \leq 776$$

SAD1 138 REV. 2/64

## EFFECT OF SLIGHT CHANGE OF SPRING RATE UPON COMPUTED SQUIRM PRESSURE

(c) BELLOWS 9115 (AISI 321) [SEE PAGE A-4]

FROM PAGE 22, TESTED $SR_A = 755$ LB/IN

COMPUTED $SR_A = 1,867$ LB/IN

$$\therefore \text{NEW } f_b = 102157 \times \frac{755}{1867} = 41{,}400 \text{ psi}$$

$$\therefore f_c = \left(41400 + \frac{755 \times 1.578\pi}{2 \times 0.011 \times 2.28}\right) \frac{E_t}{E}$$

$$= 4210\, E_t \times 10^{-6} \text{ psi}$$

RANGE OF $E_t = 8.0$ TO $8.4$ $(\times 10^6)$

$$P_{cr} = \frac{2\pi \times 755}{2.28} \times \frac{E_t}{27.5 \times 10^6}$$

$$605 \leq P_{cr} \leq 636$$

Copy

**SOLAR**
A Division of International Harvester Company

ENGINEERING REPORT
NO. M-179X
DATE 8-19-65
PAGE B-4 OF ____ PAGES
JOB NO. ____

SUBJECT: NASA BELLOWS SQUIRM PROGRAM
BY: D. SHEN

RESERVE THIS SPACE FOR BINDING.

# EFFECT OF SLIGHT CHANGE OF SPRING RATE UPON COMPUTED SQUIRM PRESSURE

## COMPARISON OF CALCULATED SQUIRM PRESSURES BASED ON COMPUTED AND TESTED SPRING RATES

| EXAMPLE BELLOWS | COMPUTED $S_{RA}$ | TESTED $S_{RA}$ | SQUIRM PRESSURE BASED ON COMPUTED $S_{RA}$ (MIN.) | SQUIRM PRESSURE BASED ON TESTED $S_{RA}$ (MIN.) | REF. PAGES |
|---|---|---|---|---|---|
| (a) 9103 | 3423 LB/IN | 2360 LB/IN | 703 psi | 681 psi | P. A-1 & P. B-1 |
| (b) 9106 | 4818 LB/IN | 2610 LB/IN | 763 psi | 737 psi | P. A-3 & P. B-2 |
| (c) 9115 | 1867 LB/IN | 755 LB/IN | 678 psi | 605 psi | P. A-4 & P. B-3 |

| EXAMPLE BELLOWS | PERCENTAGE CHANGE OF SPRING RATES USED IN COMPUTATION OF $P_{CR}$ $\frac{\text{COMPUTED } S_{RA} - \text{TESTED } S_{RA}}{\text{COMPUTED } S_{RA}} \times 100$ | PERCENTAGE CHANGE OF COMPUTED $P_{CR}$ DUE TO CHANGE OF SPRING RATES USED $\frac{P_{CR} \text{ BASED ON COMP. } S_{RA} - P_{CR} \text{ BASED ON TESTED } S_{RA}}{P_{CR} \text{ BASED ON COMPUTED } S_{RA}} \times 100$ |
|---|---|---|
| (a) 9103 | $\frac{3423-2360}{3423} \times 100 = 31.1\%$ | $\frac{703-681}{703} \times 100 = 3.13\%$ |
| (b) 9106 | $\frac{4818-2610}{4818} \times 100 = 45.8\%$ | $\frac{763-737}{763} \times 100 = 3.41\%$ |
| (c) 9115 | $\frac{1867-755}{1867} \times 100 = 59.6\%$ | $\frac{678-605}{678} \times 100 = 10.78\%$ |

SASI 138 REV. 2/64

# NASA BELLOWS SQUIRM PROGRAM

## TANGENT MODULI FOR INC. 718 & S/S 321

THE FOLLOWING CURVES WERE USED FOR SQUIRM CALCULATIONS BASED ON DRAWING DIMENSIONS

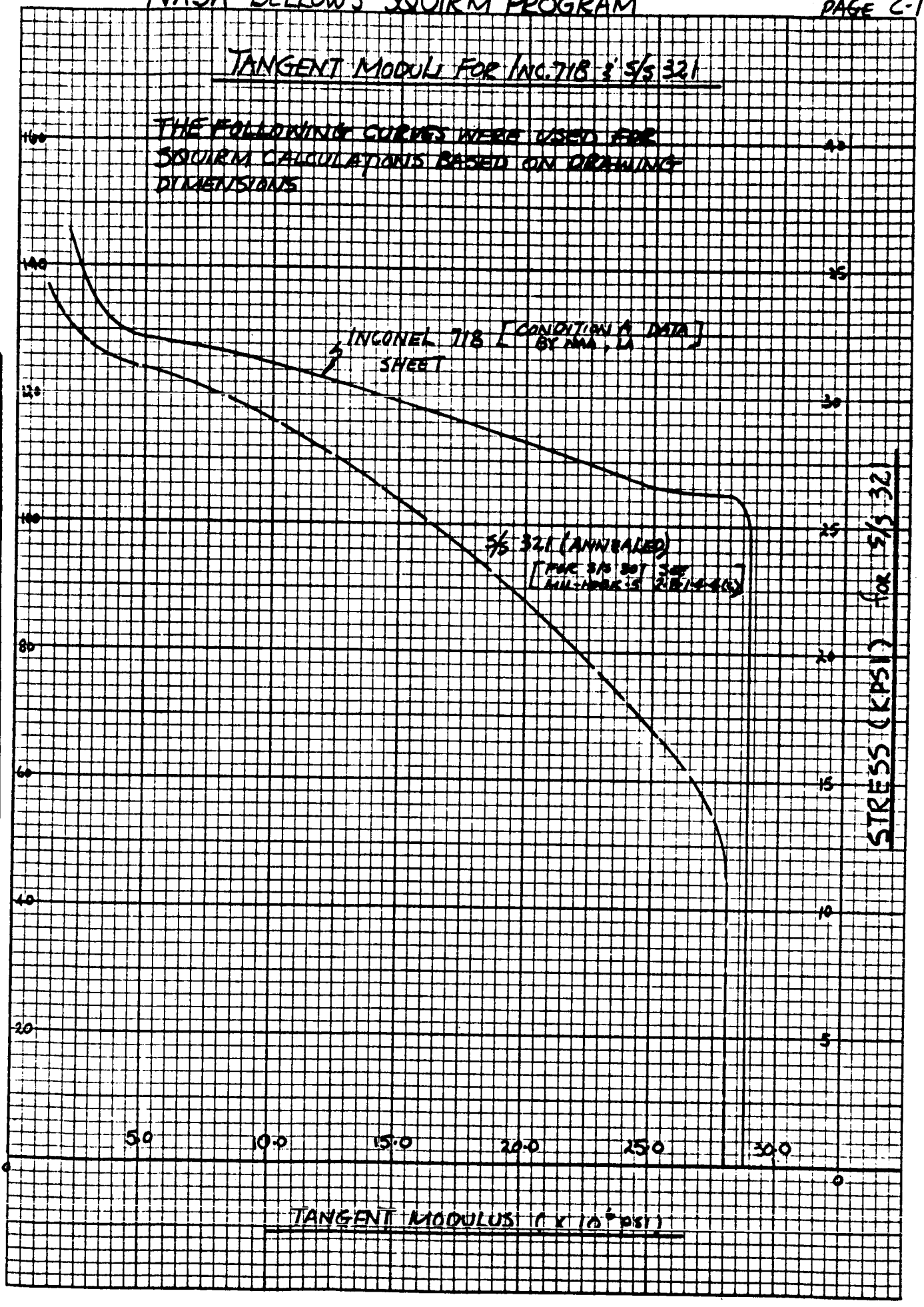

# NASA BELLOWS SQUIRM PROGRAM

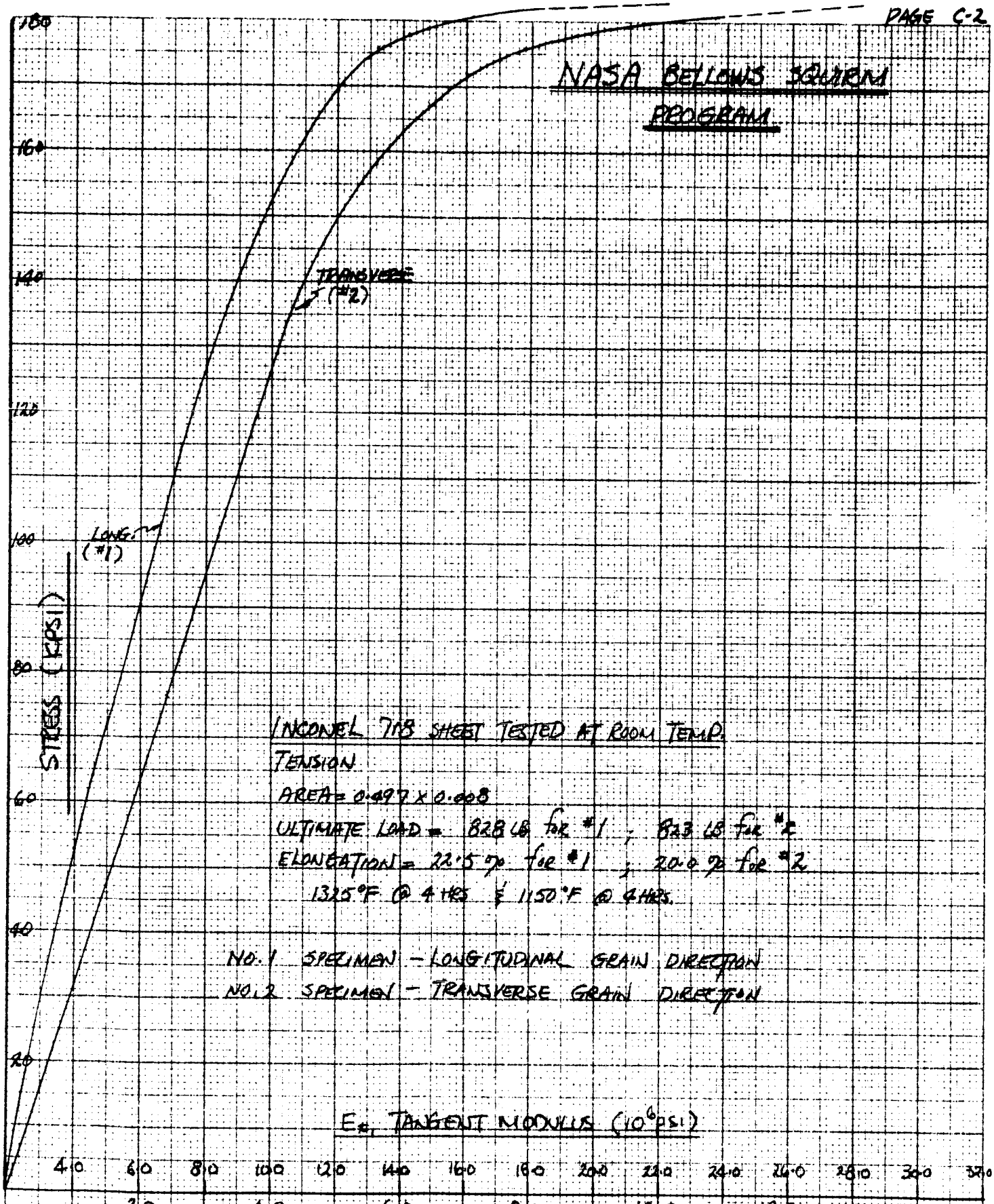


INCONEL 718 SHEET TESTED AT ROOM TEMP.

TENSION

AREA = 0.497 x 0.008

ULTIMATE LOAD = 828 LB FOR #1 ; 823 LB FOR #2

ELONGATION = 22.5 % FOR #1 ; 20.0 % FOR #2

1325°F @ 4 HRS & 1150°F @ 4 HRS.

NO. 1 SPECIMEN – LONGITUDINAL GRAIN DIRECTION

NO. 2 SPECIMEN – TRANSVERSE GRAIN DIRECTION

# NASA BELLOWS SQUIRM PROGRAM

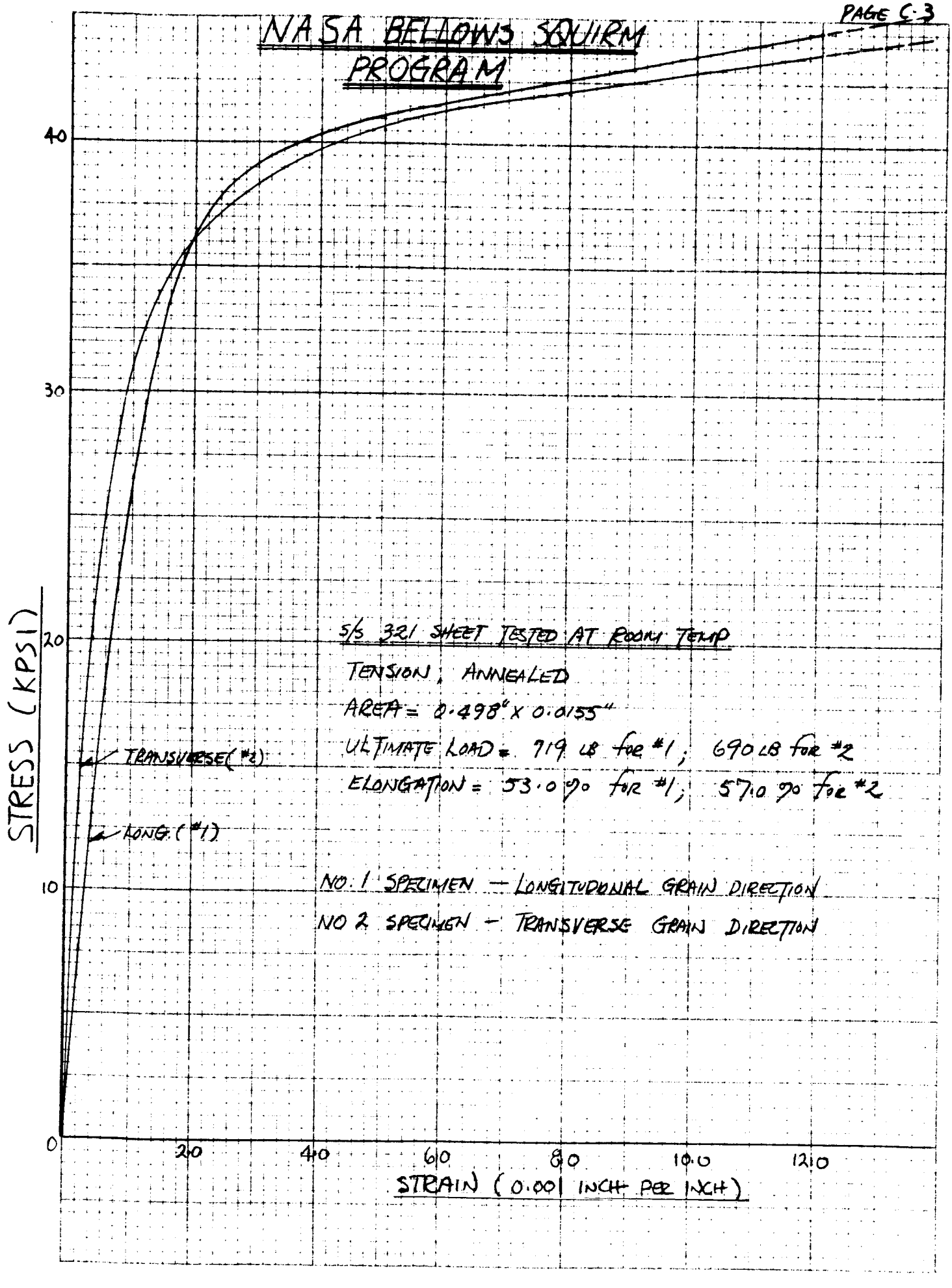


5/s 321 SHEET TESTED AT ROOM TEMP

TENSION, ANNEALED

AREA = 0.498" X 0.0155"

ULTIMATE LOAD = 719 LB for #1; 690 LB for #2

ELONGATION = 53.0 % for #1; 57.0 % for #2

NO. 1 SPECIMEN — LONGITUDINAL GRAIN DIRECTION

NO 2 SPECIMEN — TRANSVERSE GRAIN DIRECTION

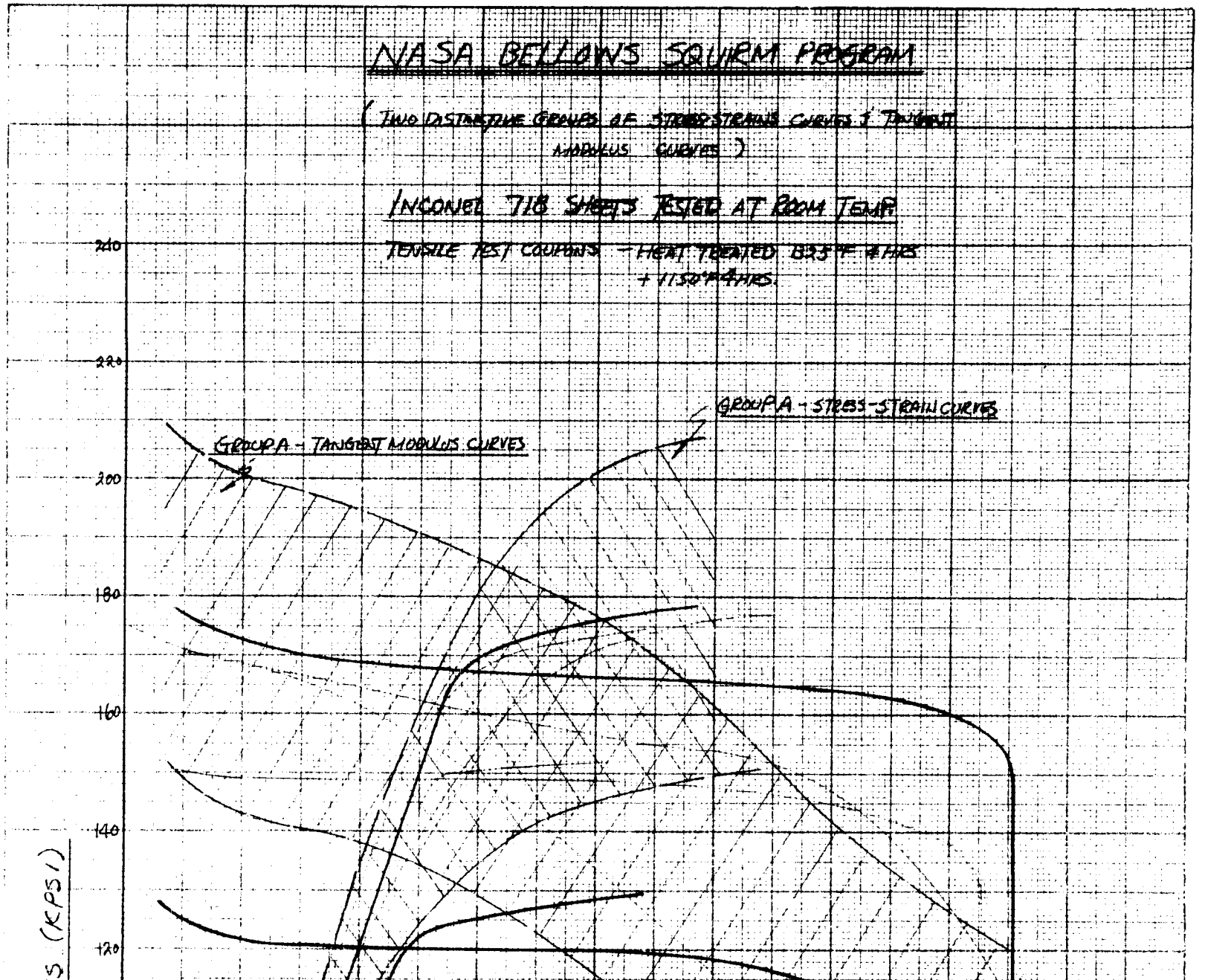
NASA BELLOWS SQUIRM PROGRAM
(TWO DISTINCTIVE GROUPS OF STRESS-STRAIN CURVES & TANGENT MODULUS CURVES)
INCONEL 718 SHEETS TESTED AT ROOM TEMP
TENSILE TEST COUPONS - HEAT TREATED 833°F 4 HRS + 1150°F 4 HRS.
GROUP A - TANGENT MODULUS CURVES
GROUP A - STRESS-STRAIN CURVES
240
220
200
180
160
140
120
S (KPSI)

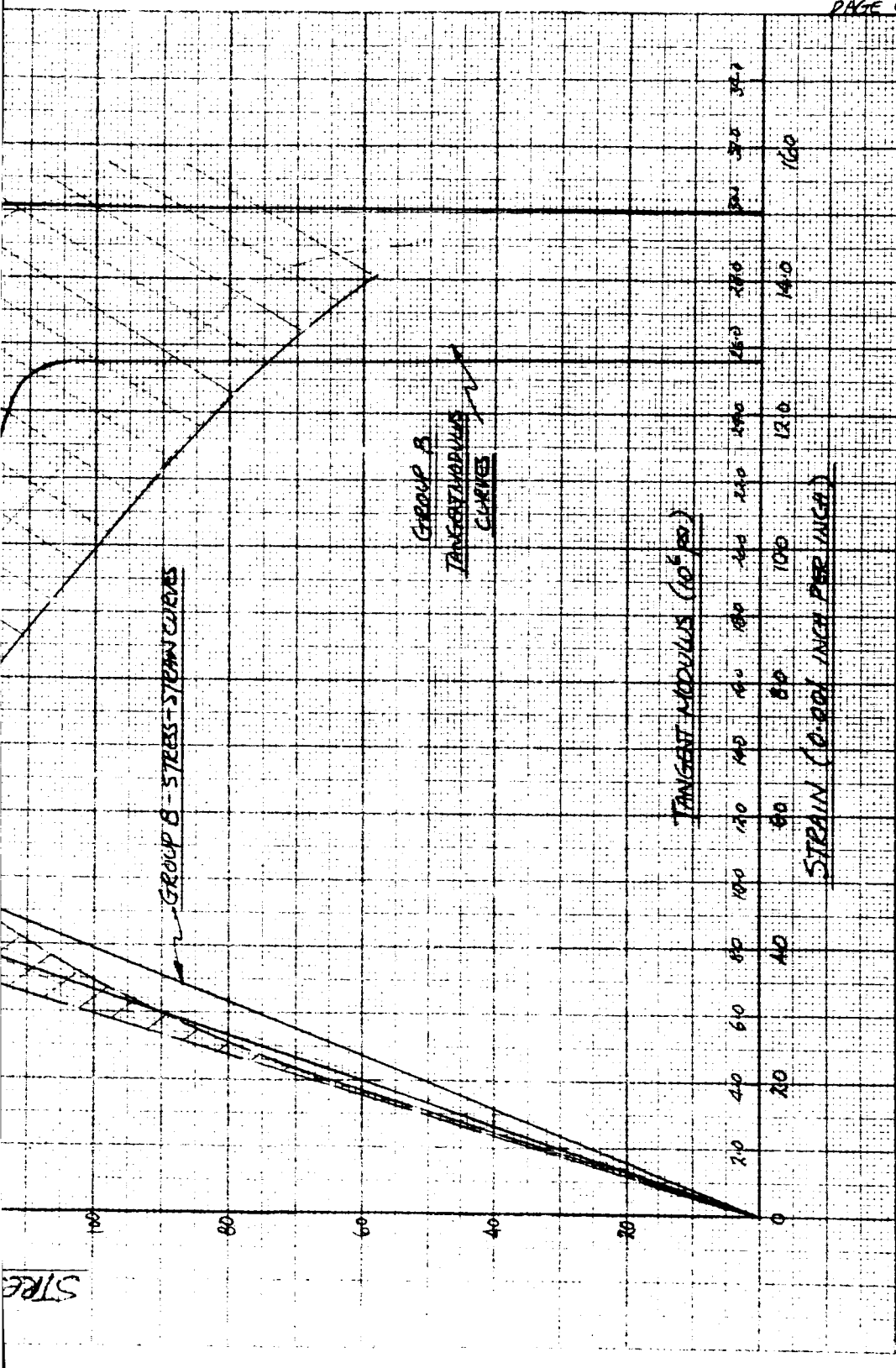
GROUP B - STRESS-STRAIN CURVES
GROUP B TANGENT MODULUS CURVES
TANGENT MODULUS (10⁶ psi)
STRAIN (0.001 inch per inch)
STRE

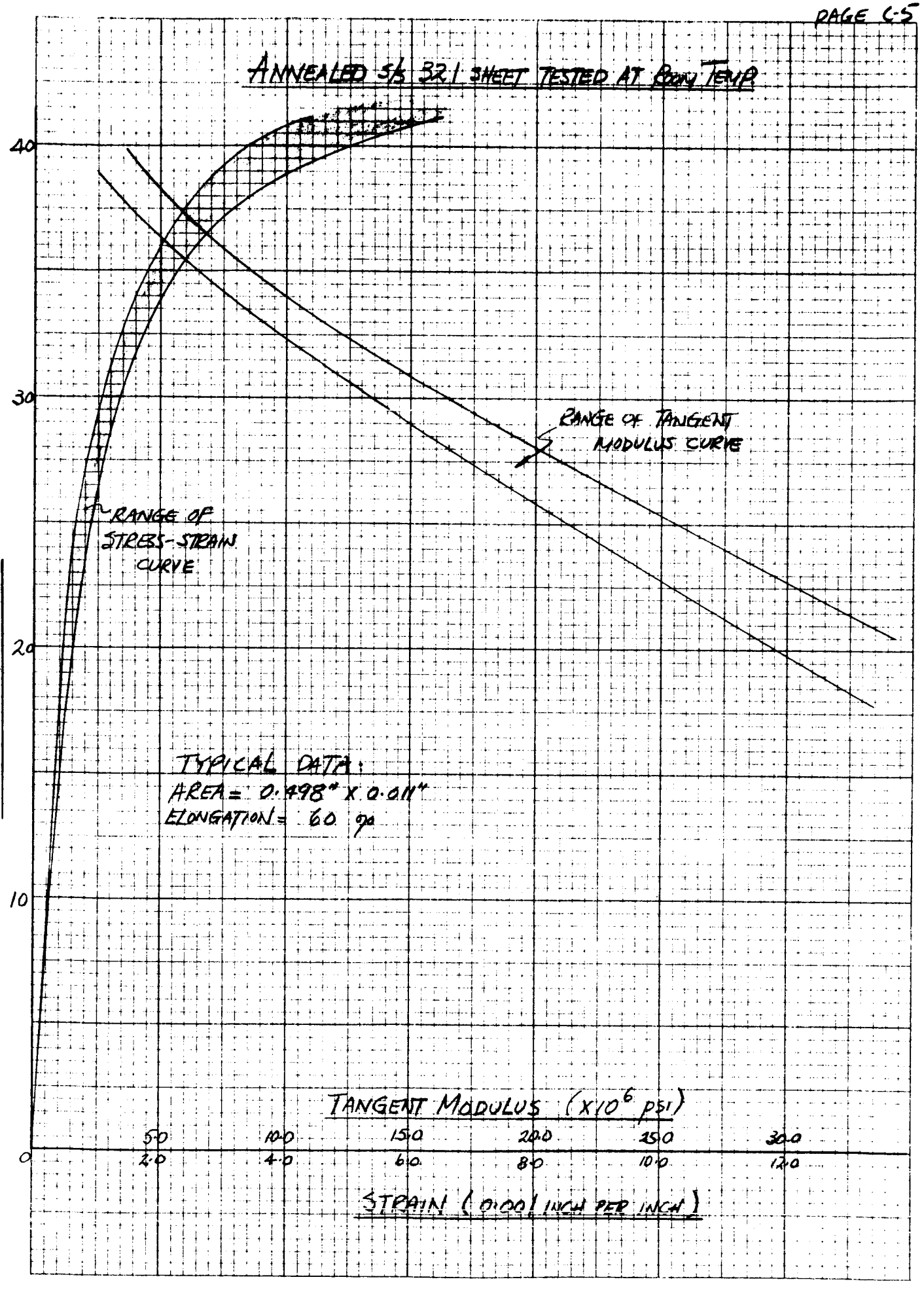
ANNEALED 5/8 321 SHEET TESTED AT ROOM TEMP
RANGE OF TANGENT MODULUS CURVE
RANGE OF STRESS-STRAIN CURVE
TYPICAL DATA:
AREA = 0.498" X 0.011"
ELONGATION = 60 %
STRESS (KPSI)
40
30
20
10
0
TANGENT MODULUS (X10^6 PSI)
5.0
10.0
15.0
20.0
25.0
30.0
2.0
4.0
6.0
8.0
10.0
12.0
STRAIN (0.001 INCH PER INCH)

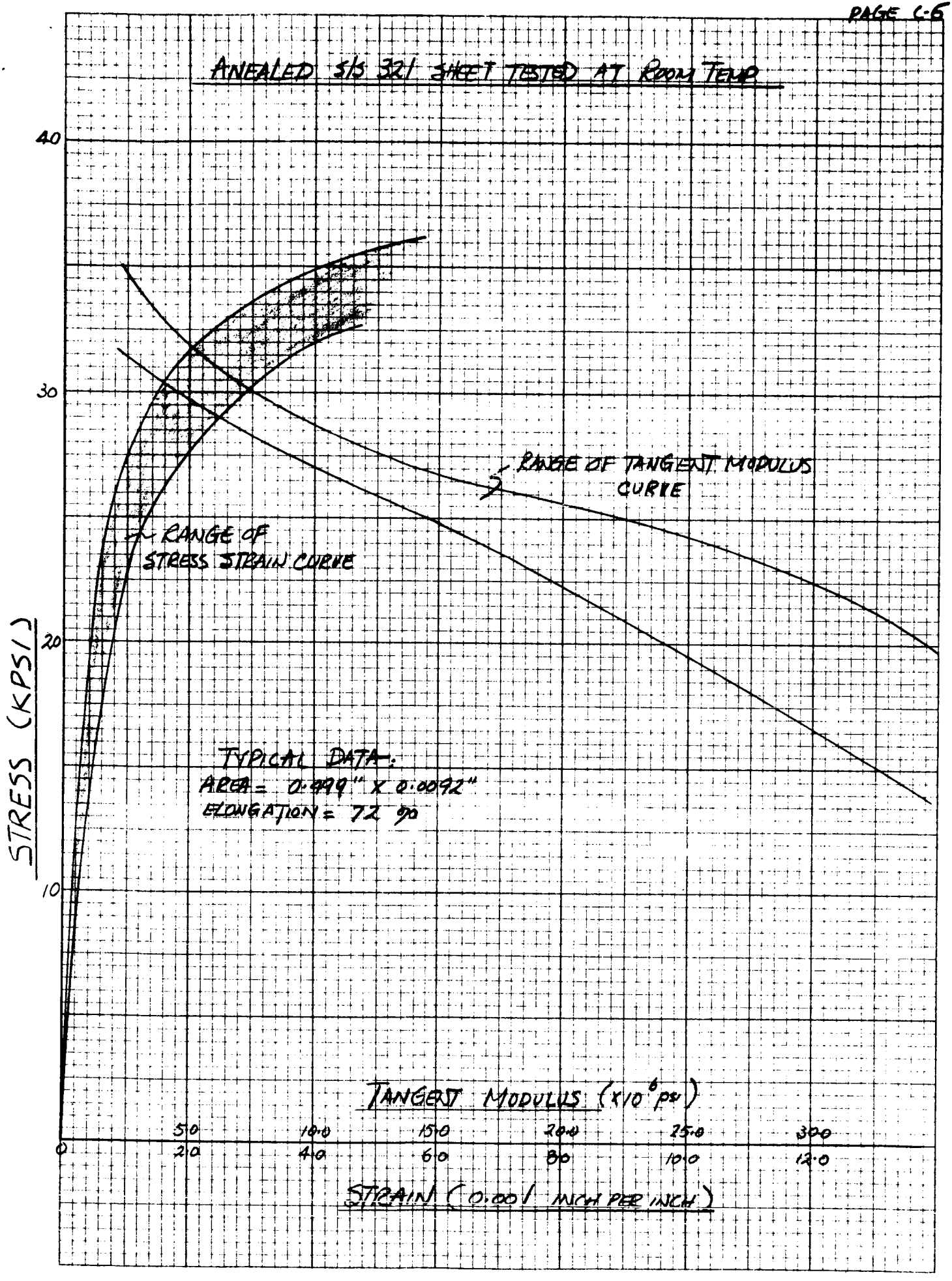

# APPENDIX II

## SOLAR RESEARCH REPORT RDR 1484B

## DEVELOPMENT TEST PROCEDURE FOR DETERMINING WEAR CHARACTERISTICS OF VARIOUS MATERIALS AND COATINGS APPLIED TO SIMULATED BALL JOINT SECTIONS

# RESEARCH REPORT

DEVELOPMENT TEST PROCEDURE
FOR
DETERMINING WEAR CHARACTERISTICS
OF VARIOUS MATERIALS AND COATING
APPLIED TO SIMULATED BALL JOINT SECTIONS
(REF: SOLAR DRAWING DSK-9434)

REPORT RDR-1484 "B"

ISSUED May 19, 1965
Revised December 7, 1965

SUBMITTED TO
Marshall Space Flight Center
Huntsville, Alabama

PREPARED BY
R. L. Neher - Research Engineer

APPROVED BY
J. E. Benawa - Research Staff Engineer

CUSTOMER REF Contract NAS-8-11303
SOLAR REF Sales Order 6-1612-7
COPY NO.

SOLAR
A Division of International Harvester Company

TABLE OF CONTENTS

## REVISION PAGE

| Rev. No. | Date | Signature | Purpose | Page and/or Figures Changed |
|---|---|---|---|---|
| (A) | 6-30-65 | By: R. L. Neher | Update and incorporate | |
| | | App: J. E. Benawa | specimen change | (A) as noted |
| (B) | 12-7-65 | By: R. L. Neher | Update and change | |
| | | App: J. E. Benawa | static load requirement | (B) as noted |
| | | By: | | |
| | | App: | | |
| | | By: | | |
| | | App: | | |

Paragraphs identified in the left margin with a circled letter have been revised or added. The letter used indicates the revision letter and date as given in the above box.

## 1.0 SCOPE

This report is written to establish a test procedure necessary to obtain basic design data and to determine optimum bearing materials and coating for special ball joint assemblies.

## 2.0 APPLICABLE DOCUMENTS

The following specifications and drawings form a part of this development test procedure.

a. 44400 - Engineering Drawing - Wear Test Fixture.

b. DSK-9434 - Test Hardware Description and Surface Finish Requirements

## 3.0 TEST EQUIPMENT AND STANDARD TEST CONDITIONS

### 3.1 Test Equipment

All instruments utilized for testing are calibrated at scheduled intervals. The equipment and instrumentation used in conducting the test program are as follows:

#### 3.1.1 Vacuum

a. Welch 5 CFM Vacuum Pump and associated equipment.
b. Veeco Thermocouple Gauge, Model GV-3l (DV-1M gauge) - Range 0-1000 microns.

#### 3.1.2 Deflection and Measurement

a. SR4 load cells - Baldwin-Lima-Hamilton, Range 0-500 pounds and 0-1000 pounds.
b. Varian G-11A Strip Chart Recorders.
c. Sanborn Oscillograph, Model 150 series.
d. SR-4 Strain Indicator - Baldwin-Lima-Hamilton, Type N.

#### 3.1.3 Miscellaneous Equipment

a. Actuating Test Fixture - Solar Drawing 44400.
b. Pressure Test Gauge - Range 0-10,000 psi.

### 3.2 Standard Test Conditions

Unless otherwise specified, maximum allowable tolerance on test conditions shall be as follows:

a. Ambient Conditions

| | | |
|---|---|---|
| 1. | Temperature | 80 ± 20 F |
| 2. | Pressure | Local atmospheric conditions 29 to 32 in/Hg. |
| 3. | Relative humidity | 20 to 95% |

b. Vacuum $10^{-1}$ to $10^{-2}$ Torr range

c. Pressure $\pm$ 1.5%

3.3 Test Reports

Solar Research Laboratories shall be responsible for the preparation of the final report. The report shall be a complete and concise record of all phases of testing with applicable data obtained from the test results. Original test data shall be retained at Solar Research Laboratories and available to Marshall Flight Space Center upon request.

(A) 4.0 TEST HARDWARE DESCRIPTION

The following test articles shall be subjected to the development test described herein. Each test article shall be identified as shown in the following table.

Typical test specimen consists of a contained block and shoe assembly as shown in Figure 1.

| TEST ITEM | SOLAR IDENTIFICATION (P/N 44400) | TEST HARDWARE DESCRIPTION |
|---|---|---|
| -2 | -7 block | Passivate/MIL-S-5002 and dip in Molydisulfide solution -Electro-film #1005 (cure cycle per DSK-9434). Mat'l: Inconel 718. |
| | -26 shoe | 4 surface finish - Mat'l: Inconel 718. |
| -1 | -7 block | Passivate/MIL-S-5002 and dip in Molydisulfide solution - Electro-film #1005 (cure cycle per DSK-9434). Mat'l: Stainless Type 321. |
| | -26 shoe | 4 surface finish - Mat'l: Stainless Type 321. |
| -3 | -7 block | 16 surface finish - Mat'l: Inconel 718. |
| | -26 shoe | 16 surface finish - Mat'l: Inconel 718. |
| -4 | -7 block | Bond Turcite Type A insert (width 0.99-1.00") to -7 block (bonding procedure per DSK-9434). Mat'l: Stainless Type 321. |
| | -26 shoe | 16 surface finish - Mat'l: Stainless Type 321. |
| -5 | -7 block | Bond Turcite Type A insert (width 0.99-1.00") to -7 block (bonding procedure per DSK-9434). Mat'l: Stainless Type 321. |
| | -26 shoe | 16 surface finish - Mat'l: Inconel 718. |
| -6 | -7 block | 16 surface finish - Mat'l: Stainless Type 321. |
| | -26 shoe | 16 surface finish - Mat'l: Stainless Type 321. |
| -7 | -7 block | Passivate/MIL-S-5002 and dip in Molydisulfide solution - Electro-film 77S (1 hour cure at 375 F). Mat'l: Stainless Type 321. |
| | -26 shoe | 16 surface finish - Mat'l: Stainless Type 321. |

| TEST ITEM | SOLAR IDENTIFICATION (P/N 44400) | TEST HARDWARE DESCRIPTION |
|---|---|---|
| -8 | -7 block | Passivate/MIL-S-5002 and dip in Molydisulfide solution - Electro-film 77S (1 hour cure at 375 F). Mat'l: Stainless Type 321. |
| | -26 shoe | 16 surface finish - Mat'l: Inconel 718. |
| -9 | -7 block | 16 surface finish - Mat'l: Inconel 718. |
| | -26 shoe | Hard chrome plate/AMS-2406C and grind 16 surface finish (.015 plating after machine grind) - Mat'l: Stainless Type 321. |
| -10 | -7 block | 16 surface finish - Mat'l: Stainless Type 321. |
| | -26 shoe | Hard chrome plate/AMS-2406C and grind 16 surface finish (.015 plating thick after grind) - Mat'l: Stainless Type 321. |
| -11 | -7 block | Coat with Haynes Stellite Alloy #12 - 16 surface finish - Mat'l: Stainless Type 347. |
| | -26 shoe | 16 surface finish - Mat'l: Stainless Type 321. |
| -12 | -7 block | Coat with Haynes Stellite Alloy #12 - 16 surface finish - Mat'l: Stainless Type 347. |
| | -26 shoe | 16 surface finish - Mat'l: Inconel 718. |
| -13 | -7 block | Torch braze Asarcon 773 insert (width 0.99-1.00") to -7 block. Dip in Molydisulfide solution - Electro-film 77S and cure 1 hour at 375 F - Mat'l: Stainless Type 321. |
| | -26 shoe | 16 surface finish - Mat'l: Stainless Type 321. |
| -14 | -7 block | Torch braze Asarcon 773 insert (width 0.99-1.00") to -7 block. Dip in Molydisulfide solution - Electro-film 77S and cure 1 hour at 375 F - Mat'l: Stainless Type 321. |
| | -26 shoe | 16 surface finish - Mat'l: Inconel 718. |
| -15 | -7 block | Torch braze Super Oilite #16 insert (width 0.99-1.00") to -7 block. Dip in Molydisulfide solution - Electro-film 77S and cure 1 hour at 375 F - Mat'l: Stainless Type 321. |
| | -26 shoe | 16 surface finish - Mat'l: Stainless Type 321. |

| TEST ITEM | SOLAR IDENTIFICATION (P/N 44400) | TEST HARDWARE DESCRIPTION |
|---|---|---|
| -16 | -7 block | Torch braze Super Oilite #16 insert (width 0.99-1.00") to -6 block. Dip in Molydisulfide solution - Electro-film 77S and cure 1 hour at 375 F - Mat'l: Stainless Type 321. |
| | -26 shoe | 16 surface finish - Mat'l: Inconel 718. |
| -17 | -7 block | Bond Teflon coated glass cloth (.014" thick) to -7 block (bonding procedure per DSK-9434). Mat'l: Stainless Type 321. |
| | -26 shoe | 16 surface finish - Mat'l: Stainless Type 321. |
| -18 | -7 block | Bond Teflon coated glass cloth (.014" thick) to -7 block (bonding procedure per DSK-9434). Mat'l: Stainless Type 321. |
| | -26 shoe | 16 surface finish - Mat'l: Inconel 718. |
| -19 | -7 block | Passivate/MIL-S-5002 and dip in Tungsten Disulfide solution - Electro-film #2606 (Cure 2 hours at 180 F and 2 hours at 400 F). Mat'l: Stainless Type 321. |
| | -26 shoe | 16 surface finish - Mat'l: Stainless Type 321. |
| -20 | -7 block | Passivate /MIL-S-5002 and dip in Tungsten Disulfide solution - Electro-film #2606 (Cure 4 hours - 2 hours at 180 F and 400 F). Mat'l: Stainless Type 321. |
| | -26 shoe | 16 surface finish - Mat'l: Inconel 718. |
| -21 | -7 block | Bond Turcite Type B insert (width 0.99-1.00") to -7 block (bonding procedure per DSK-9434). Mat'l: Stainless Type 321. |
| | -26 shoe | 16 surface finish - Mat'l: Stainless Type 321. |
| -22 | -7 block | Bond Turcite Type B insert (width 0.99-1.00") to -7 block (bonding procedure per DSK-9434). Mat'l: Stainless Type 321. |
| | -26 shoe | 16 surface finish - Mat'l: Inconel 718. |

## 5.0 TEST REQUIREMENT AND PROCEDURE

### 5.1 General Test Program

The inherent nature of development testing does not allow a precise procedure to be defined and established for the complete test. The objective of the test and the general testing method and conditions are defined as necessary to generate design data.

The exact procedures are then modified to meet the objective as data is generated.

Test items and Solar identification are shown in paragraph 4.0.

The test program shall be conducted in the manner and order outlined below.

### 5.2 Wear Test

Each specimen shall be installed in the wear test fixture and connected to the vacuum and actuating source as shown in Figure 1.

#### 5.2.1 Test Media

a. Vacuum - $10^{-1}$ to $10^{-2}$ Torr range.
b. Ambient conditions.

(A) #### 5.2.2 Test Sequence

a. Install the specimen in the test fixture and connect to the vacuum and actuating source as shown in Figure 1.

NOTE: Add 44400-41 shim to maintain the 6.000-6.001 dimensions at block-shoe interface.

Verify specimen identification and surface preparation in accordance with DSK-9434.

(A) b. Evacuate test chamber to 50 microns or less as read on the Veeco thermocouple gauge.

(B)

c. Determine and record the break-away torque of the specimen at each static load condition of Table I.

This actuating force measurement may be used as the baseline starting load condition.

Measure and record the actuation force using a Baldwin-Lima-Hamilton load cell and Varian G-11A Recorder.

NOTE: Actuating force measurement to be used to monitor the frictional force between the shoe and block surfaces as a function of time and load increments.

d. Apply static load to shoe-block assembly equal to the break-away torque value determined in step "c" or Table I.

e. Energize the actuating motor for the start of the cycle test. Testing to be conducted for a minimum of 10,000 cycles or until seizure or galling of the specimen contact surface occurs.

Galling of specimen surface area to be determined by visual (view plate window) and increase of initial actuating force as measured by the B.L.H. load cell.

NOTE: Shear load of actuating arm not to exceed 10,000 psi.

Total excursion of moving surfaces shall be $\pm$ 0.375 inch as shown in Figure 1. Cycle rate not to exceed 100 cpm.

f. Examine contact surfaces and record any scoring, etc.

g. Record total accumulated cycles and load conditions on Table I.

Return the shoe-block assembly to Manufacturing for surface preparation.

h. Repeat steps "e" through "g". Apply static load to shoe-block assembly in pressure load increments shown in Table I.

$P_A = 6.466\ cn^2$

TABLE I

(B)

WEAR TEST PROCEDURE

| Test Unit Number: | | | | | Date: | | |
|---|---|---|---|---|---|---|---|
| Condition | Hydraulic Actuator Pressure (psig) | * Approx. Load on Block-Shoe (psi) | Actuating Force Load Cell (lb) | Shaft Strain Gage Readout | Deflection (inch) | Total Accum. Cycles | Remarks |
| 1 | 310 | 1000 | | | | | * 1. Hydraulic piston area = 6.466 $in^2$ 2. Specimen contact area = 2 inches. |
| 2 | 155 | 500 | | | | | |
| 3 | 78 | 250 | | | | | |

* NOTE:

1. Break-away torque measurement of the specimen at the maximum load condition of column (3) may be used as the starting load for the initial test run.
2. Static load conditions may be varied to suit specimen requirement.

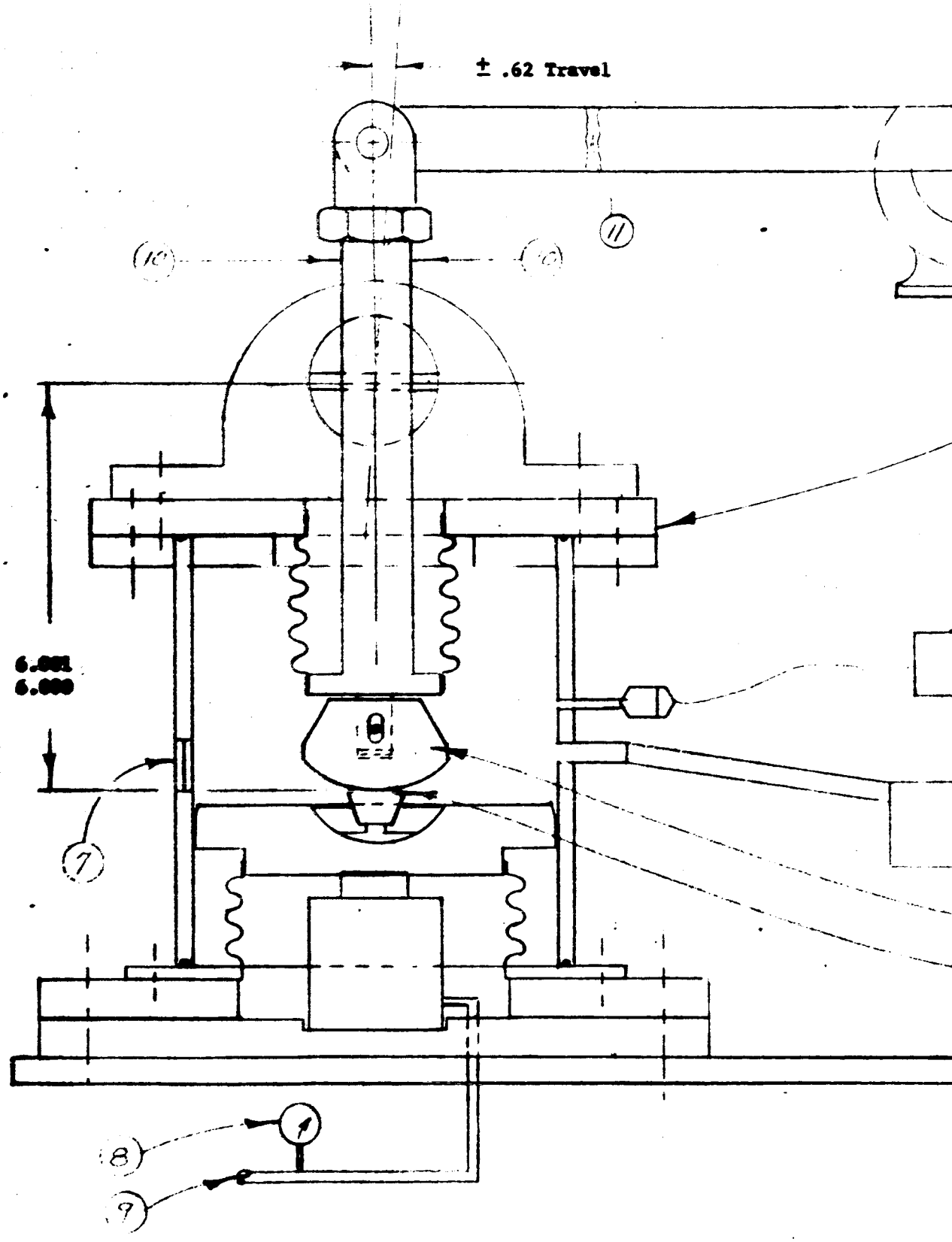
± .62 Travel
11
10
9
7
8

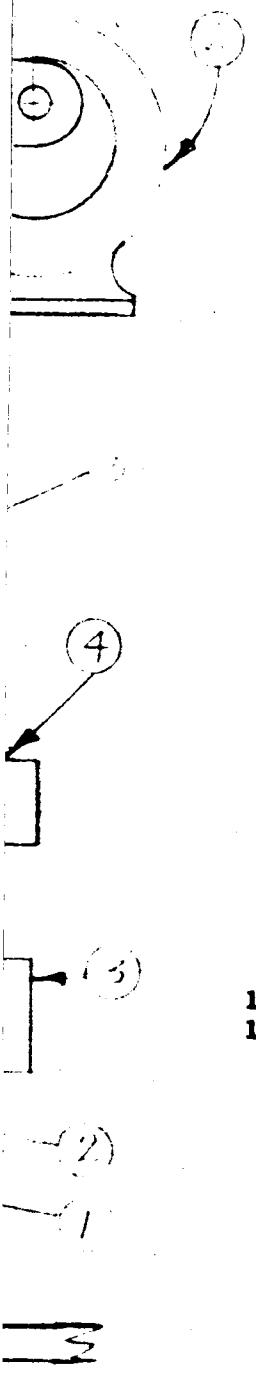

1. 44400-7 block assembly.
2. 44400-26 shoe assembly.
3. Vacuum system - $10^{-1}$ to $10^{-2}$ Torr range.
4. Veeco thermocouple gauge - [redacted] GV-31 (CV-1M Gauge) - Range 0-1000 microns.
5. Actuating fixture - Solar T/N 44400.
6. Vari-drive motor - 1 HP.
7. View port window (2).
8. Hydraulic Pressure Gauge - Range 0-10,000 psi.
9. Pressure inlet to hydraulic cylinder.
10. Strain gage location - actuating shaft.
11. Baldwin-Lima-Hamilton load cell and Varian G-11A Recorder.

Figure 1

WEAR TEST SCHEMATIC